AFRL-RB-WP-TM-2008-3052

REUSABLE MILITARY LAUNCH SYSTEMS (RMLS)

Gregory E. Moster

Structural Design and Development Branch
Structures Division

FEBRUARY 2008
Final Report

STINFO COPY

AIR FORCE RESEARCH LABORATORY
AIR VEHICLES DIRECTORATE
WRIGHT-PATTERSON AIR FORCE BASE, OH 45433-7542
AIR FORCE MATERIEL COMMAND
UNITED STATES AIR FORCE

NOTICE AND SIGNATURE PAGE

AFRL-RB-WP-TM-2008-3052 HAS BEEN REVIEWED AND IS APPROVED FOR PUBLICATION IN ACCORDANCE WITH ASSIGNED DISTRIBUTION STATEMENT.

*//Signature//

GREGORY E. MOSTER
Project Engineer
Structural Design and Development Branch
Structures Division

//Signature//

JOHN BOWLUS
Chief
Structural Design and Development Branch
Structures Division

*//Signature//

GREGORY H. PARKER, Acting Chief
Structural Design and Development Branch
Structures Division
Sensors Directorate

1. REPORT DATE *(DD-MM-YY)*	2. REPORT TYPE	3. DATES COVERED *(From - To)*
February 2008	Final	10 January 2000 – 30 September 2007

4. TITLE AND SUBTITLE	5a. CONTRACT NUMBER
REUSABLE MILITARY LAUNCH SYSTEMS (RMLS)	In-house
	5b. GRANT NUMBER
	5c. PROGRAM ELEMENT NUMBER 0602201

6. AUTHOR(S)	5d. PROJECT NUMBER
Gregory E. Moster (AFRL/RBSD)	A03N
	5e. TASK NUMBER
	5f. WORK UNIT NUMBER 0A

7. PERFORMING ORGANIZATION NAME(S) AND ADDRESS(ES)	8. PERFORMING ORGANIZATION REPORT NUMBER
Structural Design and Development Branch (AFRL/RBSD) Structures Division Air Force Research Laboratory, Air Vehicles Directorate Wright-Patterson Air Force Base, OH 45433-7542 Air Force Materiel Command, United States Air Force	AFRL-RB-WP-TM-2008-3052

9. SPONSORING/MONITORING AGENCY NAME(S) AND ADDRESS(ES)	10. SPONSORING/MONITORING AGENCY ACRONYM(S)
Air Force Research Laboratory Air Vehicles Directorate Wright-Patterson Air Force Base, OH 45433-7542 Air Force Materiel Command United States Air Force	AFRL/RBSD
	11. SPONSORING/MONITORING AGENCY REPORT NUMBER(S) AFRL-RB-WP-TM-2008-3052

12. DISTRIBUTION/AVAILABILITY STATEMENT
Approved for public release; distribution unlimited.

13. SUPPLEMENTARY NOTES
This report contains multiple technical papers that are in the public domain. Report contains color.

14. ABSTRACT
The Air Force Research Laboratory (AFRL) has developed a design environment (IPAT) and approaches to assess the performance and operational capabilities of reusable launch systems in collaboration with the NASA and industry. This approach uses the AML design environment with parametric geometry modeling. This approach has been used successfully and resulted in the Rocket Boost-Back concept under development by AFRL and SMC under the FAST ground experiment program. The RMLS program has also developed the ability to create discrete-event models and perform operational assessment which includes resource management.

15. SUBJECT TERMS
RMLS, Reusable Booster, Rocket Booster, Booster, Operationally Responsive Spacelift, ORS

16. SECURITY CLASSIFICATION OF:			17. LIMITATION OF ABSTRACT:	18. NUMBER OF PAGES	19a. NAME OF RESPONSIBLE PERSON (Monitor)
a. REPORT Unclassified	**b. ABSTRACT** Unclassified	**c. THIS PAGE** Unclassified	SAR	114	Gregory E. Moster
					19b. TELEPHONE NUMBER *(Include Area Code)* N/A

i

TABLE OF CONTENTS

1. BACKGROUND

This in-house research project was initiated in January 2000 at the request of Air Force Research Laboratory's Operational Space-lift Office (ORS) to re-establish the capability to analyze and assess reusable access to space systems. This would enable the directorate to identify and address technology deficiencies that limit the Air Forces ability to achieve the required capabilities to support our national defense needs.

The design and assessment of reusable launch systems requires multiple disciplines; therefore, multiple organizations were requested to support the Reusable Military Launch Systems (RMLS) team. These organizations included the Air Vehicles Directorate, Propulsions Directorate, Human Effectiveness Directorate, the Air Force Flight Test Center (AFFTC), NASA Kennedy Space Center (KSC), NASA Marshal Space Flight Center (MSFC), NASA Johnson Space Center (JSC), NASA Langley Research Center (LaRC), the 45 Space Wing, the 30th Space Wing, the Space and Missiles Center (SMC), and the Aeronautical Systems Center (ASC). These organizations were united by the objective to develop a common assessment capability that all would support.

Funding for this project was provided by a combination of AFRL and the organizations performing the work. Therefore, the papers and reports typically had joint sponsorship. The AFRL/RB in-house sponsorship of this project ended in September of 2007 with no efforts being supported by AFRL/RB in 2008.

2. APPROACH

The primary objectives of this effort were to develop the ability to quickly assess access to space systems in terms of performance and operational capability (reconstitution times) in order to determine technology deficiencies and make configuration and technology development recommendations. The sizing and performance objectives were achieved by developing unified analysis software by (1) using parametric geometry to approximate the configuration to be assessed, (2) teaming with domain experts, (3) using verified system sizing algorithms, (4) integrating analysis software, and (5) adding additional capability over time. The challenging task of estimating the operational capability of the systems was accomplished by collaborating with the experts and by performing assessments using a variety of software that evolved over time.

The unifying analysis software (Integrated Propulsion Tool (IPAT) maintained by AFRL/RZ) utilizes the Adaptive Modeling Language (AML) created by TechnoSoft Inc. AML was selected by AFRL because it allows geometry to be created from user selected parameters and it easily interacts with the external analysis software that team domain experts selected.

Typically, NASA, industry, and other government organizations take weeks to assess one configuration, so the first huge challenge was to select an approach that would enable quick assessments. This was achieved by deciding to approximate the geometry of the configuration to be assessed and avoid exact geometry sharing. The approximate geometry parameters were linked to parameters in the system sizing algorithms such as fuselage length, wing span, and so on. Because analysis software such as aerodynamics and aero-heating are based upon geometry, this allowed the rapid transition from empirical estimates to computational analysis. Older approaches pass IGES geometry files. IGES geometry does not maintain links with the sizing algorithms, so the links had to be recreated every time; therefore, assessments using IGES geometry took considerably longer to complete and required a great deal of effort for each assessment.

The decision to team with exerts from around the country solved several problems. It eliminated the need to develop and main local expertise, it encouraged information sharing, and it helped the dispersed teams to unite together instead of competing. This teaming was critical in developing the system sizing algorithms and supporting several national assessments such as the NASA and Air Force "One Team".

Most of the systems sizing algorithms are based upon the NASA LaRC CONSIZ software; however, each algorithm was reviewed by AFRL and ASC. During the review process, physical relationships were developed to validate them and increase their fidelity. These physical relationships gave the analyst additional insight into the parameters that drive the system mass properties. By understanding and documenting these algorithms, they were easily integrated into the IPAT environment and into other software packages that were developed later.

The sizing and performance analysis software initially used included Missile Dat Com and SHABP for aerodynamics, POST II for trajectory analysis, MINIVER for aero-heating, and

2

EXITS for TPS sizing. These software codes are widely used by the Air Force, NASA, and industry.

Operational capability estimates began by discussing flight and ground operations with NASA Johnson Space Center, NASA Kennedy Space Center, the 30th Space Wing, the 45th Space wing, and the AFFTC. All of these organizations expressed their concerns, recommendations, and provided data that was used in creating turn-time estimates. These estimates initially came from "black boxes" like the "Vision Spaceport" software developed by NASA and AFRL. The results provided no real insight in how to make significant reductions in turn-time, so they were replaced with other approaches as data became available. Several software codes worked very well such as Microsoft Project and Arena. Arena is a discrete event package that was used very successfully by NASA KSC and ASC/XP to support the RMLS team. It formed the foundation behind many of the other software packages that NASA as developed such as GEM-FLOW.

All of the above approaches and software has been used in a variety of ways since the RMLS effort first began. ASC/XP used many of the algorithms to create other approaches software codes using Phoenix Integration's Model Center software and Astrox Corporation's HySIDE.

3. RESULTS

The assessment capability was used by the Air Force to support NASA's Next Generation Launch Technology, NASA One Team, and an SMC lead Analysis of Alternatives (AOA). These assessments contributed to the Air Force taking the lead in reusable launch system technology development and NASA returning to expendable launch systems (Constellation Program). The AOA was instrumental in the creation of the ARES and FAST programs along with their associated technology development programs.

Specific uses of the assessment data are: (1) 6 DOF simulation development by the Flight Controls Division (RBC) and the Integrated Adaptive Guidance and Control effort, (2) Thermal Protection System (TPS) development by the Structures Division (RBS), (3) engine development by the Propulsion Directorate (RZ), (4) analysis software development and hypersonic programs by NASA LaRC, (5) technology development decisions by the Air Vehicles Directorate, and (6) system development recommendations by ASC/XR. The references and papers in the Appendixes provide details on much of this work.

The design environment approach is discussed in Appendices A and B though the papers "Toward An Integrated Modeling Environment For Hypersonic Vehicle Design and Synthesis" and "Collaborative Design Environment for Space Launch Vehicle Design and Optimization", respectively.

System comparisons were made in Appendices C, D, and E though the paper "Weight Growth Study of Reusable Launch Vehicle Systems", Comparative Analysis of Rocket and Air-Breathing Launch Vehicles", and " Cost Comparison of Expendable, Hybrid, and Reusable Launch Vehicles", respectively.

Turn-time capability analyses were made in Appendix F in the paper "A Discrete-Event Simulation of Turnaround Time and Manpower of Military RLVs". This paper gave AFRL an estimate of the required effort and resources required to maintain and operate an RLV.

The impact that flight operations can have on required technologies and the resources to operate a reusable booster were made in the Appendix G paper "Thermal-Based Comparison Between Rocket Boost-Back and Jet Fly-Back Booster Recovery Approaches". The research accomplished to create this paper prompted AFRL to invest further into the Rocket Boost-Back approach. This approach was later accepted by SMC and is being used in the FAST program.

The ability to perform TPS technology assessments and optimization was highlighted in the Appendix H paper "Thermal Protection System (TPS) Optimization". This is approached used in the design environment today.

Finally, the acoustic interaction of the launch vehicle and launch pad at launch was analytically and experimentally researched at NASA KSC. This work created many papers that collimated in the Appendix I paper "Noise Mitigation of Ducted Supersonic Jets for Launch Exhaust Management Systems".

All of this work combines to make a very successful and productive in-house effort that enables the Air Vehicles and Propulsion Directorates to maintain a leadership role in assessing and performing technology development for Operationally Responsive Space-lift systems.

APPENDIX A

TOWARDS AN INTEGRATED MODELING ENVIRONMENT FOR HYPERSONIC VEHICLE DESIGN AND SYNTHESIS

Jeffrey V. Zweber[*]
Design Process & Environments Team, AFRL/VASD
Wright Patterson AFB, OH 45433

Hanee Kabis[†]
Engineering Methods Group, Lockheed Martin Missiles and Fire Control
Orlando, FL 32819

William W. Follett[‡]
Computational Fluid Dynamics, Boeing, Rocketdyne Division
Canoga Park, CA 91303

Narayan Ramabadran[§]
TechnoSoft, Inc.
Cincinnati, OH 45242

ABSTRACT

The US Air Force Research Laboratory, along with its contractor partners, is developing an integrated modeling environment for the conceptual and preliminary-level design and synthesis of airbreathing, hypersonic vehicles. This effort is built on the team's successful prototype of a similar environment for rocket-powered space access vehicles. The modeling environment under development will begin by developing a 3-4 level deep hierarchy of objects that represent a hypersonic vehicle. Initially, these objects will contain only conceptual-level representations of the geometry and mass properties of the vehicle and its components. This initial information will be used with a vehicle synthesis routine to develop a "closed" conceptual design. The second step in the design process is an initial analysis of the aerodynamic and propulsive characteristics of the vehicle. These analyses will be conducted in the environment and the geometric model developed in the initial hierarchy of objects will be of sufficient fidelity to support these analyses. Next, the mass properties, aerodynamic and propulsion analysis results will be used by a trajectory simulation code, also integrated into the environment, to determine if the initial vehicle design will meet the mission performance requirements. Finally, the results of the trajectory simulation will be used to iteratively resize the vehicle until the mission requirements are satisfied. Additionally, this paper will describe the modeling environment used for this effort, lessons learned from the development of the environment for rocket-powered vehicles, and the next steps planned to expand the capabilities of the integrated modeling environment.

INTRODUCTION

The US Air Force has a renewed interest in investigating airbreathing hypersonic vehicle concepts to meet its needs for future strike and reconnaissance systems [1]. In addition, NASA is continuing its investment in hypersonic airbreathing propulsion systems and vehicle concepts for space transportation applications. In recent years, these interests have been exemplified by NASA's X-43 (Hyper-X) program [2] and the Air Force's HyTech (Hypersonic Technology) program.

Like all engineering organizations, the Air Force Research Laboratory is interested in conducting its vehicle and technology forecasting studies as quickly as possible, with as high fidelity an analysis as is feasible and with a proven, repeatable design and analysis process. The approach that the Air Force Research Laboratory team has taken is to integrate its design, analysis and modeling tools into a collaborative, network-distributed design environment.

The benefits of using an integrated design environment to reduce the time and potential errors associated with the transfer of data between design and analysis codes are well documented [3, 4]. This paper will present the initial steps in the development of an integrated modeling and analysis application for hypersonic airbreathing vehicles. This application will be developed using a modern knowledge-based engineering environment and will incorporate the lessons learned from the development of a similar application for rocket-powered space access vehicles [5]. Furthermore, the current effort will demonstrate a significant reuse of much of the software that was developed for the launch vehicle application.

ADAPTIVE MODELING LANGUAGE

For this effort, the Adaptive Modeling Language® (AML[TM]), developed by TechnoSoft, Inc., was selected as the design modeling environment. AML is a framework for Knowledge Based Engineering (KBE) that provides the ability to capture the vehicle design and analysis process and manage the data transfer between the various codes [6, 7]. The primary features of AML that led to its selection for this project are: its use of object-oriented programming and the Unified Part Model paradigm; its native understanding of geometric objects and features; and its support for multiple, simultaneous, network-distributed users.

Modeling Paradigm
The benefits of object-oriented programming (OOP) are well understood. OOP both increases the developer's ability to reuse code that was previously developed, and simplifies

---

[*] Aerospace Engineer, Senior Member AIAA
[†] Staff Research Engineer
[‡] Engineer / Scientist
[§] Software Applications Engineer

the initial development of the code. The Unified Part Model paradigm is an implementation of OOP in which the model of a given component, the fuselage for example, contains all the data about the fuselage. This paradigm helps ensure that the various models of the fuselage are consistent across the different disciplines.

To continue the fuselage example, this paradigm enforces the connection between the geometric model and the mass properties analysis. In the case of these disciplines, the mass estimating relationships (MERs), which are used to determine the vehicle's mass properties, are highly dependent on geometry (e.g., tank volume, fuselage surface area), as well as the overall vehicle weight and mission requirements. The Unified Part Model paradigm ensures that all weight items will be tracked by allowing the MERs to be included in the geometric objects. This can be visualized in the model tree shown in Figure 1. In this rocket-powered TSTO vehicle example, the tank-stack object contains both the geometry of the tanks shown and the weight and CG location of the tank.
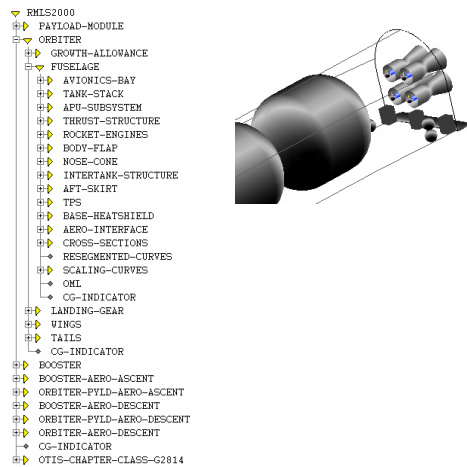

Figure 1: Unified Part Model Tree

In addition to being object oriented, AML has the ability to manage the relationships between the objects. As the model is being built; that is, as objects are being instantiated and as formulas are being coded to associate the parameters of one object with those of another object, AML is building a table of dependencies between the objects and properties of the model.

This "dependency tracking" is used to provide two computational benefits. First, dependency tracking allows AML to "smash" the values of all the variables that will change because of a change in a parameter upon which the variable is dependent. This feature means that the model will always be consistent. Once two parameters are related, the user can work with one portion of the model while not worrying that he is working with old data from another part of the model.

Related to AML's implementation of dependency tracking is its use of demand-driven computation. This feature means that for any requested calculation, only the calculations that are required will be computed, not the entire model. This feature is useful for complex models. For instance, in the fuselage model shown above, perhaps the tank geometry is calculated as an offset from the fuselage geometry. In this model, if the an aerodynamics engineer wanted to change the fuselage diameter and determine the external aerodynamic effects, the engineer would not have to wait for the tank geometry to be recomputed (or perhaps even the tank weights to be updated) because the aerodynamic calculation only requires information about the fuselage surface.

Geometric Modeling
In addition demonstrating the Unified Part Model paradigm, Figure 1 also shows AML's native geometric modeling capability. Included with AML's basic set of objects are classes to support a wide variety of commercial geometry engines. This feature means that geometric modeling is not handled as just another discipline. AML has a native understanding of solids and surfaces, can perform Boolean operations and has support for automatic mesh generation.

This capability is most easily demonstrated by considering AML's integration with Unigraphics and MSC.Patran. One of AML's supported geometry kernels is Parasolid, which is also the kernel for Unigraphics and MSC.Patran. This implementation means that AML can perform all the complex geometric calculations that are available in Unigraphics while natively transferring that geometry to MSC.Patran for meshing. Similar capabilities are available or under development for a variety of common CAD packages and commercial meshing programs.

Network-distributed (web-based) design modeling
The last major feature of AML that will be used for this application is AML's ability to allow multiple, simultaneous users to collaborate in a single engineering environment, even though they are distributed across a wide area network. AML supports two modes of operation (distributed-user collaboration and distributed-model collaboration), which can be used separately or together depending on the needs of the engineering team.

The distributed-user mode allows multiple users to interact simultaneously with a single model tree. In this mode, there is a single model that resides on a server with many users who have client interfaces on their local machine. Depending on the permissions granted, which can vary for each user, the users can view the model, change the values of model parameters, add objects to the model and even allow other users to see their current view of the model. This mode is useful for collaboration between engineers working in the same discipline. For instance, a novice aerodynamicist can receive help with the intricacies of a particular analysis code from a more senior engineer.

The second mode, distributed-model collaboration, is more useful for a multidisciplinary engineering project. In this mode, each engineer has an AML model that is tailored for his or her specific discipline. Then objects from the separate models can be connected through a central Object Request Broker (ORB). The use of an ORB allows disciplines to be added as needed. It can also allow models to connect and disconnect at will. This feature is useful for engineering teams that are spread across time zones. One discipline can start working; a second discipline can join (or rejoin) the collaboration and send and receive updates to the common objects; then the first discipline can disconnect from the collaboration.

The capability for simultaneous collaboration amongst multiple engineers will be useful for this project. Engineers from at least five different cities, spread across the United

States will be participating in the development of the hypersonic airbreathing vehicle design application.

ENGINEERING DISCIPLINES

The initial development of the integrated application will concentrate on conceptual design and synthesis of hypersonic airbreathing vehicle concepts. It is hoped that the design environment can then be expanded to model the preliminary and detailed levels of the development of a hypersonic vehicle. The authors believe this development strategy is feasible because of their experience with AML-based applications that are being used to capture and improve the detailed design of combustion engines [8].

Figure 2 shows the disciplines that are involved with the development of hypersonic vehicles. The figure also represents how the disciplines interact during the design process. Displayed in blue are the five disciplines involved in the conceptual-level synthesis of a hypersonic vehicle. Then, following sufficient iteration among these disciplines, the additional disciplines are added to refine the design of the vehicle through further iteration and studies.
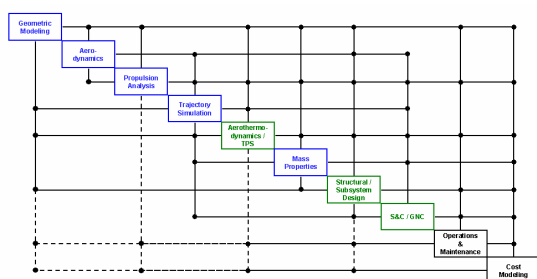

Figure 2: Hypersonic Airbreathing Vehicle Design Structure Matrix

For the effort documented here, the five disciplines that will be integrated into the application are: geometric modeling, aerodynamics, propulsion analysis (incl. flow path analysis), trajectory simulation and mass properties analysis. Additionally, this model development effort will take advantage of the inherent model and software reuse capability provide by AML's implementation of the object-oriented programming paradigm. This project will benefit greatly from the previous development of a design modeling application for rocket-powered launch vehicles [5]. Specifically, the aerodynamic analysis and trajectory simulation applications that were integrated for use on the previous effort will only require minor modifications to be applied to this application.

Synthesis and Geometric Modeling
The first step in developing a hypersonic vehicle design is to choose two configuration parameters, the vehicle class (e.g., 2-D lifting body, waverider, inward-turning or axisymmetric) and the design Mach number. Once these decisions are made, basic aerodynamic principles [9] can be used to define an initial propulsion flow path.

For the initial vehicle configurations that will be modeled in this effort, the FloGeo code from Boeing Rocketdyne will be used to generate propulsion flow path parameters for a 2-D lifting body configuration. FloGeo is method of characteristics based application that has been developed in Microsoft Excel. The application determines the necessary angles, lengths and other geometric properties of the inlet to end up with a "shock-on-lip" condition for the inlet flow at the specified design Mach number.

The next step in the design process is to develop an outer mold line (OML) model of the vehicle that is suitable for use with computational aerodynamic techniques. For this effort, a parametric OML model will be developed using AML's native geometric modeling capability. The process described here is for the 2-D lifting body class of vehicles, although a similar process could be used for the other classes of hypersonic vehicles.

The authors took this approach based on their previous experience with design modeling efforts for aerospace vehicles. They have found that developing different AML objects for different types of configurations is preferable to trying to develop a single parametric model capable of modeling the complete range of possible hypersonic vehicle configurations.

The first step in developing the OML is to model the propulsion flow path (i.e., keel line and cowl) as a set of parametric curves. The parameterization of these curves will match the output of FloGeo and may be used with an optimization procedure to improve the vehicle's performance at "off-design" Mach numbers.

Next, these curves are "extruded" to model the lower surface of the vehicle. The width of this extrusion will be determined from required internal volume of the vehicle. This required volume will be estimated initially, then verified by a mission and trajectory simulation.

Following the development the model of the vehicle's lower surface, a similar procedure is used to model the vehicle's upper surface. That is, first, a parametric curve is developed to control the shape of the upper surface, then that curve is extruded to create the upper surface model. The difference between the development of the upper surface and the lower surface is that the upper surface is designed solely based on aerodynamic and internal volume considerations, while the lower surface is strongly driven by its impacts on the performance of the propulsion system.

The last major step in developing the geometric model of the OML is to connect the upper and lower surfaces. This will be accomplished using the parametric surface modeling technique that was developed in AML for modeling aerospace surfaces. An example of this technique, used to build a parametric fuselage model, is shown in Figure 3. This fuselage geometry was built using two kinds of related profile objects termed "u" and "v" curves. These profile curves are controlled parametrically to shape and size each cross-section and the surface's behavior between the cross-sections at specified intervals. The external surface is then modeled as a nurb-surface that connects the various points that make up each profile curve.

For the OML of the 2-D lifting body class hypersonic vehicle, this profile curve paradigm will be used to connect the upper and lower surfaces. First, the edge of the upper and lower surface will be selected as the first and last v-curve for the side surface. Then points will be selected along each curve to form the starting points of a number of u-curves. Next, the u-curves will be developed freehand or with a simple mathematical formula. Finally, intermediate v-curves will be formulated or sketched freehand and the complete side surface will be automatically determined from these construction curves.
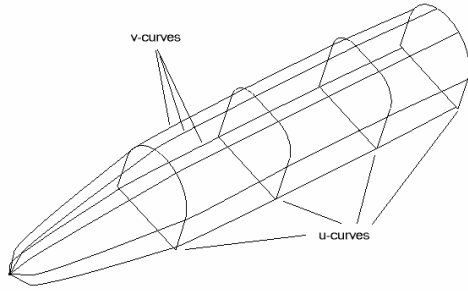
Figure 3: Fuselage Geometry Object

The final step in developing the geometric model, which will be used for computational aerodynamic and propulsion analysis, is adding control surfaces to the basic 2-D lifting body shape. There are two types of control surfaces that need to be developed, lifting surfaces and surfaces to control the propulsion flow path.

The models of the lifting surfaces (i.e., horizontal tails, vertical tails and canards) are developed in the same manner as the geometry model shown in Figure 3. Except in this case, the u-curves are airfoil sections and the v-curves are used to define the taper and twist of the lifting surface. Then, once the basic lifting surface has been modeled, it can be positioned relative to the 2-D lifting body shape and trimmed or joined to make a complete "watertight" surface.

To develop propulsion flow path control surfaces (e.g., a moving cowl lip or a moving inlet door for the turbine engine flow path of a TBCC engine), the OML that was generated by using basic aerodynamic principles, the FloGeo code in this case, must be modified.

Two methods are available to modify the OML. One option is to use Boolean operations on the OML. Using the cowl lip as an example, the process would require cutting the cowl to create the moving lip geometry; rotating the lip it to the desired angle; then trimming, extending and joining the rotated cowl lip to the remaining fixed portion of the original cowl. While this method is effective, and is commonly used by the aerospace industry, the method does not easily lend itself to design automation or optimization. The author's preferred method is to include parameters for these moving propulsion flow path surfaces in the original flow path curves that were modeled in AML. Then, a design model can be developed to automatically regenerate the lower OML surfaces when the parameters that change the propulsion flow path are varied. For the cowl lip example, the procedure would be generating a new cowl curve, extruding that curve to create the cowl surface and modifying the engine sidewalls to attach the cowl to the rest of the vehicle.

Mass Properties Estimation
The second discipline that is needed for the conceptual design and synthesis of a hypersonic vehicle is mass properties analysis. For this project, the authors have taken two approaches to integrate mass properties analysis into the design environment. The first, and simplest, method is to link an Excel spreadsheet-based weights model to AML. The second, and preferred, method is expand the AML geometry objects that were developed in the previous section so that these objects contain properties, objects and methods that will calculate estimates of the object's mass properties.

Spreadsheet-based Weights Model
The spreadsheet-based weights model that was used for this project was developed at the NASA Langley Research Center. This model consists of a main, system-level sheet with links to five discipline specific sheets (i.e., propulsion, structures, subsystems, landing gear and the thermal protection system for the airframe). The main sheet is the only one that needs to be linked to AML, with the other sheets being connected through the main spreadsheet.

The main, system-level spreadsheet takes two types of input, geometric parameters and design parameters. The geometric parameters will come from the OML model that was described in the previous section. Examples of the geometric information that is needed as inputs to the mass properties spreadsheet are: vehicle internal volume; wetted and planform areas for the fuselage and tails; surface areas covered by the various types of thermal protection systems (TPS); fuselage length; and combustor length.

The second type of inputs that are needed for mass properties analysis are determined either from mission requirements or from other, non-geometric, design decisions. Examples of these design inputs are: payload weight and volume; number and thrust level of the rocket engines, if needed for single stage to orbit vehicles; TPS unit weights, which are based on the type of TPS selected; vehicle design g-limit; and propellant fraction required.

Once the input design parameters and geometric parameters are determined, a set of mass estimating relationships (MERs) is used to determine an initial estimate of the mass properties of the vehicle. For this project, the team will use two types of MERs; one type based on component geometry and a second type based on system similarity.

An example of a geometry-based MER is Equation 1. This equation estimates the weight of the vertical tail based on the surface area of the tail. This equation was developed by fitting a curve to the historical data shown in Figure 4.

$$WT = 5 * S_{vt}^{1.09} * 0.89 \qquad [1]$$
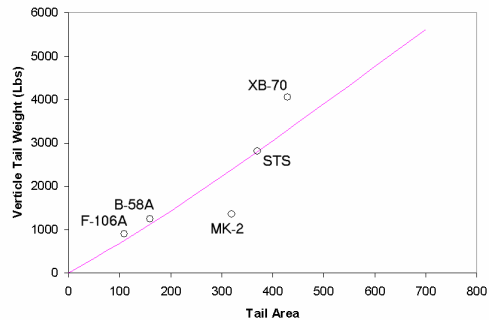
Figure 4: Vertical Tail Weight vs. Area

An example of the system similarity type of MER is the one used to estimate the mass of the vehicle's electrical system. In this case, the team estimated that the weight of the electrical system power supply will be 770 lbs, because that is the weight of the system on the Space Shuttle.

While some MERs, like the two examples presented above, are explicit, other MERs require and implicit solution method. For instance, the MER for the landing gear mass

9

strongly depends on the overall vehicle weight, which in turn is weakly dependent on the landing gear mass. This type of relationship leads to the need for an iterative process to ensure that the sized vehicle has a consistent set of mass properties.

The iteration process used with the spreadsheet-based weights model is based on determining a photographic scaling factor that makes the internal volume available match the internal volume required. This process requires the extra step of estimating component volumes as well as masses. The volume estimates are developed using a set of relationships that are conceptually similar to the MERs described above. The result of the iteration process is a scaling factor that can be used to scale or redraw the geometric model described above.

AML-based Weights Model

The major limitation of the spreadsheet-based weights model is that it is limited to photographic scaling of the vehicle that was created using the geometric modeling process. A few of the potentially useful vehicle changes that photographic scaling does not allow are: changing the vehicle's length and width independently (e.g., constraining the vehicle's length or width) or modifying the vehicle's upper surface shape to change the volume while keeping the vehicle's planform fixed.

The photographic scaling limitation will be eliminated in the second mass properties estimation method, the AML-based weights model. In this model, the mass estimating relationships will be incorporated into the geometric objects that were used to develop the OML model and geometric objects used to model the subsystems and internal components. This model will take advantage of AML's unified part model paradigm that was described above and is shown in Figure 1.

The major difference between the AML-based weights model and the spreadsheet-based weight model can be seen by examining the implementation of the vertical tail weight MER shown in Equation 1 above. In the case of the spreadsheet-based weights model, to calculate the vertical tail weight, the tail area (or the tail span and chords) must be extracted from the AML-based geometry model of the OML and input as parameters to the spreadsheet. However, in the AML-based weights modeling approach, a property called mass is added to the AML object that was already developed to model the geometry of the vertical tail. This new property can be programmed to calculate the weight of the vertical tail using the tail area or other parameters that are already available in the vertical tail object. These parameters are already available because they were needed for the geometric model.

The vertical tail weight model also exemplifies the paradigm that the methods for calculating the weights of each component of the vehicle will be developed as part of the object that also contains the top-level, conceptual geometric information about vehicle. Note however, that the fidelity of the geometric model and mass properties calculation may vary from vehicle component to vehicle component. For instance, the power system may be represented by boxes of fixed volume and weight, while the landing gear model may be made up of many additional geometric pieces (i.e., tires, brakes, struts, etc.) and have a complex MER based on takeoff weight, landing speed and runway surface.

Once MERs are integrated with a sufficient number of the AML objects to represent all of the major weight items, an iterative procedure must be developed in AML to ensure that the MERs are consistent. Like the spreadsheet-based weights model, this iteration will involve changing the size of the vehicle. However, because the mass properties estimate is tightly tied to the geometric components, design engineers will be able to develop more complex sizing routines. For instance, tail areas could be sized based on stability considerations and the vehicle's width could be constrained to accommodate an integer number of fixed sized airbreathing engines. This flexibility should allow the design team to synthesize feasible vehicles more easily.

Propulsion Flow Path Analysis

The bulk of the effort associated with this project will be the integration of ramjet and scramjet design and analysis tools into the AML environment. The first decision that needs to be made is what fidelity of propulsion flow path analysis is needed for conceptual-level design and synthesis of a hypersonic vehicle. Above, we described the FloGeo code, which will predict the on-design performance of the propulsion system. While this may be sufficient for the synthesis of cruise vehicles, a better prediction of the vehicle's off-design performance is needed for the design of accelerator configurations for access-to-space applications.

For this effort, the low-fidelity method that the authors have chosen to determine the performance of propulsion system is a combination of three codes. Together, Rocketdyne's FAST code, along with MCIA and L1IA from Lockheed Martin, provide tip-to-tail analysis of the propulsion flow path. MCIA will analyze the vehicle's inlet from its nose to the beginning of the isolator, FAST is an "engine deck" that will model the isolator and combustor, while L1IA will complete the analysis from the end of the combustor through the nozzle.

In addition to integrating these codes into AML, objects and methods will need to be developed to ensure that the flow conditions are consistent between MCIA and FAST as well as between FAST and L1IA. Finally, an AML procedure will be developed to create a table of propulsive forces and moments at various flight conditions (i.e., Mach Number, dynamic pressure and angle of attack). This table is needed for use with the trajectory simulation tool.

An alternate method was considered for calculating the off-design performance of the propulsion system. This method has two advantages. First, it is a single analysis code and second, it was already integrated into AML under a previous effort. The code that was considered is SRGULL [10] from NASA's Langley Research Center.

SRGULL uses the same approach for analyzing propulsion flow path as was described above. Namely, the flow path is divided into a forebody/inlet region, a combustor section and the nozzle. In SRGULL, the program is divided into subroutines to handle each section as opposed to the separate codes that were described above. As for the fidelity of the code, the calculations in the forebody/inlet and nozzle regions are 2-D or axisymmetric with 3-D corrections and the combustor flow is calculated using a 1-D method.

The inputs required by SRGULL are the flow path geometry, the flight conditions, fuel type and throttle setting. When the code was integrated with AML, a user interface

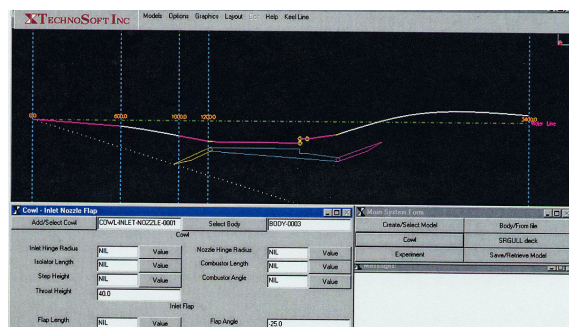was also developed. A sample of the user interface is shown in Figure 5.

Figure 5: Example of the User Interface for Keel Line Modeling for the SRGULL Analysis Code

Even though SRGULL was already integrated into AML, it was not used for this project. This decision was made because the team was not comfortable with the code, whereas the team has extensive experience with the other codes described above. The authors have found that this situation occurs often. Typically, engineers have invested a considerable amount of time and effort in learning and improving the software tools that they use regularly and they are not willing to change software just because it is already part of an integrated process. The authors believe that each organization's design process is unique and that any integrated design environment must be tailored to support the process that already exists within an organization.

Aerodynamic Analysis
The next discipline considered, aerodynamic analysis, does allow the authors to take advantage of codes that were previously integrated into AML. For this effort, the team was comfortable with using Missile DATCOM [11], PANAIR [12] and S/HABP to determine the conceptual-level aerodynamic characteristics of the vehicle. Missile DATCOM is a semi-empirical code that can determine the forces and moments on a cylindrical or nearly cylindrical body, with small protuberances and axisymmetric finsets, over a wide range of Mach numbers. Some error will occur in using Missile DATCOM to analyze hypersonic vehicle shapes, however the team will use PANAIR to correct the calculation. PANAIR is a general-purpose aerodynamic code that uses a linear panel method. PANAIR is capable of determining the pressures on bodies and surfaces of arbitrary shape at subsonic and supersonic speeds. The final aerodynamic code that will be used is S/HABP (Supersonic/Hypersonic Arbitrary Body Program). S/HABP uses first order methods to calculate the pressures on arbitrarily shaped bodies and lifting surfaces at supersonic and hypersonic speeds.

Along with integrating these codes into AML, a limited visualization capability has also been developed in AML. For example, Figure 6 shows a simple plot of aerodynamic data and Figure 7 illustrates a typical body pressure distribution.

The final step in developing the aerodynamic analysis objects for hypersonic vehicles is implementing a method for determining or describing which portions of the OML are associated with the propulsion flow path and which areas are outside the propulsion flow path. This is very important for hypersonic vehicles because of the vastly different

analyses that are used in each area. For instance, for a 2-D lifting body shape, the pressures, forces and moments on the entire lower surface of the vehicle are calculated using the propulsion analysis tools and the loads on the sides and upper surface of the vehicle are determined using regular aerodynamic analysis tools. Finally, the forces and moments on the external sidewalls and cowl of the engine need to be calculated by either the propulsion or aerodynamic analysis tools. Ultimately, what is needed is a procedure for determining a single set of resultant aeropropulsive forces and moments that vary as a function of flight condition and engine throttle setting.
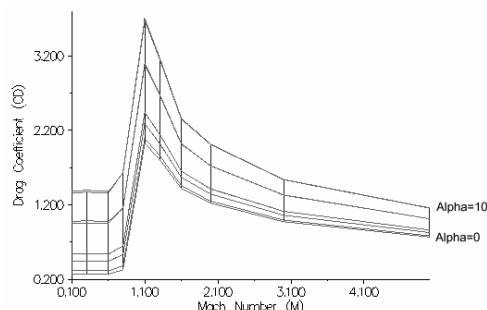

Figure 6: C_d for a Typical Wing-Body Vehicle as a Function of Mach Number as computed by Missile DATCOM
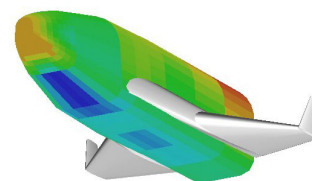
Figure 7: Pressure Distribution on a Fuselage as Predicted by PANAIR

Trajectory Simulation
The final discipline needed to "close" the design of a hypersonic vehicle is trajectory simulation. Trajectory simulation is used to determine and verify that the amount of fuel available in the vehicle is sufficient perform the desired mission (i.e., cruise a specified distance or accelerate to a desired staging point).

The trajectory simulation is used in an iterative process to determine the final, "closed", conceptual design. An iterative process is needed because the fuel fraction is a required input to the mass properties analysis. The vehicle closure process that will be used this hypersonic vehicle sizing application is:

1. Guess a required fuel fraction for the vehicle.
2. Specify a design for the propulsion flow path and OML of the hypersonic vehicle. (Note: both steps 1 and 2 are highly dependent on the design engineer's experience and personal preferences.)
3. Calculate the vehicle's mass properties based on the geometric model, the fuel fraction required and other mission parameters. (Remember that another iterative process is needed here to ensure that the MERs are consistent.)
4. Calculate the aeropropulsive forces on the vehicle for the flight conditions of interest.

11

5. Use a trajectory simulation code to calculate the fuel fraction that would be required for this vehicle to perform the desired mission.
6. Compare the results of step 5 with the guess from step 1 to determine if the fuel fraction required is consistent for this vehicle. If not, modify the vehicle's OML from step 2, adjust the guess of the fuel fraction required and repeat the process. (Note: depending on the type and magnitude of the changes to the OML, the aeropropulsive force calculations from step 4 may not need to be repeated.)

For this effort, two commonly used trajectory simulation and optimization codes, POST [13] and OTIS [14], will be considered. Both POST and OTIS have been integrated, to some level, in AML under previous efforts.

The methods that were used to integrate POST and OTIS exemplify the tradeoffs that are possible in all code integration problems. The main consideration that needs to be made when planning a code integration project is how much of the original functionality of the code will be available to the user of the integrated design application. Typically, as more functionality is made available in the integrated application, more discipline specific, or code specific, experience is required of the user. However, limiting the functionality of the integrated code usually also limits the range of designs that can be examined and limits the code reuse benefits of the object oriented programming paradigm.

Under previous efforts, POST was integrated using a "variant" approach, while the integration of OTIS was more comprehensive.

The variant approach required that a trajectory simulation engineer develop a complete simulation input file for the problem using existing procedures. Then, the engineer identified which parameters and data tables would change (and could change) when the baseline vehicle is redesigned. Finally, a method was developed to create a new input file for the simulation code by automatically changing the few parameters and tables that were previously identified.

A more comprehensive level of integration was developed for the OTIS 3.0 simulation code. The goal of this integration was to ensure that the complete functionality of the code was available in the integrated application. For OTIS, this also required the creation of a complex user interface. This is because the code has many settings available and these settings may be changed in each phase of the input. Note: phases can refer to changes in flight objective (e.g., minimum time climb or best altitude cruise) or changes in vehicle configuration (e.g., after launch vehicle staging or after weapons release).

Because of the complete level of integration of OTIS, it was expected that the main user of this portion of the integrated application would be an experienced OTIS user. For this reason, the developers chose to develop the user interface in pages that correspond to sections of the OTIS input file. A portion of the main user interface form is shown in Figure 8.

Furthermore, the AML programmers developed a basic online help interface for OTIS. The main feature of this help system is easy access to the definitions of the variables that are defined in OTIS. The developers have found that the

cryptic abbreviations used by OTIS are one of the main concerns for new OTIS users. A sample of this help interface is shown in Figure 9.

Figure 8: Main User Interface Form for OTIS in the Integrated Application

Figure 9: Help Screens for Defining OTIS Variables

The final significant part of the OTIS integration project was the development of a simple trajectory plotting object. This plotting object was developed mainly for use by the experienced OTIS user while debugging their setup of the trajectory simulation. A sample plot that was created using this capability is shown in Figure 10.
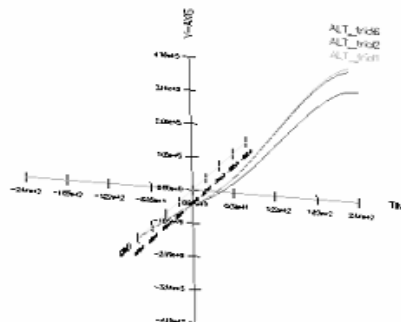
Figure 10: AML Trajectory Plotting Example

Based on their experience with these two integration efforts, the authors hope that a "happy medium" between the two approaches can be found. The POST integration is too limited and the OTIS integration exposes functions of the program that are very rarely, if ever, used for the simulation of hypersonic, airbreathing or rocket-powered launch or cruise vehicles. The team hopes to develop a user interface that is both robust and relatively easy to use by an engineer who is new to the trajectory simulation discipline.

INITIAL APPLICATION

The authors are currently working with two different hypersonic, airbreathing vehicle configurations. One configuration is a 2-D lifting body class vehicle, similar to NASA's X-43 (Hyper-X) configuration, shown in Figure 11. The second configuration is an axisymmetric, rocket-based combined cycle (RBCC) powered, SSTO vehicle, similar to the GTX configuration [15], shown in Figure 12.

Figure 11: Hyper-X Configuration

Figure 12: GTX Configuration

The geometric modeling efforts have been split between the two configurations. As mentioned above, many distinct OML modeling objects were developed for each configuration because they are such significant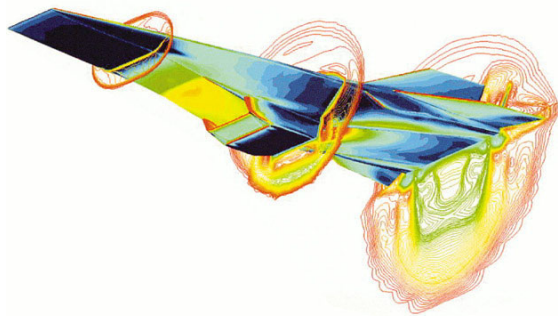ly different configurations. Also, the MERs that are integrated with the geometric objects will have to be tailored for each configuration.

For instance, the fuel tank models for each configuration will be significantly different. For the 2-D vehicle, the tanks will be conformal. That results in a more complex geometric model, even at the conceptual-level, and a MER which will estimate that the conformal tank is heavier than a cylindrical one for the same surface area, volume and/or pressure. However, for the axisymmetric vehicle, the fuel tanks will be mostly conical. These tanks can be modeled with simpler geometric objects and require MERs that predict a tank that weighs less than the conformal tank for similar design conditions.

For the other disciplines (i.e., propulsion flow path analysis, aerodynamic analysis and trajectory simulation), most of the author's effort to date has concentrated on the 2-D lifting body configuration. This decision was based on the author's previous experience in modeling these configurations as well as the availability of analysis codes and experimental results for configurations of this class.

CONCLUSIONS

This effort has resulted in an integrated design modeling application for the conceptual-level design and analysis of hypersonic airbreathing vehicle configurations. Additionally, the authors believe that this application can form the basis of a more complex design environment that is capable of refining the design of hypersonic vehicles to the preliminary level.

To be called a preliminary-level design and analysis application, additional disciplines are needed. Specifically, two disciplines, aerothermal analysis and finite element structural analysis, are needed to provide physics-based mass properties information. Aerothermal analysis will provide the temperatures and heat fluxes to which the vehicle will be exposed during its mission. This information can then be used to size the thermal protection system of the vehicle, which makes up a significant portion of the total vehicle weight. Ongoing efforts [5] could be expanded to integrate aerothermal analysis tools into AML. Finite element methods (FEM) can be used to size the main structural components (including the tanks) based on the loads they will see during a mission. The weights of these size components can then be estimated more accurately. The integration of FEM into AML is being explored under a separate effort [16].

Another discipline that is encountered during preliminary design is flight control. The major tasks of this discipline are the development of flight control laws, sizing of the elements of the flight control system, and the development of a six degree-of-freedom (6DOF) model of the vehicle. Codes like MATLAB or MATRIXx are commonly used for these tasks and because they are modern software products, information can easily be linked between these programs an AML.

Finally, higher fidelity aerodynamic and propulsion analysis methods will be needed during the preliminary design process to generate the pressures, forces and moments to feed into the FEM and flight control disciplines.

REFERENCES
1. Tirpak, John A., "Mission to Mach 5", *Air Force Magazine: Journal of the Air Force Association*, Vol. 82, No. 1, January 1999.
2. Engelund, W. C., "Hyper-X Aerodynamics: The X-43A Airframe-Integrated Scramjet Propulsion Flight-Test Experiments", Journal of Spacecraft and Rockets, v. 38, no. 6, Nov-Dec 2001, pp 801-802.
3. Kowal, D., Zarda, P. R. and Baum, F. "Web-based Design and its Impact on the Engineer", presented at the 3rd International Conference on the Intelligent Processing and Manufacturing of Materials, Richmond, BC, CANADA, July 29-August 3, 2001.
4. Zweber, J. V., Stevenson, M. D., Bhungalia, A. A., Catron, S. J., Hartong, A. R. and Grandhi, R. V., "A Web-based Collaborative Application for Aerospace Vehicle Design and Analysis ", presented at the 3rd International Conference on the Intelligent Processing and Manufacturing of Materials, Richmond, BC, CANADA, July 29-August 3, 2001.

5. Bhungalia, A. A., Zweber, J. V. and Stevenson, M. D., "Thermal Protection System Analysis in an Integrated Design Environment for Launch Vehicles", AIAA paper 2002-0595, presented at the 40th AIAA Aerospace Sciences Meeting & Exhibit, Reno, NV, January 14-17, 2002.

6. *Adaptive Modeling Language Reference Manual,* Version 3.1.3, TechnoSoft Inc., Cincinnati, OH, 1999.

7. The Adaptive Modeling Language. A Technical Perspective, TechnoSoft, Inc., Cincinnati, OH, http://www.technosoft.com/docs/brochure99.pdf

8. TechnoSoft, Inc. web site, http://www.technosoft.com/gallery/11.htm

9. Anderson, John D., Jr., *Modern Compressible Flow with Historical Perspective, 2nd Ed.,* McGraw-Hill, New York, 1990.

10. Pinckney, S. Z, Ferlemann, S. M., Mills, G. and Takashima, N., "Program Manual for SRGULL, Version 1.0: Second Generation Engineering Model for the Prediction of Airframe-Integrated Subsonic / Supersonic Combustion Ramjet Cycle Performance", NASA Langley Research Center Report HX-829, July 2000.

11. Blake, W., "Missile DATCOM Users Manual" AFRL-VA-WP-TR-1998-3009, February 1998.

12. Public Domain Aeronautical Software web site, http://www.pdas.com/panair.htm

13. Powell, R. W., Striepe, S. A., Desani, P. N., Braun, R. D., Brauer, G. L., Cornick, D. E., Olson, D. W., Peterson, F. M. and Stevenson, R., "Program To Optimize Simulation Trajectories (POST): Volume II, Version 5.2, Utilization Manual", NASA Langley Research Center, Hampton, VA, October 1997.

14. Paris, S. W. and Hargraves, C. R., *OTIS 3.0 Manual*, Boeing Space and Defense Group, Seattle, WA, 1996.

15. Trefny, C., "An Air-Breathing Launch Vehicle Concept for Single-Stage-to-Orbit", AIAA paper 99-2730, presented at the 35th AIAA / ASME / SAE / ASEE Joint Propulsion Conference and Exhibit, Los Angeles, CA, June 20–23, 1999.

16. Blair, M. and Canfield, R. A., "A Joined-Wing Structural Weight Modeling Study", AIAA paper 2002-1337, presented at the 43rd AIAA / ASME / ASCE/ AHS/ ASC Structures, Structural Dynamics & Materials Conference, Denver, CO, April 22-25, 2002.

APPENDIX B

Collaborative Design Environment for Space Launch Vehicle Design and Optimization

Mark D. Stevenson
2856 G Street, B79
Wright Patterson AFB, OH 45433, USA

Alicia R. Hartong
1970 Monahan Way, B11A R021
Wright Patterson AFB, OH 45433, USA

Jeffrey V. Zweber, Amarshi A. Bhungalia
2210 8th St., B146 R301
Wright Patterson AFB, OH 45433, USA

Ramana V. Grandhi
College of Engineering and Computer Science
Dept. of Mechanical and Materials Engineering
3640 Colonel Glenn Hwy.
Dayton, OH 45435, USA

The design of a hypersonic cruise or space launch vehicle is a large undertaking requiring the team effort of many engineers having expertise in the areas of aerodynamics, propulsion, structures, flight control, performance and mass properties. As the design takes shape, specialists are requested to design such things as the crew station, landing gear, interior layout, weapons location, and equipment installation. The completed vehicle design is a compromise of the best effort of many talented engineers. It should be clear that the design process is a complex integration effort requiring the pulling together and blending of many engineering disciplines.
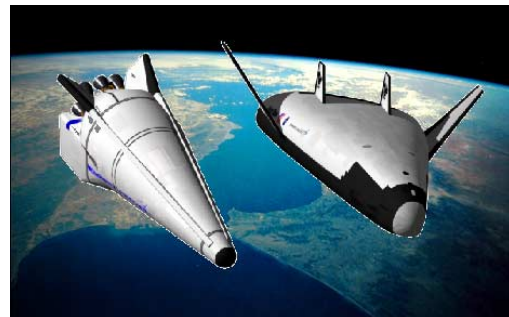

Figure 1: Trans Atmospheric Vehicles

Like all organizations, the Air Force is interested in conducting its vehicle studies as quickly as possible with as high fidelity an analysis as is feasible and with a proven, repeatable design and analysis process. This research is in support of an approach formulated by engineers at Wright Patterson Air Force Base who seek to integrate design and analysis tools into a collaborative, network-distributed design environment. The benefits of using an integrated design environment to reduce the time and potential errors associated with the transfer of data between design and analysis codes are well documented.[1,2] This research presents the integration of an initial set of space access and future strike vehicle analysis codes designed to improve the entire conceptual-level design process and documents the advantages of using the tools in a collaborative, network-distributed environment. This paper focuses on the design environment including geometry modeling, object design, discipline interactions, and design tools built for this effort including weight, propulsion, and trajectory analysis.

REUSABLE LAUNCH SYSTEMS

Both the US Air Force and NASA have indicated that next-generation reusable launch systems are needed within the next few years. Indications of the area's high importance can be seen through funding of projects like the X-33 and Hyper-X experimental launch concepts. At this stage of the study program, similar technologies and vehicle concepts are being examined to meet both the space access and future strike requirements. Consequently, rapid assessment of a Reusable Military Launch Systems is becoming increasingly important. There is a large array of RMLS options and promising configurations must be selected quickly for higher fidelity analysis. Furthermore all proposals must be analyzed uniformly using the same base-lined analysis tools and objective constraints.

The initial user of the web-based, collaborative application for launch vehicle design is the Air Force's Reusable Military Launch System (RMLS) analysis team. The core of this team has members from five different organizations that are located in four different buildings at two different bases. The team focuses on capability assessment for both future strike and space access vehicles. The goal is to impartially judge RMLS designs without restrictions on mode of operations. These modes include Horizontal Takeoff-Horizontal Landing, Vertical Takeoff-Horizontal Landing, and Vertical Takeoff-Vertical Landing. The team will also judge vehicle configuration options such as air breathing vs. rocket based propulsion and Two Stage to Orbit vs. Single Stage to Orbit.[3,4] A better understanding of the RMLS design space will dictate future areas of research and development needed to increase the viability of promising configurations.
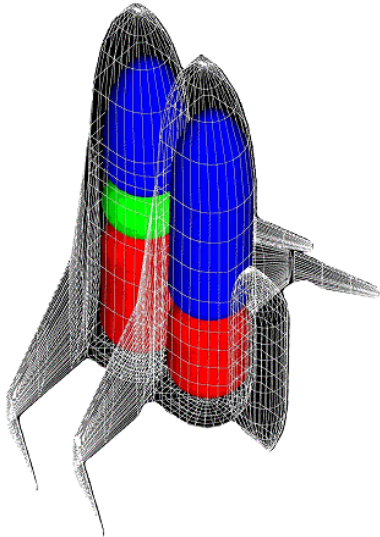
Because of the distributed nature of the team, the initial method used to conduct analyses was to pass files manually via email and a web site bulletin board. This system is sufficient for the relatively small team. However it has obvious areas of inefficiency in communication. Moreover there exists the possibility of errors being introduced due to data translation and loss of configuration control. An improved design and analysis process was needed to prevent these potential errors and to allow the RMLS team to efficiently interact with technology experts from other government agencies, industry and academia.

The current vehicle under study is an in-house design of a fully reusable TSTO. The design (Figure 2) is a departure from the Bimese concept of identical booster and orbiter stages arranged "piggy-back" with an external payload mounted on the orbiter. The in-house concept consists of a booster and orbiter with a similar aeroshape but internal differences. Future vehicles under consideration include a stacked (serial burn) version of the Bimese concept and an air-breathing design.

Figure 2: Reusable Military Launch System

LAUNCH VEHICLE DESIGN ENVIRONMENT

The conceptual-level design process for hypersonic and space access vehicles is dominated by geometric modeling, aerodynamics, aerothermodynamics, engine performance (air-breathing or rocket) analysis, trajectory simulation, mass properties analysis and cost modeling. This process is shown in Figure 3 as a design structure matrix. A design structure matrix is used to graphically display the interactions between the various disciplines in a design process.[5] Each block in Figure 3 represents a different analysis code. These codes could be further associated with different engineers, different computers or even computer platforms.

The process starts with a designer formulating a possible outer moldline of the vehicle. This can be done anywhere from a "back of the envelope" sketch to lofted model in a CAD package. From the geometry, the aerodynamic, propulsion and mass properties analysts generate their models. Using the results of these analyses, a set of trajectories or missions is simulated to determine if the concept vehicle will meet its requirements. Then, from the results of the trajectory simulation, an aerothermoelastic analysis can be performed to determine the heating loads on the vehicle and subsequently
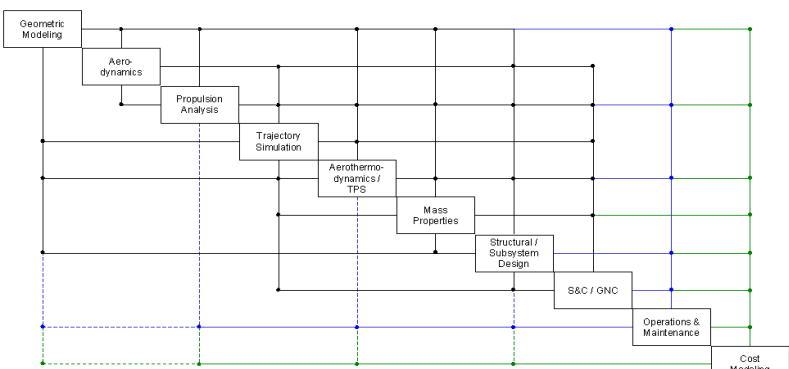

Figure 3: Design Structure Matrix

size the thermal protection system (TPS) and internal structure. The TPS size affects the geometric model by reducing the available internal volume for fuel and payload. Conventionally, this design cycle is repeated, varying geometric parameters, until the size and shape of the vehicle converges to the smallest vehicle that will perform a given set of missions.

One of the well-known shortcomings of this process is that it takes far too long for the design to progress to a point where operations, logistics and life cycle cost analyses are performed.[6] The long-term goal of this research is to demonstrate that, by integrating all the launch vehicle design disciplines into a collaborative design environment, the design data can be fed to the cost and operations disciplines sooner. In addition, by capturing the design process, the results of these analyses can be fed back to the conventional, conceptual design disciplines. By removing the manual data transfer steps, more design iterations can be accomplished in the same amount of engineering time.

The current status of the project is that some tools for the geometric modeling, aerodynamic analysis, propulsion analysis, trajectory simulation and mass properties disciplines have been integrated. Structural weight and aerodynamic results are calculated directly from an initial geometry specification, with the total weight being determined by adding the thermal protection system (TPS), propulsion system, payload and propellant weights. These three disciplines (mass properties, aerodynamics, and propulsion) provide the data that is needed by the trajectory simulation code to determine if the vehicle meets mission requirements (altitude and inclination angle). Finally, an iterative process is employed to vary the vehicle's fuel fraction ratio, and consequently the overall size of the vehicle, to correctly size the vehicle and propulsion system for a specified mission, or to determine that a specific vehicle class will not work for the required payload and orbit.

The Adaptive Modeling Language

For this effort, the Adaptive Modeling Language (AML) developed by Technosoft Inc., was selected as the design-modeling environment. AML is a framework for Knowledge Based Engineering that provides the ability to capture the launch vehicle design and analysis process and manage the data transfer between codes. It is by using the logical functions and calculations in AML, to capture process knowledge and design intent, that the significant timesavings in performing repeated analyses on a family of designs can be achieved. Previous research has demonstrated this knowledge capture in AML models for structural analysis and cost modeling.[7] The current version of AML has a wide variety of features that make it well suited for developing applications to capture a complex, multidisciplinary design process.[8] Perhaps the most important and least unique feature of AML is that it is an object-oriented language. A consensus has been reached in the software industry that object-oriented programming is vital for ease of software development and reuse. By applying the object-oriented paradigm to engineering models, AML allows the reuse of these models (objects). A well-formulated model will represent the component in general, parametric terms. For instance, the 747 and F-16 have very different wing shapes and sizes, but both wings can be represented by the same set of parameters (i.e., aspect ratio, root chord, taper ratio, airfoil section, twist distribution, dihedral and sweep angle). By developing a wing model this way, the same object can be used to model both aircraft.

A second important feature of AML (inherited from its Allegro Common LISP infrastructure) is its hierarchical, dynamic part-model. This feature is what makes AML "adaptive"; that is, models do not need to be recompiled to change the object hierarchy. The subobjects can be added interactively or specified in the definition of the class that was chosen for the top-level model (or in the definition of classes that were added as subobjects). This capability also allows objects and their properties to be added, edited or deleted independent of the order of instantiation. Included in the hierarchical structure is the Unified Part Model paradigm. This paradigm allows the model of a given component, the wing for example, to contain all the data about the wing that will be required by the various analyses. For instance, the wing model could contain a panel aerodynamic model, which would be used for low-speed calculations; a finite-element model of the wing box, which would be used for structural analysis; a second aerodynamic model that includes control surfaces, which would be used for stability analysis; and a thermal model, which would be used to size the wing's thermal protection system.

This modeling paradigm allows the model to grow as the design matures and new parts are created or new analyses are required. By keeping all the design information in a unified model, the "bookkeeping" of the data can be simplified. AML has built-in dependency tracking and demand-driven calculation capabilities to assist in this data management. *Dependency tracking* is important for ensuring that each discipline of the model is working with the current set of design parameters. With a manual design or configuration management system, it is easy for the various discipline specific models to get out of sync. AML automatically builds and maintains a list of dependencies. This list is updated as the objects are instantiated or deleted; or as the formulas associated with a property are changed. AML's dependency tracking also works in the other direction. That is, AML maintains a list of the properties that are affected by each property. The *demand-driven calculation* feature is complimentary to the dependency tracking capability. While the dependency tracking capability notifies all the parts of the model that have been affected by a change in a design parameter, the demand-driven calculation feature ensures that the only calculations to be performed are those needed for the current item of interest.

The last important feature of AML that will be covered here is the Graphical User Interface (GUI) included in AML. AML provides the powerful ability to automatically generate GUI's from an objects coding, eliminating the need for a designer to specifically develop a GUI structure. When writing an object, a developer specifies which parameters should be included in the user interface with only minor modifications in the parameter classes used. AML builds the GUI's during runtime. This eliminates a substantial volume of required coding from an object and reduces object development time. Additionally, when a design is being run over a network, form information does not need to be transmitted because the forms are part of an objects code, and generated on each individual client machine.

Collaborative design requires a distributed set of users running various analyses, possibly hundreds of miles apart. Bringing together a set of analysis tools under a unified environment is only a first step in achieving a fully integrated collaborative environment. Because of the large number of disciplines, an application would be extremely inefficient if limited to a single computer. A new feature being added to AML, under an Air Force Dual Use Science and Technology program termed Web-Based Design Environment (WDE) allows users to be distributed over a wide area network.[9] Users log into a server that contains the vehicle model via a standard WDE browser. Vehicle geometry modification and analysis can then be performed real-time over the network. The browser is platform independent and can access analysis codes on any computer across the entire network. By allowing pieces of the model to reside on different machines, each computer can specialize in a single discipline. This reduces the number of analysis codes needed and can save money by reducing the required software licenses and simplifying the system administration. The tool only passes parameter values of the model, which means that a high-fidelity graphical model requires a very small bandwidth.[10] Security and design configuration control issues are addressed within the modeling environment.

DESIGN DISCIPLINES

Design begins with geometry or an array of geometric considerations. Preferably the geometry object should be fully parametric, allowing the user to change shape into any other shape under consideration. However, the author has found that a single geometric object capable of all design configurations is not desired. The large number of parameters (e.g. number of fuselage cross sections, cross section geometries, cross section positions, wing type, and wing location) for a design forces a user interface to be complicated and unwieldy. There are a number of design possibilities, creating a huge array of very different vehicle designs. A series of parametric models tailored for each vehicle class (e.g. 2-D air-breathing and rocket based lifting body) is being created as part of the ongoing RMLS research. Using only a few parameters these models can be rapidly changed to any vehicle design within a given class. When a desired vehicle falls outside a class, other classes may have to be used or built to accommodate the new vehicle. A new parametric model takes about two weeks to create. The Bimese parametric vehicle class developed in conjunction the RMLS team at WPAFB for the current research with the help of TSI is shown in Figures 2, 8, 10, and 12. The model is able to be non-photographically stretched for vehicle sizing and includes links to previously mentioned analysis tools. The geometry objects developed for this class will also be used for future horizontally stacked configurations.

Rocket Engine Design Code

A focus for any launch vehicle design is centered on the propulsion system. Engine selection impacts several crucial design decisions including fuel type and associated fuel tank selection. Fuel fractions for SA/FS vehicles can be as high as 90% so fuel selection becomes a very important issue. Hydrogen fuels have a higher ISP (a measure of the overall energy contained in a rocket) but are less dense and require cryogenic tanks. Hydrocarbon fuels require smaller fuel pumps that reduce the size and weight of the rocket engine. Trade-offs for both fuel types require detailed analysis to determine the best fuel type for a specific rocket configuration. The importance of the propulsion system requires a rapid rocket design and performance analysis tool for vehicle modeling. The Parametric Rocket Model [11], developed at Wright Patterson AFB, uses a historical data trend approach primarily taken from "Design of Liquid Propellant Rocket Engines".[12]

The author chose to incorporate the simple Parametric Rocket Model into the AML environment because of its simplicity and fast run times. Additionally it provides information required for other analysis codes with a minimal input. The basic procedure for designing the propulsion system using the Parametric Rocket Model is as follows:

1. Select a specific rocket type and fuel, the characteristic velocity and combustor pressure, ratio of specific heat, propellant flow per unit throat area and characteristic combustor length based on previous engine designs are set. This represents the performance level of the engine class.
2. Given the specified nozzle expansion ratio(s) and nozzle type (1 position, 2 position, or dual bell) a nozzle thrust coefficient is calculated as a function of altitude.
3. Thrust at a reference throat area is then calculated as a function of altitude.
4. Given the specified thrust at a specified altitude, a scale factor is calculated that is applied to the reference thrust function to obtain the specified thrust.
5. The scale factor is also applied to the reference throat area to properly scale the geometry.

An example of how engine performance parameters are calculated are the equations used for exit nozzle pressure. The theoretical nozzle expansion ratio is calculation using Equation 1, where γ is the specific heat for a given fuel type, p_e is an assumed exit pressure and p_{cns} is the chamber (nozzle stagnation) pressure for a given fuel. This doesn't include boundary layer displacement correction, heat transfer or shifting γ effects, but it is close to actual values. The exit pressure is then calculated using Equation 2, where ε is the desired expansion ratio. Equations 1 and 2 are related to each other so a Newton-Rhapson iteration method is used for convergence. The iteration is performed on $1/\varepsilon$ because it is more linear than ε.

$$\varepsilon_{th}(p_e, p_{cns}, \gamma) := \frac{\left(\frac{2}{\gamma+1}\right)^{\frac{1}{\gamma-1}} \left(\frac{p_{cns}}{p_e}\right)^{\frac{1}{\gamma}}}{\sqrt{\frac{\gamma+1}{\gamma-1}\left[1 - \left(\frac{p_e}{p_{cns}}\right)^{\frac{\gamma-1}{\gamma}}\right]}}$$

Equation 1: Theoretical Expansion Ratio

$$p_e(\varepsilon, p_{cns}, \gamma) := root\left(\frac{1}{\varepsilon} - \frac{1}{\varepsilon_{th}(p_e, p_{cns}, \gamma)}, p_e\right)$$

Equation 2: Exit Nozzle Pressure

A plot of engine performance (given by thrust coefficient) for several nozzle types vs. altitude is plotted in Figure 4. The plots are characteristic of typical engine performance curves. The discontinuity in the graph for the Space Shuttle Main Engine (SSME) 150 2p (two position) nozzle is a result of moving a secondary nozzle into position at a specific altitude. The method has been correlated with advanced LH-LOX and RP-1-LOX engines. This simple model calculates thrust and Isp as a function of altitude, weight and geometry of the engine based on thrust at a specified altitude, rocket type, nozzle type (1-position, 2-position, or dual bell nozzle), and expansion ratio.
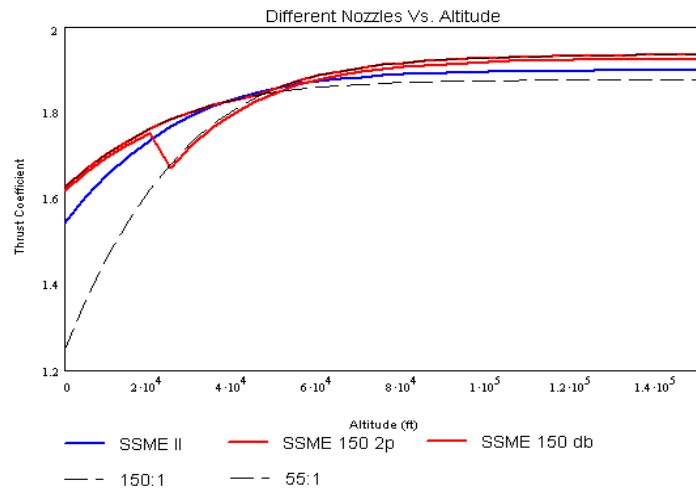
Figure 4: Engine Performance

19

Simply changing one parameter such as fuel type can radically change the engine geometry; Isp, thrust, and weight are also affected.

Weight Analysis

Weight analysis is a crucial aspect of RMLS design. Too much vehicle dry mass and fuel fractions will never be high enough to get a payload to orbit. Additionally, weight and aerodynamic parameters such as G-loading, calculated from trajectory and aerodynamic analysis, drive structural sizing.

Figure 5: Engine Geometry

Weight analysis equations tend to be strictly proprietary information tightly held by their parent organizations. Consequently no commercial off the shelf weight estimation software was found that suited the RMLS design group. Weight estimation software should be simple, use available information associated with the model and track the physics well. To build weight estimation software, engineers at WPAFB compiled historical trends in launch vehicle design as a way to predict future vehicle designs. Data was compiled from Air Force Flight Dynamics Lab reports produced in the 1970's and 1980's including the Space Shuttle, NASP and BETA vehicle.[13,14,15,16,17,18]
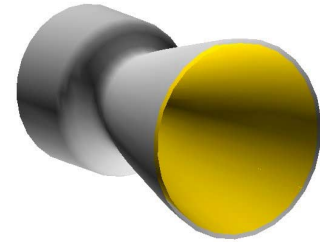
Weight Estimation

The weight analysis software was written directly into the AML environment, and highly coupled with the geometry. Component weights are generally calculated from a vehicle's gross weight, empty weight or geometry (also a function of gross weight). For example, Figure 6 plots the relationship of tail area with tail weight. The relationship is almost linear for a variety of vehicles. The vehicles used for this comparison are the XB-70 Valkyrie (Mach 3 USAF experimental bomber 1964-1969), STS (Space Shuttle), F-106A Delta Dart (supersonic USAF operational interceptor 1956-1960), B-58A Hustler (Supersonic USAF Operational Bomber 1960-1970), F-4 MK-2 Phantom (Supersonic USAF Operational Fighter 1965-1992). The actual relationship used for the weights equation (Equation 3) was chosen to match the Space Shuttle data. Because this weights equation is based on geometry, which is based on gross vehicle weight, iteration of the overall vehicle is required to close the vehicle size and weight calculations. Component weights can be known values, such as an electrical system power supply that has been set at 770 lbs based on Space Shuttle requirements. Setting a weight to a deterministic value is equivalent to pulling a known power supply off the shelf and adding it to the model. Component weights can also be a simple equation or expanded into geometrical objects depicting sub-system placement. Components can be further broken down into constituent parts for increased model fidelity. The basic procedure for calculating an overall vehicle weight using the system is as follows:

1. Guess the empty weight fraction
2. Calculate component weights based on initial guess
3. Sum the weights and determine difference in empty weight calculations
4. Size the vehicle and adjust the empty weight guess
5. Iterate until vehicle closure

Figure 6: Historical Weight Trends

$$Weight = 5 * Svt^{1.09} * 0.89$$

Equation 3: Tail Weight Estimation

Once the weight estimation and sizing procedure are complete, the model is run through trajectory analysis that is used to update the propellant fraction. The weight estimation procedure is then rerun iteratively with trajectory analysis until overall vehicle closure. This research has discovered that only two to three iterations are required to close the vehicle.
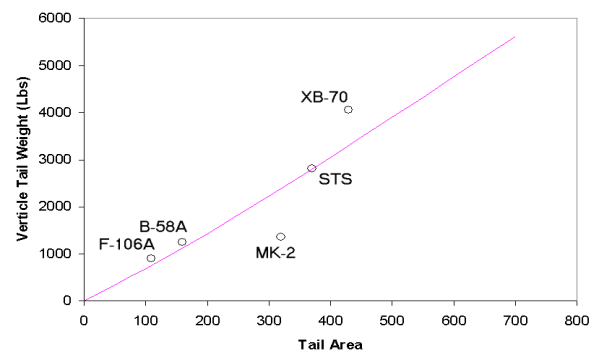
20

Thermal Protection System Weight Estimation

As part of the weight estimation process, Thermal Protection System (TPS) weight must be addressed. The model uses a simple water-line scheme to estimate what TPS types are needed in what areas. With the knowledge that the vehicle will re-enter the atmosphere at a specified angle (i.e., 30°) surfaces that are in direct line with or at specified increments from the stagnation points are calculated. With the knowledge that surfaces nearest the stagnation points will require the highest temperature TPS, a lookup table of TPS materials (based on Shuttle tiling) is used to place tiles in specific regions. The density and thickness of the tiles is then used to calculate the entire weight of the TPS.

A more physics based approach for predicting TPS design is currently under development through an Air Force Small Business through Innovative Research (SBIR) program. Using high fidelity aerodynamics and heating analysis calculated directly from the geometry of the rocket design and its trajectory profile, the transient heating profile will be coupled with a TPS optimization routine. The thickness of the TPS is varied so that a maximum temperature on the inner rocket structure is not exceeded throughout the trajectory. The heating loads are then applied to the Finite Element model of the inner vehicle structure for sizing. The updated vehicle weight can then be sent back to trajectory analysis in an iterative cycle until vehicle closure. This will not only yield higher fidelity TPS design, but will also include the transient effects in the heating profile. Currently most TPS designs are sized to the point in the trajectory that yields the highest temperature; this overestimates the required TPS and consequently increases the weight of the vehicle.

Weight Estimation Error

There are errors in the weight estimation routines. The vehicles currently being analyzed are roughly five percent under weight, based on historical vehicle designs. The additional weight is accounted for using a weight correction factor, but additional work needs to be done to model vehicle weight better. Five percent under estimation is a considerable factor considering that the RMLS type vehicles may have growth factors of 30 or more. The higher fidelity methods previously discussed could be used to refine the weight synthesis equations for future increased model accuracy. Additionally, members of the RMLS team have modeled aerospace partners design to compare and verify the analysis. Results have shown a good comparison between the reports. Additionally, the comparison found that a few parameters in the model weight were not feeding back into the weight estimation scheme. Future studies will allow higher confidence in the model. Despite these errors, the current weight estimation routines are a good start to capturing vehicle weight, and accurate enough for the level of fidelity desired.

The weight estimation software developed is only for preliminary design. The author knows there are dangers to base weight estimation on historical data trends. This is especially true when the only data point that has been built and flown is the Space Shuttle that was designed for an immense 80,000-pound payload and is an operational nightmare. The Space Shuttle is not a good data point, but it is widely used because it is the only point available. Future work may incorporate higher fidelity tools, which will benefit from the vehicle-sizing starting point this tool gives. Additionally, the physics in the higher fidelity tools could then be captured to increase the accuracy of the preliminary weights equations developed.

Trajectory Analysis

As previously discussed, trajectory analysis is an integral part of RMLS design. The two main trajectory analysis codes used within the industry are OTIS (Optimal Trajectories by Implicit Simulation) and POST (Program to Optimize Simulated Trajectories). Within the aerospace industry, the author has found that new codes are not easily accepted, and various organizations (even within the RMLS team) live and die by their selected code with no thought of change. Consequently both codes have been integrated into the environment using program wrappers. However, the author favors OTIS because its solutions have yielded better results, coupled with the ability to use more parameters and constraints.

OTIS 3.0 is a FORTRAN77 program for simulating and optimizing the point mass trajectories of a wide variety of aerospace vehicles. The version used at Wright Patterson AFB was recently compiled for

use on NT-based windows machines. The most advanced simulation uses implicit integration to generate an open-loop optimal control of a prescribed vehicle.[9] OTIS was designed more like a math program; give it a series of parameters (possibly hundreds), constraints and objectives, and it will solve for the optimal mathematical solution. POST is also a FORTRAN 77 program for a generalized point mass with discrete parameter targeting and optimization.[19] POST behaves more like a traditional trajectory program; give it a series of parameters (under 100), constraints, objectives and a trajectory that the user thinks is good, and it will yield a slightly better trajectory. POST has the benefit of being fast but is hampered by only running in DOS mode on PC-based machines. The POST integration uses a LISP function to traverse the tree to collect data, reformatting it into an input text file required by POST. The text file must then be sent to the trajectory analyst to run POST and send back the updated fuel fractions.

The OTIS 3.0 integration currently only contains the specific information relevant to a particular RMLS class of vehicles. The properties allowed in a specific model are tailored such that a limited set of trajectories can be performed, reducing the incredibly large array of options OTIS 3.0 allows. This reduces the strain on a user of the tool by reducing the number of properties understood and checked during program execution. The few properties relevant to a given design are easily accessible within the design environment. However, the initial trajectory file relevant to a particular vehicle class is required to be generated by an expert user of OTIS 3.0. Trajectory analysis is extremely complicated, and eliminating the expert entirely from the design process would be impossible. Vehicle configuration properties such and aerodynamics, weight, engine propulsion are automatically formatted into the OTIS format, and the updated fuel fractions are automatically read back into the collaborative environment for automated iterative design.

Aerodynamic Analysis

The aerodynamic analysis application used for the Bimese trade studies was Missile DATCOM. DATCOM requires geometry to be broken down into simple known components and then uses empirical equations of the known shapes to calculate the desired aerodynamic coefficients for the overall vehicle. Consequently only simple geometry can be modeled using DATCOM. Multiple bodies also pose a problem becuase they are not handled in DATCOM. The author chose to model the orbiter and the booster separately, with the payload treated as a protuberance on the orbiter. The drag of the orbiter and booster is then summed. The calculated drag using this method ignores whatever interference exists between the wings, which adds to the drag calculation. But this decreases at higher Mach numbers and is not unreasonable to ignore. To check this assumption, a CFD model is being run for the concept. However, the results are not expected soon because of the huge computational expense of CFD analysis.

The analysis shown in Figure 7 demonstrates the expected drag rise going through Mach 1.0; the large increase is a result of the NACA 0012 airfoil chosen for the Bimese concept. The analysis is consistent with predictions on how the model should behave, allowing confidence in the aerodynamic analysis.

Figure 7: Coefficient of Drag Calculation Using DATCOM

For a sanity check a more detailed analysis could be performed using PANAIR, an example of an analysis of the Bimese concept is shown in Figure 8. PANAIR is a linear aerodynamic solver using the technique of boundary elements (commonly referred to as aerodynamic paneling). Surface geometry is "body-fitted" with an array of quadrilateral panels. Continuous surface singularities (both sources and doublets) are distributed using a number of schemes to meet a number of needs.[20] The program is accurate but requires longer run times, and is not applicable to the quick trade studies desired for the RMLS team. Additionally, PANAIR requires a continuous structured body grid that is difficult to model around protuberances such as wings in an automated fashion. The RMLS Bimese model was not constructed with PANAIR in mind so the wings could not be included in the PANAIR analysis. Consequently, only the body is analyzed in Figure 8 and the analysis cannot be compared with DATCOM. Both aerodynamic analysis objects contain information on how to break the smooth geometry of the model into their respective application inputs. No additional user work is required to run the analysis within the limits of the Bimese concept.
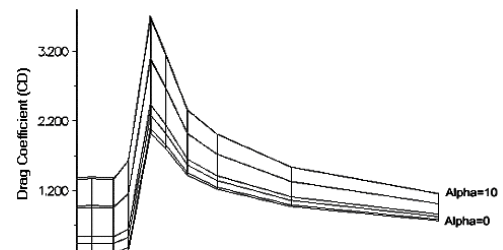
Future work will include adding ZONAIR to the list of aerodynamic analysis tools included in the environment. ZONAIR is a panel method aerodynamic solver based on ASTROS for very accurate results with limited computational time. A benefit of ZONAIR is that meshing can be unstructured, allowing input grids to be automatically generated. Additionally, multiple wingsets will be able to be modeled.
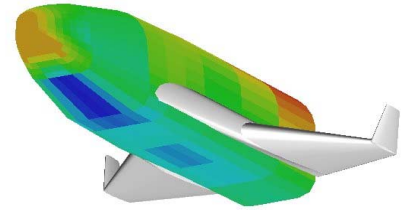

Figure 8: PANAIR Pressure Distribution on RMLS Bimese Vehicle

EXCERSIZING THE MODEL

The majority of the research has focused on the design environment development, and, as a result, the majority of this research is concerned with the environment and associated analysis modules. However the environment is only a foundation for rapid trade studies. Using this tool, the author performed various trade sweeps of the Bimese concept. The vehicle sizing routine incorporating weights and propulsion takes 60-180 seconds (sizing both the orbiter and booster) running on a Pentium III processor with 500 Mbytes RAM. The time difference depends on how many sizing iterations are required (which depends on how close original model sizing guess is to final design). Initial trajectory analysis using POST must be run offline because of the limitations of POST (which must be run in DOS mode), so trajectory and its required aerodynamics analysis are not run in an automated fashion. The input file required for the automated OTIS 3.0 analysis has recently been built and will be used to run through the series of designs the RMLS team wants to look at. With the limited number of analysis tools incorporated (weights, aerodynamics, propulsion, and trajectory) only a few trade study parameters can be considered. But the parameters considered are critical to design formulation. Trade study parameters able to be handled by the model include payload sizing, thrust to weight ratio, fuel selection for both booster and orbiter, wing thickness, rocket nozzle type, and staging velocity. The author will limit discussion to the first three trade studies mentioned.

Payload Sizing

Payload size comes from mission requirements. The payload size trade study performed shows what a top-level mission change will cost in terms of vehicle weight for a given design. In this study, the author changed the payload weight from 4k to 64k pounds, sized both the orbiter and booster vehicles and plotted the
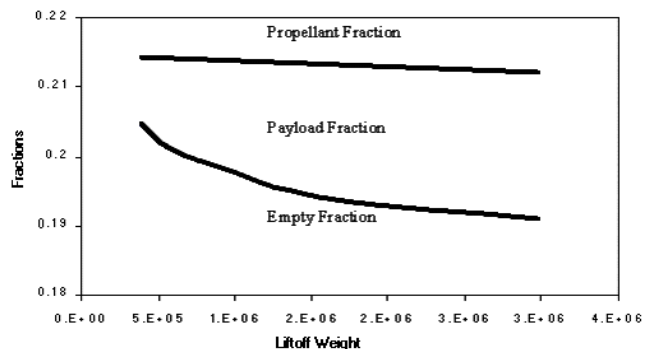
Figure 9: Vehicle Fractions Based on Fuel

resulting overall vehicle fractions in Figure 9. In this plot, the propellant fraction (Pf) plotted is 1-Pf (i.e., about 76% of the vehicle weight). If the ordinate was scaled to one, the entire area between the Pf curve and one would represent the propellant fraction. Payload fraction is the difference between propellant fraction and empty weight. The empty weight plotted is the true empty weight of the vehicle. The increase in the empty weight fraction at the lower vehicle gross weight is largely a result of nearly constant TPS weight, resulting in greater weight fractions. The propellant fraction was held constant at 76% for the payload sweep; the slight decrease seen is a result of

Figure 10: Payload Sizing Comparison

23

the weight equations not summing the weights properly. Within the range of payloads that were analyzed, greater vehicle efficiency is realized with larger payloads. At a lower liftoff weight, no payload is able to fit within the vehicle.

The vehicles at the extremes of the analysis (4k and 64k pound payloads) are shown in Figure 10. Notice that the sizing is not photographic. The wings grow at a faster rate in comparison with the fuselage. This is a result of the wings depending on the empty weight of the vehicle to maintain an acceptable rate of sink, span loading, and wing loading during landing conditions. The weight mainly depends on the size of the fuel tanks, the engine, and thrust structure, which depend on the fuel volume. Volume is a cubic function, so a small change in the fuselage will lead to a large increase in weight. The planform area only grows by the square of the increase in fuselage size, so if the fuselage grows by a factor of two, the weight increases by a factor of eight, and the wings increase a factor of four.

Thrust-to-Weight Optimization

In the second analysis sweep the thrust-to-weight ratio of the orbiter was varied and plotted as a function of vehicle dry weight (Figure 11). Thrust-to-weight and propellant fractions are closely related; higher thrust to weight ratios require less vehicle fuel fractions. Iteration was required with the trajectory analysis to solve for the fuel fraction. The results ranged from 77.5% at a thrust to weight ratio of 1.0 to 74.5% at a thrust to weight ratio of 1.8. Because the orbiter operates at high altitudes, the thrust to weight effect on vehicle weight is mostly a result of gravity losses (a

Figure 11: Thrust to Weight Optimization

factor of ΔV). Consequently there is only a small shift in dry weight and slight differences in vehicle design. The increase in dry weight at higher thrust to weight ratios results from limiting the G-loading on the vehicle. Additional increases in thrust only add additional engine weight to the vehicle. An optimum thrust-to-weight ratio is found to be between 1.3 and 1.7.
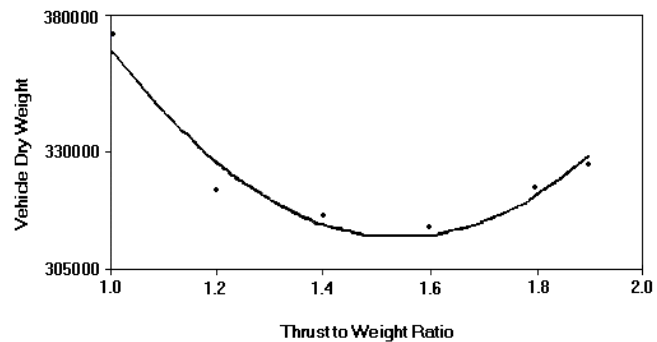
Fuel Selection

In this study, the fuel of both the orbiter and booster where set to either a hydrocarbon (kerosene) or hydrogen based fuel with a LOX (liquid oxygen) for the oxidizer. The vehicles in Figure 12 show that the hydrogen-fueled concept is much larger than the hydrocarbon design. This is a result of the very low density of hydrogen, which requires a larger volume for the same propellant mass, increasing the volume required to store it. However, the vehicle dry weight is still roughly the

Figure 12: Fuel Selection Vehicle Comparison

same for both concepts. In fact, further studies have shown that the hydrocarbon design could be made lighter than the hydrogen concept by increasing the staging Mach number. The non-photographic scaling in the vehicle concepts results from the same sizing constraints of the payload trade study. Further analysis is required, particularly in the operations area, to determine the o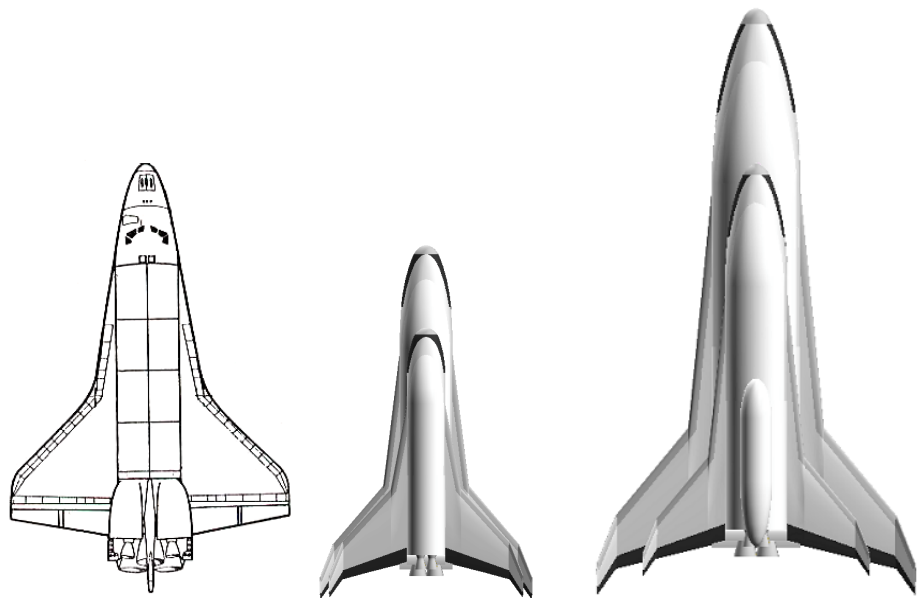ptimal staging mach number. The scaled picture of the Space Shuttle is included only as a yardstick as to the size of these concepts.

SUMMARY

The Reusable Military Launch System design environment under development at WPAFB has demonstrated dramatic design and analysis timesavings. The collaborative design environment currently incorporates parametric geometry, aerodynamics, mass properties, aeroheating, rocket propulsion, and trajectory analysis disciplines for the Bimese rocket configuration currently under study by the RMLS team. Continuing Research will incorporate additional analysis tools and optimization techniques for complete vehicle formulation. As the number of analysis objects grows, the usefulness and efficiency of the tool will increase. Further trade study analysis will define optimal vehicle design. These trade studies include:

- o Load-factor
- o Allowable wing loading
- o Number of engines (engine out capability)
- o Engine type
- o Fuel selection
- o Parallel vs. serial burn
- o Staging Mach number

However, performing various single degree of freedom trade studies does not necessarily produce optimal results. The interconnectivity of the various disciplines found in the design structure matrix almost guarantees non-linear results that must be analyzed as a whole. Future work will include optimization across the disciplines to produce optimal vehicles for particular mission categories. The research reported here has created a design environment for rapid design analysis at a conceptual level. This work will be useful for assessing optimal design solutions and will dictate future air force requirements and direction for building RMLS vehicles. This is only the beginning of a much larger process. With additional object creation, higher fidelity analysis will be achieved.

BIBLIOGRAPHY

1. Bhungalia, A. A., Zweber, J. V. and Stevenson, M. D., "Integrated Aerodynamic and Geometric Modeling for Hypersonic Vehicle Design", ASME paper DETC/DAC-14267, presented at the 26th ASME Design Automation Conference, Baltimore, MD, September 10-13, 2000.

2. Stevenson, M. D., Bhungalia, A. A. and Zweber, J. V., "Integrated Trajectory Analysis for Transatmospheric Vehicle Design", AIAA paper 2000-4817, presented at the 8th AIAA/USAF/NASA/ISSMO Symposium on Multidisciplinary Analysis and Optimization, Long Beach, CA, September 6-8, 2000.

3. Stanley, D., *et al.,* "Rocket Powered Single Stage Vehicle Configuration Selection and Design", AIAA 93-1053, Feb. 1993.

4. Freeman, D., Stanley, D., Camarda, C., Lepsch, R., Cook, S., "Single Stage to Orbit: A Step Closer", AIF 94-V3.534, Oct 1994.

5. Olds, J., Bradford, J., Charania, A., Ledsinger, L., McCormick, D., and Sorensen, K., "*Hyperion*: An SSTO Vision Vehicle Concept Utilizing Rocket-Based Combined Cycle Propulsion", AIAA paper 99-4944, presented at the 9th International Space Planes and Hypersonic Systems and Technology Conference, Norfolk, VA, November 1-5, 1999.

6. Prasad, B., *Concurrent Engineering Fundamentals: Integrated Product and Process Organization,* Volume I, Prentice-Hall, Upper Saddle River, NJ, 1996.

7. Zweber, J. V., Blair, M., Kamhawi, H., Bharatram, G. and Hartong, A., "Structural and Manufacturing Analysis of a Wing Using the Adaptive Modeling Language", AIAA paper 98-1758, presented at the 39th AIAA/ASME/ASCE/AHS/ASC Structures, Structural Dynamics and Materials Conference, Long Beach, CA, April 20-23, 1998.

8. *Adaptive Modeling Language Reference Manual: Version 3.0*, TechnoSoft Inc., Cincinnati, OH, 1999.

9. "Web-based Design Environment", DUS&T Program Report to Congress, Air Force Projects for Fiscal Year 1999, http://www.dtic.mil/dust/cgr/af00cgr.htm#airforce19

10. Meltzer, Pete, "Web-based tool speeds up weapon system design", Skywrighter, WPAFB, OH, 26 May, 2000.

11. Livingston, John, "A Parametric Rocket Model", USAF, WPAFB, OH, 2000.

12. Huzel D., Huang D., Rocketdyne Div, N. America Aviation Inc., "Design of Liquid Propellant Rocket Engines", NASA SP-125, 1967.

13. Klich, P., MacConochie, I., NASA Langley, "Mass Estimating Techniques for Earth-To-Orbit Transports with Various Configuration Factors and Technologies Applied", SAWE Paper No. 1315, 38th Annual Conf. Of SAWE, NY, NY 7-9 May 1979.

14. MacConochie I., Klich P., NASA Langley, "Techniques for the Determination of Mass Properties of Earth to Orbit Transportation Systems", NASA TM-78661, June 1978.

15. NASA Johnson Space Center, System Definition Branch: Technology and Project Implementation Office, "Design Mass Properties II: Mass Estimating and Forecasting for Aerospace Vehicles Based on Historical Data", JSC-26098, November 1994.

16. HYCAD – Equations developed by ASC/XR 1985 and 1988.

17. Olds, John, Dissertation NC State 1993, Appendices A and B.

18. Forbis, J., Woodhead, G., Boeing Military Airplanes, "Conceptual Design and Analysis of Hypervelocity Aerospace Vehicles: Vol 1. Mass Properties, Part 1 Transatmospheric Vehicle Weights (TAVWTS)", WL-TR-91-6003, July 1991.

19. Powell, R. and Braun, R., "Program to Optimize Simulated Trajectories (POST)", NASA Langley Research Center, Hampton VA, Oct. 1997.

20. Blair, M., Moorhouse, D., Weisshaar, T., "System Design Innovation Using Multidisciplinary Optimization and Simulation", AIAA 2000-4705

APPENDIX C

Weight Growth Study of Reusable Launch Vehicle Systems

Adam F. Dissel[*] and Ajay P. Kothari[†]

Astrox Corporation, College Park, Maryland 20740

John W. Livingston[‡]

Aerospace Systems Design and Analysis ASC/XRE, Wright–Patterson Air Force Base, Ohio 20742

and

Mark J. Lewis[§]

University of Maryland, College Park, Maryland 20742

Using a wide spectrum of completed air-breathing and rocket-powered launch vehicle baseline configurations, an assessment was undertaken to ascertain each vehicle system's scaling response to empty weight growth. To establish the growth behavior, each vehicle's baseline solution was modified for percentage increases or decreases in the baseline empty weight from $+10\%$ to -10%, after which each vehicle system was then re-solved. The identification of the trends in these solutions enabled the determination of the growth factor for each vehicle configuration. The growth factor characterizes the system's sensitivity to changes in structural weight arising from technological uncertainty. Systems with high growth factors represent a greater amount of design risk because they may rapidly scale out of control if expected technology levels fail to materialize. This understanding may also be applied to measure the extent of improvements possible from application of more advanced technology. Several other figures of merit were also used to evaluate the growth solutions, including empty weight, wetted area, and gross weight. The assessment concluded that single-stage air breathers have a higher response to weight uncertainty than two-stage configurations with the horizontal takeoff mode being more sensitive than vertical takeoff. Two-stage air-breathing configurations, whereas exhibiting lower growth factors, differed greatly from each other in total empty weight across the growth cases with the vertical takeoff mode roughly half the weight of comparable horizontal takeoff configurations. Two-stage reusable rocket configurations also show low scaling weight growth factors and empty weights and are relatively insensitive to small percentage growth changes.

Nomenclature

f_{FX} = fixed weight fraction
f_P = propellant fraction
f_S = baseline scaling structural fraction
f_{SN} = scaling structural fraction
GF_{FW} = fixed weight growth factor
GF_{SW} = scaling weight growth factor
W_E = empty weight
W_{FX} = fixed weight
W_G = gross weight
W_P = propellant weight
W_{PAY} = payload weight
W_S = scaling weight
W_{SN} = new scaling weight

I. Introduction

DURING the past two decades, there have been several failed attempts at the development of reusable rocket or air-breathing launch vehicle systems. Single-stage-to-orbit (SSTO) vehicle concepts such as the National Aerospace Plane (NASP), the

*Research Engineer, also Graduate Research Assistant, University of Maryland; adissel@umd.edu. Student Member AIAA.
†President, 3500 Marlbrough Way Suite 100. Senior Member AIAA.
‡System Design Engineer, Aeronautical Systems Center/Aerospace Systems Design and Analysis.
§Professor, Department of Aerospace Engineering. Fellow AIAA.

Mcdonnell Douglas Delta Clipper Experimental (DCX), and the Lockheed Martin X-33 are among those programs canceled. A contributing cause to the demise of these programs was the impact of vehicle growth arising from inaccurate predictions in the attainable level of technology. This phenomenon was particularly apparent in the NASP program, which, by the time of its cancellation, had grown in physical scale many times beyond initial forecasts. The X-33 met a similar fate when the expected propellant tank weight became unachievable due to technology problems with the planned composite tanks. The substitution of heavier, more traditional tanks into the nearly complete vehicle would have resulted in a system now unable to meet its mission goals.

The incorporation of a healthy design margin is a widespread approach to addressing such growth problems in launch vehicles and has been used routinely in aircraft design and sizing. However, launch vehicles possess a much steeper growth response than most aircraft, and whereas a significant design margin may mitigate the growth risk of a multistage launch vehicle, even a 50% margin can be insufficient for a single-stage launcher. A successful reusable launch vehicle program must understand and compensate for these growth effects and focus its efforts on both the realistic estimation of used technology levels and the targeted improvement of those technologies with the greatest system growth impact. This consideration is doubly important for immature and evolving technologies such as hypersonic air-breathing propulsion.

The work presented in this paper represents a broad effort to characterize the growth behavior of a wide-ranging suite of potential reusable launch vehicles for access to space. The reference mission for each configuration solution is a 20,000 lb payload placed into a 100 nm low Earth orbit (LEO). The configurations considered extend across the spectrum of both SSTO and two-stage-to-orbit (TSTO) air-breathing and rocket vehicles and hybrid combinations of the two and includes both horizontal-takeoff-horizontal-landing (HTHL) and vertical-takeoff-horizontal-landing (VTHL) flight modes. The goal of this growth study is *not* to present a single best vehicle design or launch mode; rather, the investigation seeks to characterize the

growth sensitivity and resulting design risk that must be addressed to be successful with each given configuration.

II. Design Methodology

All vehicles in this design study have been configured with the HySIDE code developed by Astrox Corp. [1]. The code is a component-based, object-oriented design package within a systems engineering software environment. HySIDE uses analytical solutions and tabulated data as available rather than detailed computational fluid dynamic solutions to be speedy and flexible while still maintaining a high degree of accuracy. Use of the code's rapid design and analysis capabilities allows for the quick systematic comparison of hundreds of design parameters and input cases.

To design a hypersonic vehicle, the code uses the freestream Mach number and altitude at a chosen design point and specified bow shock strength, from which the method of characteristics and streamline tracing methods [2] are used to form the inlet surface. After the trace, the surface inviscid forces are known, as is the inlet exit flow state. A quasi-one-dimensional combustor model is used to model the mixing and burning of hydrogen or hydrocarbon, and a combustor surface is defined. The nozzle flowfield is then also created using the method of characteristics. An external surface joins the inlet capture area and nozzle exit. A reference temperature boundary layer method is then applied to determine the viscous forces, heat transfer, and boundary layer displacement thickness on each surface. The aerodynamic forces are determined by integrating the pressures on each surface's gridpoints [3]. A rocket vehicle is analyzed with similar methods, but without the internal flowpath surfaces.

The code has the ability to perform analysis in a completely integrated fashion (propulsion–airframe–massproperties–aero–gravloss–heating–volumes, etc.). Individual components include either hypersonic air-breathing or rocket engines integrated into a full vehicle model; their performance is calculated over the complete mission trajectory. Vehicle sizing is done in an iterative loop. The vehicle is scaled until the volume available for the fuel is equal to the fuel volume needed based on individual component weights and

densities. The code calculates the volumes and areas of all the components and from this subtracts the volumes of payload, equipment, thermal protection system (TPS), etc. The resulting volume is multiplied by a tank packaging efficiency as a measure of how well the tank shape is able to use the available volume. The resulting value is the volume available for propellant, and must equal the fuel volume required to complete the mission trajectory to "close" the vehicle. All of the components will require resizing as the vehicle is continuously scaled to match all of these requirements simultaneously.

Several standard codes, such as Missile Datcom for aerodynamics, have been integrated into the code's suite of analysis tools. Setup time for the complete analysis of a new system requires several days, and once the included components of the specific vehicle system are connected, the system calculations for each solution run are done in about ten minutes on a standard desktop PC. The code has the ability to model 21 different commercially available rocket engines as well as air-breathing scramjet-based engines and traditional turbine engines using a variety of inlet geometries. Reusable and expendable rocket geometries are also included.

III. Alternative Configurations

The baseline versions of the 18 configurations analyzed for this study were set up and solved during previous investigations as documented in [4,5]. Figure 1 identifies these configurations and their baseline gross takeoff weights (GTOW) [the Space Transportation System (STS) and XB-70 Valkyrie are included for scale reference]. As seen from the figure, the study investigated 18 vehicle configurations: nine SSTO and nine TSTO. All of the SSTO vehicles were hypersonic air-breathing vehicles differing by inlet type, propellant selection, low-speed propulsion cycle, and takeoff mode. The TSTO configurations included three pure-rocket systems as well as air-breathing vehicles combined with either an upper-stage rocket orbiter or first-stage rocket booster. The air-breathing vehicles used either an inward-turning "IN" inlet or more traditional wedge "2D"-type inlet geometry. The low-speed propulsion cycles for all

SSTO-VTHL

2D-RB(H2)
816,776 lbs
370 tonnes

IN-RB(H2)
574,272 lbs
260 tonnes

2D-RB(HC)
702,916 lbs
319 tonnes

IN-RB(HC)
502,816 lbs
228 tonnes

STS Stack
4,400,000 lbs
1,996 tonnes

SSTO-HTHL

IN-RB(H2)
724,934 lbs
329 tonnes

IN-RB(HC)
817,393 lbs
371 tonnes

2D-RB(H2)
1,255,020 lbs
569 tonnes

2D-RB(HC)
1,418,680 lbs
644 tonnes

2D-TB(HC)
1,489,350 lbs
676 tonnes

TSTO-VTHL

HCR / HCR
1,440,000 lbs
653 tonnes

HCR / HR
1,188,000 lbs
539 tonnes

HR / HR
1,035,000 lbs
469 tonnes

HCR / 2D-RB
718,811 lbs
326 tonnes

HCR / IN-RB
524,916 lbs
238 tonnes

TSTO-HTHL

XB-70
534,000 lbs
242 tonnes

Turbine(HC) / 2D-RB
629,951 lbs
286 tonnes

2D-TB(HC)/ HR
836,365 lbs
379 tonnes

2D-RB(H2) / HR
1,033,590 lbs
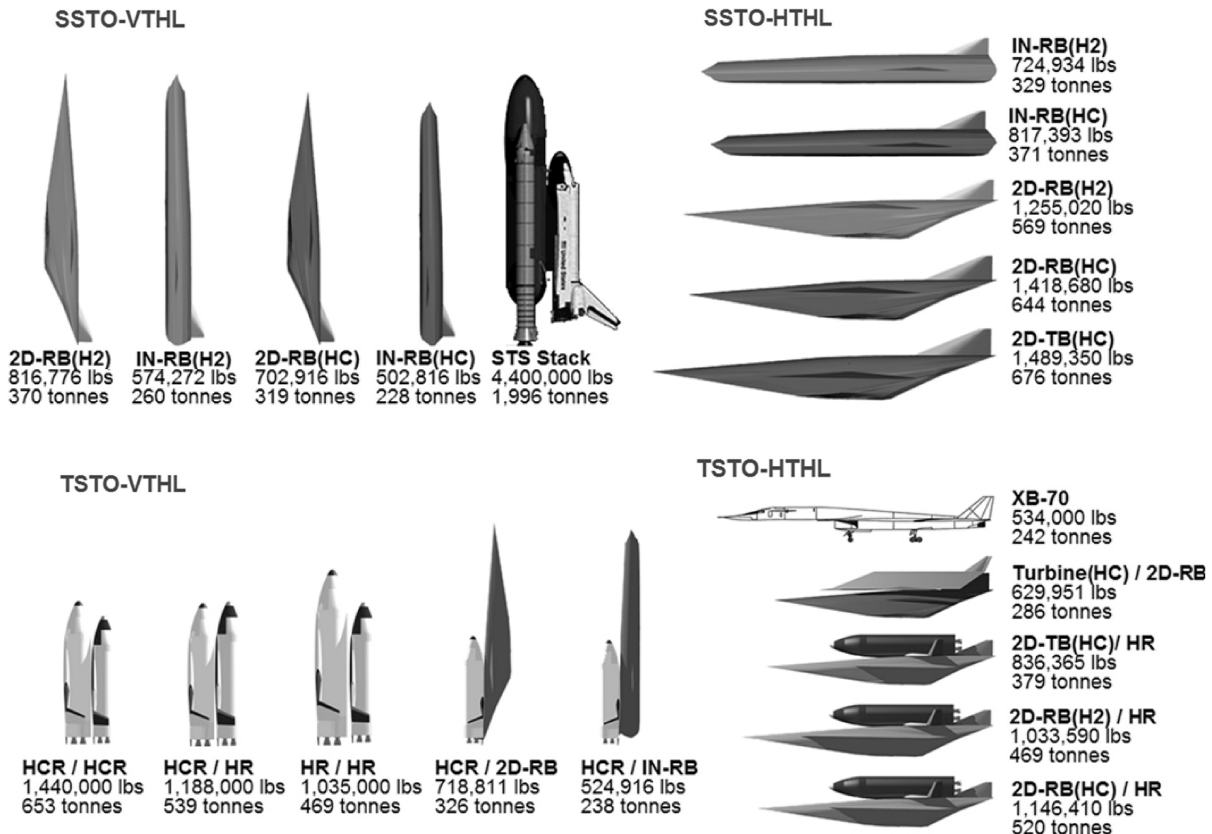469 tonnes

2D-RB(HC) / HR
1,146,410 lbs
520 tonnes

Fig. 1   Investigated configurations: baseline GTOW and scale comparison.

Table 1 Investigated configurations: propellant and empty weight fractions

Vehicle name	Configuration type	Propellant fraction					Empty weight fraction				
		−10%	−5%	0%	+5%	+10%	−10%	−5%	0%	+5%	+10%
IN-RB(H2)	SSTO VTHL	0.729	0.729	0.729	0.730	0.730	0.224	0.230	0.236	0.241	0.246
IN-RB(HC)	SSTO VTHL	0.754	0.754	0.754	0.754	0.755	0.195	0.201	0.206	0.211	0.216
2D-RB(H2)	SSTO VTHL	0.755	0.754	0.752	0.752	0.752	0.213	0.218	0.223	0.228	0.232
2D-RB(HC)	SSTO VTHL	0.777	0.777	0.776	0.776	0.776	0.185	0.190	0.195	0.200	0.203
IN-RB(H2)	SSTO HTHL	0.727	0.728	0.728	0.728	0.730	0.231	0.238	0.245	0.250	0.255
IN-RB(HC)	SSTO HTHL	0.757	0.757	0.757	0.758	0.762	0.207	0.214	0.219	0.224	0.229
2D-RB(H2)	SSTO HTHL	0.754	0.753	0.752	0.752	0.753	0.220	0.227	0.232	0.237	0.241
2D-RB(HC)	SSTO HTHL	0.780	0.780	0.778	0.779	no soln	0.197	0.203	0.207	0.212	no soln
2D-TB(HC)	SSTO HTHL	0.700	0.700	0.701	no soln	no soln	0.279	0.282	0.286	no soln	no soln
HR/HR	TSTO VTHL	0.795	0.792	0.790	0.787	0.785	0.182	0.187	0.191	0.195	0.199
HCR/HR	TSTO VTHL	0.847	0.845	0.843	0.842	0.840	0.133	0.136	0.139	0.141	0.145
HCR/HCR	TSTO VTHL	0.873	0.871	0.869	0.868	0.866	0.111	0.113	0.116	0.119	0.121
HCR/IN-RB	TSTO VTHL	0.756	0.754	0.752	0.751	0.750	0.198	0.205	0.210	0.215	0.219
HCR/2D-RB	TSTO VTHL	0.772	0.770	0.768	0.767	0.765	0.194	0.199	0.204	0.208	0.213
2D-RB(H2)/HR	TSTO HTHL	0.719	0.713	0.706	0.700	0.694	0.257	0.265	0.275	0.283	0.290
2D-RB(HC)/HR	TSTO HTHL	0.746	0.740	0.735	0.727	0.722	0.233	0.241	0.248	0.257	0.264
2D-TB(HC)/HR	TSTO HTHL	0.613	0.602	0.593	0.585	0.576	0.358	0.371	0.383	0.394	0.404
Tutbine/2D-RB	TSTO HTHL	0.512	0.500	0.489	0.481	0.473	0.448	0.464	0.479	0.491	0.502

air breathers was provided by either integrated rockets "-RB" or turbines "-TB" operating on hydrogen "(H2)" or hydrocarbon "(HC)" fuel. All air breathers assumed hydrogen scramjets and integrated hydrogen rockets for postscramjet ascent to orbit. One HTHL vehicle used a pure turbine-powered booster as a first stage. Where used, the pure-rocket stages are notated by propellant; hydrocarbon-fueled rockets (HCR) or hydrogen-fueled rockets (HR). The TSTO notation in the figures is listed as "Stage1/Stage2."

In addition to the baseline solutions, this study used the design code to produce four additional growth solutions for each system concept, which corresponded to percentage changes in the total baseline empty weight for −10, −5, +5, and +10%. These data solutions are required to determine the sensitivity or growth factor for each of the concepts. The propellant and empty weight fractions for the closed data points for the different empty weight growth percentages are shown in Table 1.

The tabulated data show that, with the exception of the largest TSTO air breathers, the majority of the configurations exhibit very small changes in propellant fraction across the different growth solutions. This observation supports the simplification that the propellant fraction can be considered approximately constant.

A. Sizing Equations and Growth Factors

Insight into how vehicle systems are sized can be had by developing and examining a set of relatively simple equations derived from the "sizing equation." These expressions can be employed to determine the weight impact of different growth scenarios without the need to re-solve each system in detail. For the purposes of this analysis, the total vehicle weight is divided into four categories: propellant weight, fixed weight, scaling weight, and payload weight. The propellant weight includes all propellants used for launch ascent, as well as for orbital positioning and maneuvering. The fixed weight is the sum of all the vehicle components that do *not* scale with vehicle sizing during closure, such as payload bay fixtures and mounts, payload bay doors, nonscaling avionics, etc. The scaling weight is the sum of the weights of the spacecraft that *do* scale with increasing or decreasing size. Most major subsystems and structure items fall into this category, including propellant tanks, thermal protection surfaces, airframe, wings, landing gear, engines, etc. The vehicle gross weight is the sum of all four weight categories:

$$W_G = W_P + W_{FX} + W_S + W_{PAY} \tag{1}$$

The scaling and propellant weight fractions are simply the respective weights divided by the total gross weight:

$$f_S = \frac{W_S}{W_G} \tag{2}$$

$$f_P = \frac{W_P}{W_G} \tag{3}$$

To determine the growth factors, a sizing equation is needed that properly captures the scaling behavior seen in the design code solutions. It will be useful to express the gross weight in terms of the fixed weight, and scaling and propellant weight fractions:

$$W_G = \frac{W_{PAY} + W_{FX}}{1 - f_S - f_P} \tag{4}$$

This sizing equation is very useful for a wide range of aircraft types and missions. The scaling and propellant weight fractions are indeed quite close to constant over a reasonably large range of sizes for a given design layout, engine design, and mission. The empty weight is simply the sum of both the scaling and fixed structural weights:

$$W_E = W_S + W_{FX} = f_S W_G + W_{FX} \tag{5}$$

Substituting for gross weight, an empty weight equation is obtained in terms of the scaling weight fraction and fixed weight:

$$W_E = f_S \frac{W_{PAY} + W_{FX}}{1 - f_S - f_P} + W_{FX} \tag{6}$$

Equations (4) and (6) yield the gross and empty weights as functions of fixed weight, payload weight, propellant fraction, and scaling structure fraction. For constant values of fixed weight and payload weight, the vehicle may be sized with the two fractions.

B. Correction with Analysis Results

The preceding sizing equations will require values for the scaling weight fraction and the vehicle fixed weight that will enable the equations to approximate the gross and empty weights of the data solutions. To this point, there has been no effort made to distinguish the empty weight into either scaling or fixed weight types. Presupposed values for these quantities that could have been part of the design setup will likely not produce sufficient data agreement if used in the sizing equations. The discrepancy is attributable to the nonlinear behavior of the solution of an integrated vehicle. Component level weight estimations are based on many varied parameters; some items scale with surface area or vehicle volume, whereas others are determined based on the gross or empty weights. The fixed weight and scaling weight fractions are varied until they best fit the actual design code data points, in effect determining how much of the empty weight is actually behaving as fixed weight vs scaling weight. Negative values of the term reduce the amount of empty weight acting like fixed weight, whereas positive values increase the amount. Figures 2 and 3 illustrate the effect of different
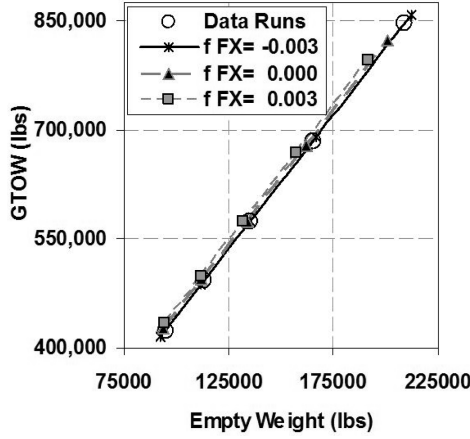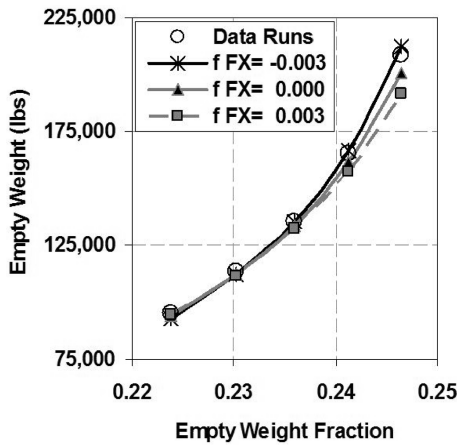
Fig. 2 GTOW matching with IN-RB(H2) data.

Fig. 3 EW matching with IN-RB(H2) data.

values of f_{FX} in matching the gross and empty weights of the design code data points.

The figures show that for the VTHL SSTO IN-RB(H2) vehicle, a good data agreement is achieved with a f_{FX} value of -0.003. The scaling fraction is then simply the empty fraction minus the fixed weight fraction. The fixed and scaling weight fractions were accordingly determined for each of the configurations. We now have smooth analytic relationships for each of our alternative designs, which can be differentiated to determine growth behavior.

IV. Empty Weight Growth Factors

An empty weight growth factor is a measure of the scaling response in vehicle empty weight due to an increase in either the vehicle's fixed weight or scaling weight. The fixed weight growth factor determines the change in a given vehicle system's empty weight for an increase in the fixed weight of the system, as would occur for an increased payload requirement; whereas the scaling weight growth factor reflects the change in empty weight due to a change in the vehicle's own scaling structural weight.

A. Fixed Weight Growth Factor

An increased fixed weight requirement will trigger an increase in the vehicle's size as it is scaled up to closure. The growth response is straightforward, because the vehicle model weight estimating parameters do not change for changes in fixed weight, remaining fixed at the baseline values. The fixed weight growth factor is the derivative of the empty weight in Eq. (6) taken with respect to the fixed weight and will be a constant value for a given system and suite of technology assumptions.

30

$$\frac{dW_E}{dW_{\mathrm{FX}}} = \frac{f_S}{1 - f_S - f_P} + 1 \tag{7}$$

The fixed weight growth factor may be expressed in terms of weight or the weight fraction:

$$\mathrm{GF_{FW}} = \frac{W_{\mathrm{PAY}} + W_{\mathrm{FX}} + W_S}{W_{\mathrm{PAY}} + W_{\mathrm{FX}}} \tag{8}$$

$$\mathrm{GF_{FW}} = \frac{1 - f_P}{1 - f_S - f_P} \tag{9}$$

B. Scaling Weight Growth Factor

The scaling weight growth factor is a measure of the scaling response in vehicle empty weight to an increase in the unit weight of the vehicle structure. This increase often arises due to a change in the estimation of the corresponding weight of some structural technology, such as a heavier or lighter weight TPS tile type. The scaling weight growth factor can therefore be used as a measure of the vehicle's response to the technological uncertainty inherent in the development of any future system, and as such was the principal figure of merit applied in this investigation. A general aerospace vehicle scaling reaction to such an increase proceeds as follows:

1) A previously closed vehicle solution experiences an increase in a structural unit weight.

2) That percentage increase multiplied by the total amount of that structural component present in the closed solution results in an additional amount of weight that must now be carried by the vehicle.

3) The vehicle solution is no longer closed, meaning it no longer contains sufficient fuel to successfully execute the mission with the now heavier vehicle. The weight addition acts as a perturbing influence that triggers a scaling up of the vehicle solution to reclose the vehicle.

4) As the vehicle grows in response to the weight change it must also now do so with a correspondingly higher unit weight. This double impact causes a much larger change in the reclosed vehicle's empty weight vs the original empty weight than just the addition of the perturbing change in structure weight alone.

5) The empty weight growth factor is obtained by differentiating the empty weight scaling Eq. (6) with respect to the weight change and is the slope of the delta empty weight/delta perturbing weight curve at the point of the vehicle solution.

As previously mentioned, each vehicle system was reclosed in HySIDE for percentage increases in the total baseline structural (empty) weight from -10% to $+10\%$. The empty and gross weight sizing equations were applied to curve fit through the five solution points for each system. For reasons that will become clear further on, the empty weight equation is first rewritten in terms of a new scalable weight W_{SN}:

$$W_E = \left(\frac{W_{\mathrm{SN}}}{W_G}\right) \frac{W_{\mathrm{PAY}} + W_{\mathrm{FX}}}{1 - W_{\mathrm{SN}}/W_G - f_P} + W_{\mathrm{FX}} \tag{10}$$

Differentiating with respect to the scalable weight yields

$$\frac{dW_E}{dW_{\mathrm{SN}}} = \left(\frac{1}{W_G}\right) \frac{W_{\mathrm{PAY}} + W_{\mathrm{FX}}}{1 - W_{\mathrm{SN}}/W_G - f_P}$$
$$+ \left(\frac{W_{\mathrm{SN}}}{W_G}\right) \frac{W_{\mathrm{PAY}} + W_{\mathrm{FX}}}{(1 - W_{\mathrm{SN}}/W_G - f_P)^2 W_G} \tag{11}$$

Pulling the common terms to the front of the equation,

$$\frac{dW_E}{dW_{\mathrm{SN}}} = \left(\frac{1}{W_G}\right) \frac{W_{\mathrm{PAY}} + W_{\mathrm{FX}}}{1 - W_{\mathrm{SN}}/W_G - f_P} \left[1 \right.$$
$$\left. + W_{\mathrm{SN}} \frac{1}{(1 - W_{\mathrm{SN}}/W_G - f_P) W_G} \right] \tag{12}$$

Simplifying the bracketed term in the preceding equation gives

$$\frac{dW_E}{dW_{SN}} = \left(\frac{1}{W_G}\right)\frac{W_{PAY} + W_{FX}}{1 - f_{SN} - f_P}\left(\frac{1 - f_P}{1 - f_S - f_P}\right) \qquad (13)$$

The final step is to substitute equivalent fractions for the weights. This step reintroduces the original baseline scalable weight fraction f_S and is the reason for the introduction of the new (nonbaseline) scaling weight fraction f_{SN}. It is important to note that at the baseline solution point, $f_{SN} = f_S$. The scaling weight growth factor is now given by the following equation:

$$GF_{SW} = \frac{(1 - f_S - f_P)(1 - f_P)}{(1 - f_{SN} - f_P)^2} \qquad (14)$$

The growth factor may be alternatively expressed in terms of weights:

$$GF_{SW} = \frac{(W_{PAY} + W_{FX})(W_{PAY} + W_{FX} + W_S)}{(W_{PAY} + W_{FX} + W_S - W_{SN})^2} \qquad (15)$$

Combining these growth factor equations with those for empty and gross weight allows for the estimation of vehicle weights and growth response by simply choosing different values of the scaling structure fraction. Note that when $f_{SN} = f_S$, Eqs. (14) and (15) degenerate into Eqs. (8) and (9).

Once obtained, the scaling weight growth factor may be used for quickly performing multiple individual system component technology assessments without the need to re-solve each system separately. Thus employed, the growth factor is a powerful way to determine which configurations pose less of a design risk. Once a particular vehicle's scaling behavior is understood, it can be coupled with further analyses to determine an appropriate design margin. Livingston [6] has combined the growth factor process with defined uncertainty bands on the vehicle technology to determine the growth point required to achieve an 80% probability of successful closure based on the assumed maturity of the technology.

V. Additional Figures of Merit

A. Empty Weight

At this level of analysis, the total vehicle system empty weight may be reasonably employed as the main cost driver of a launch vehicle system. Most of the launch operation and flight refurbishment costs, as well as the initial development and procurement costs of a launch vehicle scale roughly with empty weight [7]. When comparing the empty weights as a rough measure of the approximate cost and feasibility of designing and constructing the vehicle, it should be remembered that the use of conformal tanks, active TPS, and other new technologies will result in an air-breathing vehicle that "pound for pound" will likely cost more than a pure-rocket vehicle. Although existing rocket technology is more mature than the emerging hypersonic air breathers, the requirement for highly operable and reliable rocket engines for post air-breathing orbital ascent will require more investment [8] in rocket engine capabilities.

B. Wetted Area

The amount of wetted area impacts the vehicle's performance, weight, and operational cost. For the heating conditions present during either the air-breathing trajectory or atmospheric reentry, all the exposed area of a hypersonic vehicle will require some level of TPS. When the heating over a certain area exceeds the limits of current materials technology, then those areas must be actively cooled. The reduction of TPS area yields a double benefit, the first being a reduction in weight, and the second a reduction in the time and cost of TPS refurbishment [9]. Conversely, runaway growth in vehicle size leads to multiplying maintenance cost. TPS maintenance is a major part of the space shuttle's refurbishment costs. State of the art and future advanced passive TPS materials may require less maintenance than previous TPS materials. However, the actively cooled panels on future hypersonic vehicles are a new TPS system that is likely to require a fair amount of inspection and between flight refurbishment. The air-breathing stages need substantial active cooling on leading edges and through the inlet, combustor, and nozzle.

C. Gross Weight

Vehicle gross takeoff weight is often cited as a principal metric of comparison between different vehicle configurations. However, the vehicle gross weight is not as useful a figure of merit as the three listed earlier. The major constituents of the gross weight for the vehicles are the propellants required. Compared with the cost of acquiring and maintaining the vehicle, the cost of purchasing, storing, and handling each flight's propellant is nearly insignificant. Although a higher gross weight vehicle for a given design and mission may represent a lower performing propulsion system, it is the impact of that performance on the vehicle's empty weight and surface area that are of primary interest. However, the gross weight was included in this study because it does give quick insight into the scaling of parameters that have to do with the fueled vehicle, such as propulsion thrust requirement, pad limitations, and in the case of horizontally launched vehicles, the wing and landing gear sizing. It is also used to determine if a particular HTHL vehicle baseline or grown solution has exceeded the runway bearing load limitation, which, for this study, was assumed to be 1.5×10^6 lb.

VI. Results

As mentioned, the 18 vehicle configurations were all re-solved for empty weight percentage changes of $-10, -5, +5$, and $+10\%$, thus representing an additional 72 closed vehicle solutions in addition to the original 18 baseline closures. The discussed measures of merit were determined for each solution point and are presented in the following section. In each of the remaining figures, each individual vehicle system is shown at the five solution points such that the general trend in each is readily estimated. The data thus presented yield valuable insight into a broad range of possible vehicle growths; both positive and negative. If it is determined that the baseline technology assumptions used for this study are too optimistic, one need only shift up to a higher $+\%$ solution point on each vehicle growth curve to reassess the impact of a more conservative performance estimate. The growth factor results presented from this point forward are all scaling weight growth factors.

A. Growth Factor Figure Notation

The next two figures show the scaling weight growth factor vs empty weight trends for SSTO and TSTO configurations. The five solutions for each vehicle are represented as points on the figures with trend lines connecting them. The filled symbols represent the baseline solution; the two open symbols below this point are the -5 and -10% solutions, and the two open symbols above the baseline point are the $+5$ and $+10\%$ solutions. There are a few configurations whose closure points extend off above the scale of the figure axis, in which case only the negative percentage solutions may appear.

Represented in Fig. 4 are the scaling weight growth factors vs empty weights for the SSTO air-breathing configurations. The configurations differ by inlet type and low-speed rocket propulsion segment fuel selection. The figure shows that the VTHL inward-turning air breather with a hydrocarbon-fueled, low-speed propulsion segment has the lowest baseline growth factor and empty weight of the SSTO configurations. The VTHL all-hydrogen versions have slightly higher baseline growth factors. This difference becomes magnified as the solutions are run at the $+5$ and $+10\%$ cases. As seen, the distance between the baseline solution point and the $+5\%$ point is greater for the vehicles with higher baseline growth factors than for those with lower baseline growth factors. The higher growth response necessitates further scaling to reclose the vehicle. This behavior is only amplified when considering the distance to a further closure point. For example, at the $+10\%$ point, the VTHL inward-turning (HC) vehicle has increased its growth factor by 6 and
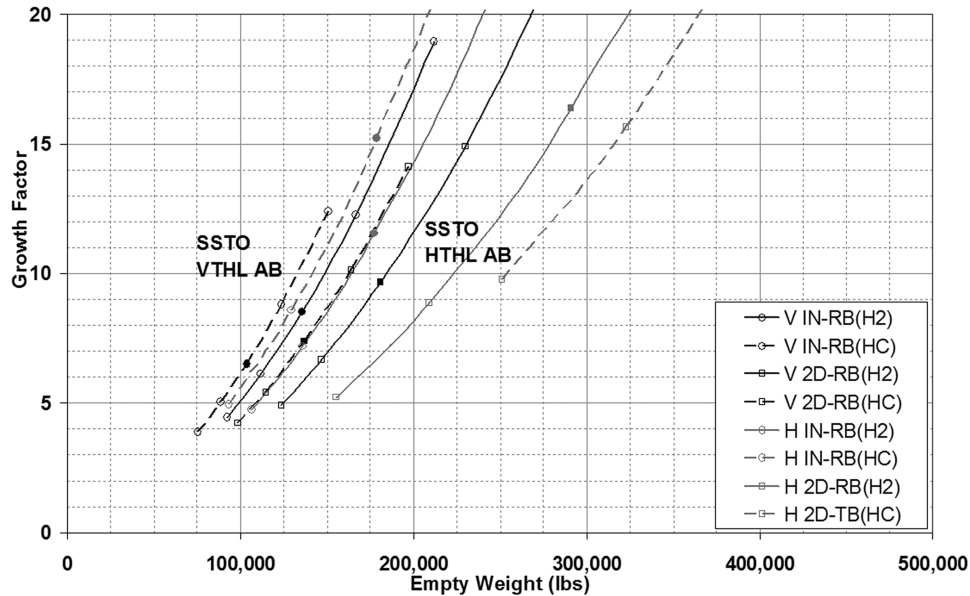
Fig. 4 Growth factor vs empty weight: SSTO, VTHL, and HTHL air breathers.

its empty weight by 50,000 lb, whereas the all-hydrogen version of the same configuration has increased by more than 10 in growth factor and over 80,000 lb in empty weight. Compared to the vertical SSTO vehicles, the baseline solution points for the HTHL configurations are shifted towards higher values of scaling weight growth factor and empty weight. The higher growth factors cause small differences in the configurations to be magnified, thus resulting in a sparser concentration of the baseline solutions than was seen for the VTHL vehicles. This accelerated growth response is due to conditions pertaining to the horizontal takeoff mode of these configurations. The wing area and landing gear of an HTHL vehicle are sized with respect to the vehicle gross weight. As the gross weight increases, these subsystems increase at a faster rate than equivalent systems on VTHL vehicles in which the wing area and landing gear are sized for the smaller empty weight increase. The larger wing area of the HTHL vehicles results in significant drag losses during the high-speed ascent portion of the hypersonic trajectory. These gross weight interactions are also the reason why the use of hydrocarbon fuel in the low-speed rockets used by some of the SSTO HTHL configurations now causes an increase in growth response. The lower performance hydrocarbon fuel drives up the gross weight of the

vehicle and thus enters into the wing/gear scaling problem afresh. These factors combined together cause the SSTO HTHL configurations to be more sensitive to growth than the SSTO VTHL configurations. Indeed, for the technological assumptions of the current study, some of the HTHL vehicles are already exhibiting a nearly runaway scaling response at the +5% closure point. The poorest performer of the four HTHL vehicles shown is the SSTO air breather with integrated turbines for low-speed propulsion. Its baseline point has a very high empty weight and growth factor and does not even appear on the figure, although its lower −5 and −10% closure points do. Having higher growth sensitivity does not summarily invalidate the potential of an SSTO HTHL. For the applied technological estimations, the SSTO VTHL vehicles are an improvement over the SSTO HTHL configurations in terms of empty weights and growth sensitivity. Because the same technology estimates and methods were consistently applied for common subsystems in the solutions of vehicles employing either launch mode, closing the resulting size gap would require large changes to technologies and assumptions peculiar to the particular launch mode. Technological possibilities for improving the performance of the SSTO HTHL vehicles with respect to the SSTO VTHL vehicles
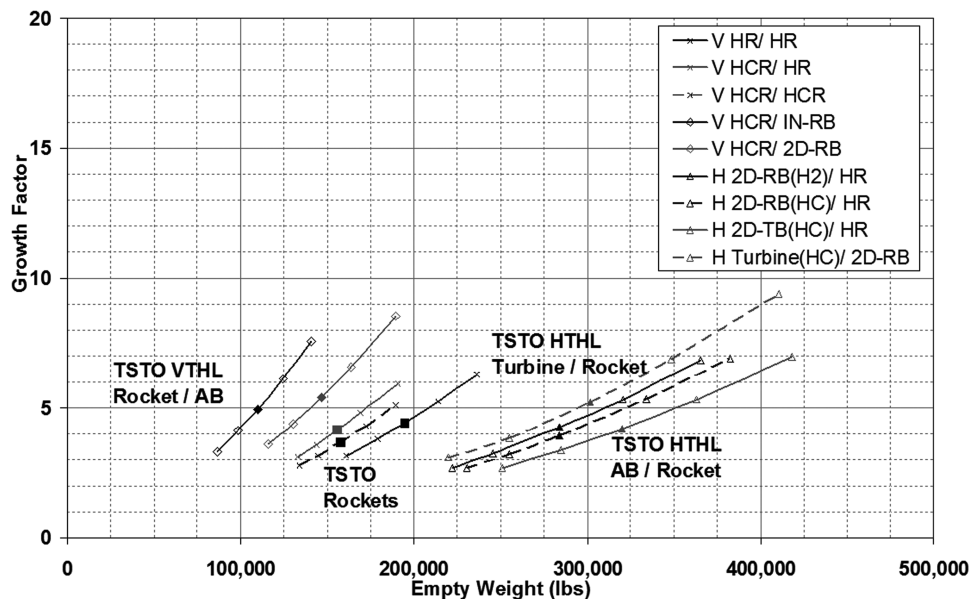

Fig. 5 Growth factor vs empty weight: TSTO configurations.

might include magnetic rail launch or increased takeoff speed. Likewise, the size gap could be reduced by conditions that might adversely and uniquely affect the SSTO VTHL configurations. It is possible that the SSTO VTHL concepts could get larger and the SSTO HTHL concepts could get lighter, but it is unlikely that the gap between them would close completely. The sizing trends observed in these growth trades should be considered carefully; the high degree of growth variability shown in these results for either SSTO launch mode precludes any final selection judgment until the considerable uncertainties in basic hypersonic vehicle component technologies and integration issues are reduced.

The TSTO configurations are considered next, and their growth solutions are shown in Fig. 5. The effect of staging on growth response is quite visibly communicated by the concentrated solutions shown. The empty weight of the three pure-rocket vehicles varies by only ∼80,000 lb across the whole growth percentage range. The smaller changes of the TSTO rockets are indicative of a robust system that is well suited to absorbing moderate changes in weight and therefore exhibits less design risk. Because of the subdued growth behavior of the TSTO rocket configurations, there is little variation among the three vehicles even though their propellant configurations are quite different. Also included in Fig. 5 are two additional TSTO categories that employ either HTHL air-breathing boosters with upper-stage rockets (three vehicles), or an HTHL turbine booster with an upper-stage hypersonic air breather (one vehicle). Once again, the use of staging moderates the scaling response; however, the combined empty weight of the TSTO HTHL systems using air-breathing stages is double that of the TSTO rockets. The TSTO HTHL vehicles show a larger spread in the location of the different closure points, but are still more concentrated than the SSTO HTHL air breathers. Although these configurations only increase a few points in growth factor from the baseline point up to the +10% case, it is important to note that they have gained ∼100,000 lb in empty weight in doing so. The final two configurations of the figure are vertically launched rocket boosters with upper-stage air breathers. These TSTO VTHL vehicles are less than half the empty weight of the previous TSTO HTHL vehicles. These two TSTO VTHL configurations also show fairly low scaling weight growth factors and scaling response; however, they have much steeper trend lines. This may lead to the erroneous conclusion that these vehicles are scaling faster than their TSTO HTHL counterparts. The opposite is actually true; the closure points on the steeper trend indicate less resulting empty weight growth from the same scaling response. The actual +5% solution points for both the VTHL and HTHL configurations are at a growth factor of between 6 and 7, so both categories actually experienced similar growth factor increase but with very different outcomes in terms of empty weight response.

B. Measures of Merit Figure Notation

The next four figures show the results of each closure solution for the general figures of merit chosen for this study. For the following figures, results are only presented for the best two vehicles from each general configuration category with the exception of the SSTO HTHL air-breathing vehicles, where three vehicles were presented to show the results of the SSTO turbine-based vehicle. The results are presented in bar charts with the vehicle closures for the −10% case on the front row, and the +10% case on the back row. Each bar is labeled with the actual solution point data. There are no positive (+%) growth data for the SSTO HTHL turbine-based vehicle on the far right of the figures because that configuration was impossible to close at even the +5% growth case. The +10% solution point for the SSTO HTHL 2D hydrogen rocket-based vehicle is not shown due to blowing up in a similar fashion. A vehicle thumbnail image is included to represent each configuration category and to provide ready identification of each group of data.

Figure 6 represents the scaling weight growth factors across the different closure solutions for the best two vehicles of each configuration category. In the figure, TSTO configurations are to the right, and SSTO configurations are to the left. This figure again
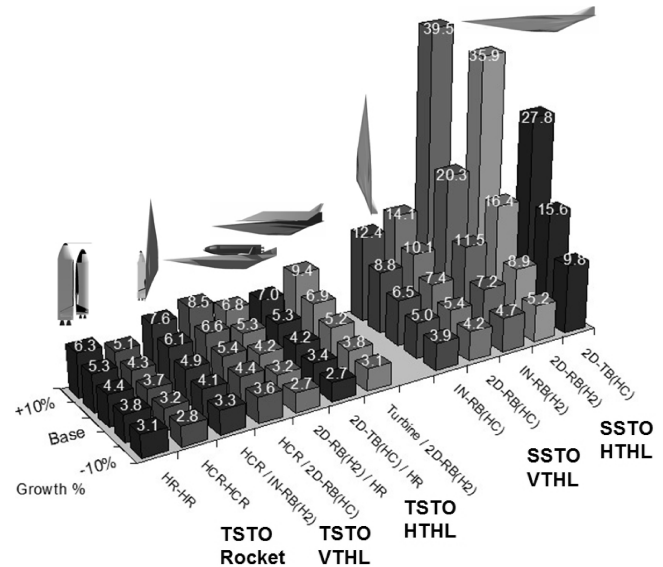
addresses the low growth factors of TSTO configurations vs SSTO. The growth factor data suggest that the development of an immature technology such as hypersonic propulsion should first be applied in a more forgiving TSTO configuration to gain experience and develop the technology and then apply that understanding to the SSTO, in hopes of achieving the lower percentage closure points.

The amounts of total vehicle empty weight for each system are shown in Fig. 7. The empty weight results for the TSTO vehicles differ markedly from each other. The three highest empty weights for the TSTO vehicles are for the two TSTO HTHL configurations and they are double the amount for the two TSTO VTHL configurations. A more detailed analysis of the causes of the differences between these configurations is contained in [5]. The highest empty weights in the SSTO category are also attributed to the SSTO HTHL vehicles, which, due to higher growth response, become larger than the SSTO VTHL vehicles. Another interesting observation is that the three different configurations using turbines for the low-speed trajectory segment have the three highest empty weights of all the configurations studied.

The total wetted area for each vehicle is represented in Fig. 8. The trends seen for wetted area follow the same patterns as those observed for the empty weight. As mentioned, the wetted area is a
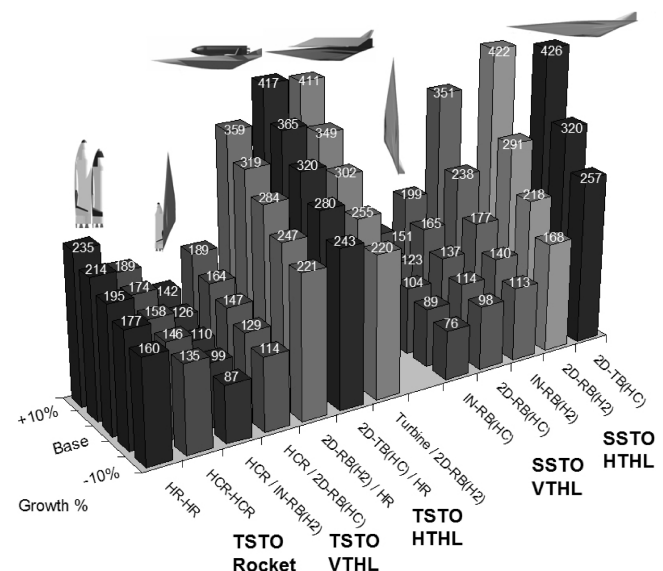

Fig. 6 Empty weight growth factors.

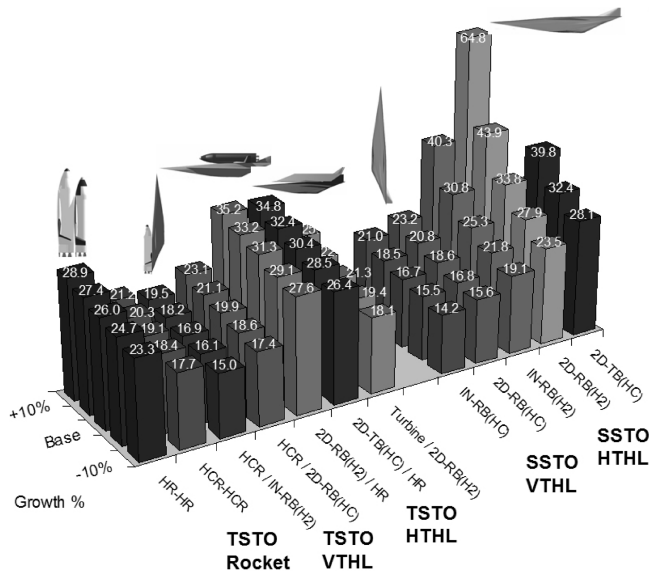Fig. 7 System empty weights, klb.

33

Fig. 8 Total wetted areas, kft^2.

strong driver for the amount of maintenance and refurbishment costs and turn time for a reusable launch vehicle. As with empty weight, not all wetted area is the same. For example, the rockets used as first stage boosters never see any substantial heating and therefore get by with much less capable TPS. In contrast, the hypersonic air-breathing vehicles all require advanced high-temperature passive TPS over every exposed portion of the vehicle's external surface and internal flowpath except for the flowpath regions that are actively cooled.

The final measure of merit is the vehicle gross weight shown in Fig. 9. This is one figure of merit in which the pure rockets come out fairly high due to their higher propellant fractions. The gross weights of some of the SSTO HTHL vehicles in this study have exceeded the assumed runway load limitation of 1.5×10^6 lb for some of the closure solutions. At +10%, all SSTO HTHL air breathers are above this limit with the exception of the all-hydrogen, inward-turning vehicle. The SSTO HTHL turbine-based vehicle is right at the limit already for its baseline case. These solutions were all for 20,000-lb payload to LEO. It is easy to foresee from the trends in this figure that any substantial increase in that payload could invalidate all of the HTHL vehicles at any positive growth percentage from operations staged from existing runways. The SSTO and TSTO VTHL vehicles have the lowest total gross weights of all the vehicles.
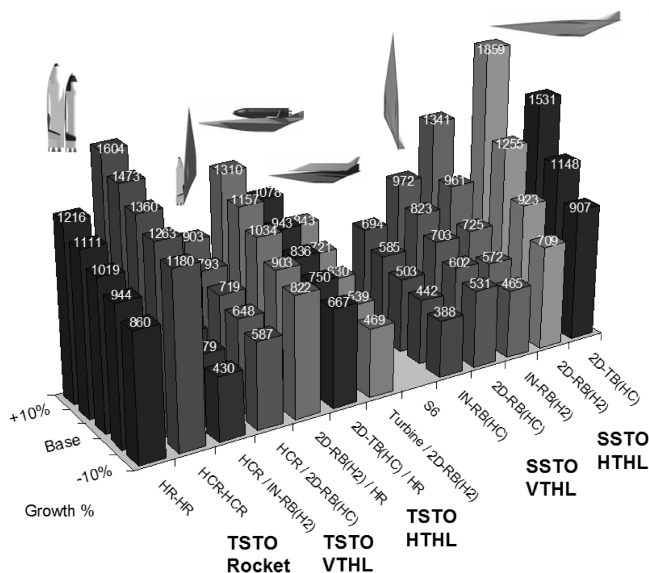
VII. Conclusions

This investigation considered 18 vehicle systems, many different configurations of air breathers and rockets, and performed a broad growth investigation to characterize the scaling behavior of each vehicle system. The general growth sensitivity conclusions that may be drawn as a result of this study are listed next. For more detailed conclusions contrasting individual baseline vehicles with each other, the reader is referred to [4,5].

For vertically launched TSTO rockets:

1) The use of staging greatly reduces the scaling behavior of these systems.

2) The three vehicle solutions for this category have very similar scaling weight growth factors and exhibit minor increases in empty weight for even large growth percentages.

3) Design success is very likely through the employment of a moderate growth margin during development.

For SSTO air breathers:

1) SSTO configurations have higher baseline scaling weight growth factors than the TSTO configurations and are highly susceptible to large increases or decreases in weight and scale for even small growth percentages.

2) For the configuration assumptions of the present study, the empty weights and scaling response of the SSTO VTHL configurations was consistently less than that observed for the SSTO HTHL configurations, with the all-hydrogen-fueled SSTO VTHL vehicles being more variable than those with hydrocarbon-fueled, low-speed propulsion segments.

3) For the HTHL SSTO configurations, the use of hydrocarbon rocket propulsion for the low-speed segment and its corresponding increase in vehicle gross weight exacerbates the growth response compared to the all-hydrogen configurations. The SSTO turbine vehicle had the highest baseline empty weight and most severe scaling response of all the configurations studied.

For TSTO air breathers:

1) As with the TSTO rockets, the use of staging benefits the TSTO air-breathing vehicles, both VTHL and HTHL.

2) Although the HTHL TSTO air breathers exhibit low growth factors (compared to SSTO), the magnitudes of the changes in weight and scale for larger growth percentages is considerable due to the higher baseline empty weights of these configurations.

3) The VTHL TSTO air breathers are consistently less than half of the total empty weight of the HTHL TSTO configurations across the applied growth percentages. Although similar to the HTHL TSTO air breathers in growth factor, the magnitudes of the changes in empty weight and scale are much less at the higher growth percentages.

Many of these observed trends have been recently corroborated by other researchers. The configurations investigated by Hank et al. [10] were analogous to many of those presented here. Other SSTO configurations were examined by Orloff , which, although similar to those of this study, used additional propellant configurations such as completely hydrocarbon-fueled configurations and vehicles using duel-fuel scramjets.

In summary, a sufficient understanding and allowance for the growth response of a particular launch configuration is vital in helping to assure a successful vehicle program. As applied to an SSTO configuration, this understanding and determination becomes of paramount importance due to the severity of the scaling response. This makes it nearly impossible to accurately set the final scale and size of the vehicle unless there is near-perfect certainty in the performance and technology of the system beforehand. Failure to appreciate or account for the severity of that response has directly contributed to the demise of previous SSTO attempts. Indeed, there are many areas of basic research ranging from the estimation of conformal hydrogen tank weight to the accounting of trim-drag and aeroelastic effects that must be addressed before the highly growth-sensitive SSTO configurations can be designed with more certainty. The TSTO configurations have lower scaling weight growth factors, indicating vehicle systems that more easily absorb design or technology changes during the development program without

Fig. 9 System gross weights, klb.

34

extreme increases in size and weight. A program with such a vehicle is many times more likely to be successful at incorporating the actual design numbers once the vehicle design has been frozen. The use of staging is a very beneficial way to reduce growth behavior and provides an intermediate point where uncertain or emerging technologies may be applied and matured in a system with a lower inherent design risk before being attempted on a more exacting SSTO configuration. A high scaling weight growth factor does *not* necessarily invalidate a particular vehicle design; it is just a measure of how much more certainty and confidence must be had in the solution parameters to be successful with that design.

Acknowledgments

References

[1] Kothari, A. P., Tarpley, C., McLaughlin, T. A., Suresh Babu, B., and Livingston, J. W., "Hypersonic Vehicle Design Using Inward Turning Flowfields," AIAA Paper 96-2552, July 1996.

[2] Billig, F. S., and Kothari, A. P., "Streamline Tracing, a Technique for Designing Hypersonic Vehicles," ISABE Paper 33.1, Sept. 1997.

[3] Kothari, A. P., Tarpley, C., and Pines, D., "Low Speed Stability Analysis of the Dual Fuel Waverider Configuration," AIAA Paper 96-4596, Nov. 1996.

[4] Dissel, A. F., Kothari, A. P., and Lewis, M. J., "Comparison of Horizontally and Vertically Launched Air-Breathing and Rocket Vehicles," *Journal of Spacecraft and Rockets*, Vol. 43, No. 1, 2006, pp. 161–169.

[5] Dissel, A. F., Kothari, A. P., and Lewis, M. J., "Investigation of Two-Stage-to-Orbit Air-Breathing Launch Vehicle Configurations," *Journal of Spacecraft and Rockets*, Vol. 43, No. 3, 2006, pp. 568–574.

[6] Livingston, J. W., "Comparative Analysis of Rocket and Air-breathing Launch Vehicles," AIAA Paper 2004-6111, Sept. 2004

[7] Bowcutt, K., Gonda, M., Hollowell, S., and Ralston, T., "Performance, Operational and Economic Drivers of Reusable Launch Vehicles," AIAA Paper 2002-3901, July 2002.

[8] Bowcutt, K., and Hatakeyama, S. J., "Challenges, Enabling Technologies and Technology Maturity for Responsive Space," AIAA Paper 2004-6005, 2004.

[9] Rooney, B. D., and Hartong, A., "A Discrete-Event Simulation of Turnaround Time and Manpower of Military RLVs," AIAA Paper 2004-6111, Sept. 2004.

[10] Hank, J. M., Franke, M. E., and Eklund, D. R., "TSTO Reusable Launch Vehicles Using Airbreathing Propulsion," AIAA Paper 2006-4962, July 2006.

[11] Orloff, B., "Comparative Analysis of Single Stage to Orbit Rocket and Air-Breathing Vehicles," M.S. Thesis, Air Force Institute of Technology, Wright–Patterson AFB, OH, June 2006.

J. Martin
Associate Editor

APPENDIX D

Comparative Analysis of

Rocket and Air-breathing Launch Vehicles

John W. Livingston[*]
USAF, WPAFB, Ohio, 45433

Abstract

This paper compares and contrasts reusable rocket and air-breathing launch vehicles. Various rocket systems are compared including reusable Two Stage To Orbit (TSTO) and hybrid systems. Air-breathing systems include TSTO and Single Stage To Orbit (SSTO) designs. Both vertical and horizontal takeoff systems are investigated. Vertical takeoff, staged rocket systems are the clear choice for systems fielded in the next 10 years. Some vertical takeoff SSTO systems look very promising. Horizontal takeoff systems are much larger, have less margin and consequently higher growth factors.

Nomenclature

ATS   = Advanced Technology Suite
CAV   = Common Aero Vehicle, reentry vehicle
HC   = Hydrocarbon
HTHL   = Horizontal Takeoff Horizontal Landing
LH   = Liquid Hydrogen
lox   = Liquid Oxygen
OMS   = Orbiting Maneuvering System
RBCC   = Rocket Based Combined Cycle
RCS   = Reaction Control System
RLV   = Reusable Launch Vehicle
SOA   = State of the Art
SSTO   = Single Stage To Orbit
TBCC   = Turbine Based Combined Cycle
TPS   = Thermal Protection System
TSTO   = Two Stage To Orbit
VTHL   = Vertical Takeoff Horizontal Landing
WER   = Weight Estimating Relationship

I.   Introduction

THIS paper presents the results of many years of studying and modeling space access systems for the purpose of comparing and contrasting their merits and liabilities and assessing technology impacts. A wide range of vehicle types have been examined ranging from VTHL rockets to HTHL airbreathers, both TSTO and SSTO.

For the last few years we have been a member of the Reusable Military Launch System (RMLS) team. This is an ad hoc team composed of members from the Air Force, NASA and industry. Our objective has been to investigate the various reusable launch system options available for meeting national needs: Air Force, NASA and commercial. There are many concepts with widely varying attributes. This makes it extremely difficult to sort through them, find

---

[*] System Design Engineer, Aeronautical Systems Center /Aerospace Systems Design and Analysis, ASC/ENMD, Bldg 11a, 1970 Monahan Way.

useful Figures of Merit (FOM) and make meaningful comparisons. This paper summarizes some of the team's findings.

II. Missions

We have been considering 3 possible mission categories:

1) Rapid Global Ordinance Delivery
The rapid global delivery mission is to deliver ordinance via CAVs to any place on the globe from CONUS. This is primarily a suborbital or once-around mission. Payload class is 15-40k lbs delivered to an easterly once-around orbit. Vehicle turn time is critical in order to keep the fleet size down and bring costs closer to those of regular bombers.

2) Operationally Responsive Space Lift
This mission stresses on-demand, flexible launch capabilities. Payloads are in the 10-15k lbs range delivered to an easterly 100 nm orbit, but at least 4k lbs delivered to a polar orbit. Again, rapid turn time is important, but probably not as critical. Both military missions have the most pressing need for rapid, low cost operations and probably the largest fleet sizes.

3) Low Cost Space Transportation
Commercial and NASA lift requirements are wide ranging, with NASA manned missions requiring the largest payload at around 60k lbs to an easterly low earth orbit. Turn times are not as critical as for the military missions.

This paper concentrates on reusable systems, but finding enough missions to justify a RLV is a major problem. The current number of worldwide launches is below 100 per year and The United States' share is much smaller. If the number of annual launches remains near present levels, expendable systems will continue to be economically viable. First partially reusable then fully reusable launch systems become more attractive as the number of annual launches increases, but only if costs, especially maintenance, can be kept low. For this reason partially reusable systems are included in this study.

For the purposes of this study, systems were sized to deliver an 8 ft diameter x 30 ft long 15k lb payload to an easterly orbit. The results are not sensitive to the payload size and are applicable over a wide range.

III. Measures of Merit

Ultimate figures of merit such as robustness, flexibility, risk, safety, mission cost and total life cycle cost are not very useful during the wide ranging conceptual phase of systems design and analysis. Needed are a few figures of merit which are good indicators for the above. This paper will make use of the following:

1) Empty Weight
Empty weight is a good indicator for development and acquisition costs. It is widely used at this stage of analysis, and is often used along with material types and complexity.

2) Complexity
Overall system complexity impacts development and acquisition costs and risks. Measuring complexity is not very quantitative and can be subjective, but is worth noting. One typically counts the number and type of major subsystems and the complexity of their interactions. Maintenance man-hours is a reasonable measure of this as well, though it does bring in the quality of the development process, in that the reliability of the subsystems are part of the equation.

3) Wetted Area
Wetted area is a good indicator for Thermal Protection System (TPS) related costs. TPS is a major contributor to maintenance man hours and turn time.

4) Uncertainty
Uncertainty estimates in conjunction with growth factors indicate technology readiness level and help set appropriate management margins for system development. The impacts on various uncertainties within the system are estimated using a Monte Carlo technique.

5) Growth Factor
There are many different growth factors. The one we are interested in is the empty weight growth factor. It is defined as the growth in system empty weight needed to restore full system flight performance in response to a change in weight. It is obtained by differentiating the system sizing equation with respect to a change in weight. It

grows asymptotically as the system approaches its performance limit. High growth factors combined with uncertainties can yield extreme variations in the final size. This is especially true of HTHL SSTO systems.

    6)   **Maintenance Man-Hours per launch cycle**

Average total man-hours of maintenance needed to prepare the complete system for its next luanch is a major contributor to operating and life cycle costs. Modeling maintenance man-hours has been a major effort of team member Brendan Rooney and is reported in **Reference 1**.

As a final observation, gross liftoff weight is *NOT* a particularly good figure of merit for this type of wide ranging comparative analysis, because it does not differentiate between propellants and hardware. Hardware is extremely expensive to develop, acquire and maintain, whereas propellants, even hydrogen, cost practically nothing by comparison.

IV.   Alternative System Concepts

Some of the system concepts evaluated are shown in **Figure 1**. Numerous rocket, scramjet and turbine propulsion combinations are considered. TSTO and SSTO systems are looked at, as are vertical and horizontal takeoff systems.

This paper reports on 17 different launch system concepts, and more are being added. All systems are fully reusable except the hybrid systems.

A brief description of each of the systems follows. More details can be found in the references. The system's identifying nomenclature is used in the included graphs.
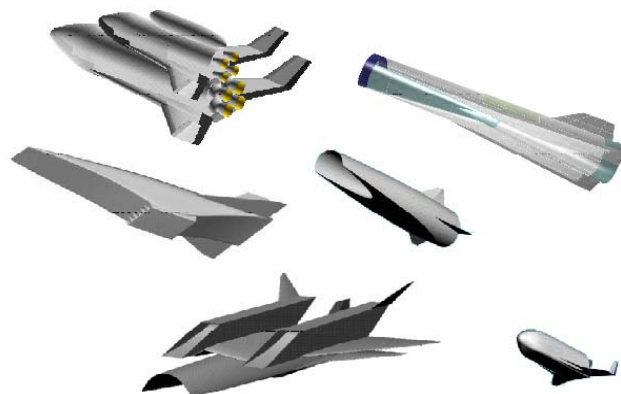
Figure 1. Some of the system concepts compared.

TSTO Rocket Systems

All of the TSTO rocket systems are VTHL and stage at 7000 fps. The boosters use turbofans to return to base. They are all serial burn. Earlier studies looked at parallel burn systems, including Bimese glide back boosters. They did not compare well to the simpler serial burn systems.

RP RP   RP1/lox engines in both stages

M M   Methane engines and subsystems in both stages

M M w   Methane engines in both stages, and Inconel structures

Multi-Stage Hybrid Rocket Systems

These systems all have reusable first stage boosters similar to the fully reusable boosters and stage at the same velocity.

RP RP   High performance RP1 /lox engines are used on the expendable upper stage

RP LH   LH/lox upper stage

RP S2   Two solid rocket upper stages

VTHL SSTO Rocket Boosted Scramjet Systems

All of the VTHL SSTO systems use rockets to boost up to the scramjet takeover Mach Number. All of these systems use LH fueled scramjets, and all use LH/lox rockets for final insertion into orbit.

V HC 2D   RP1/lox boost rockets, 2D scramjets.

V HC Inw   RP1/lox boost rockets, One Inward turning scramjet

V LH Inw   LH/lox boost rockets, One Inward turning scramjet.

VTHL TSTO Rocket Boosted Scramjet Systems

The VTHL TSTO rocket boosted scramjet systems utilize reusable first stage boosters which stage above Mach 2.5 and glide back to base. All of these systems use liquid Hydrogen fueled scramjet upper stages with LH/lox rockets for final insertion into orbit

V HCR /2D   RP1/lox booster with a 2D scramjet upper stage

V HCR /SJ   RP1/lox booster with an inward turning scramjet upper stage

HTHL SSTO Scramjet Systems

All of the HTHL SSTO scramjet systems transitioned to scramjet above Mach 2.5. All of these systems use liquid Hydrogen fueled scramjets with LH/lox rockets for final insertion into orbit.

H LH 2D   LH/lox boost rockets with 2D scramjets

H LH Inw   LH/lox boost rockets with inward turning scramjets

H HC Inw   RP1/lox boost rockets with inward turning scramjets

HTHL TSTO Scramjet / Rocket Systems

All of the HTHL TSTO scramjet / rocket systems utilize scramjets on their booster stages and stage at approximately Mach 10. They all use a LH/lox rocket orbiter stage similar to the TSTO rocket systems, but with the addition of more TPS to deal with the more severe aero heating during ascent.

TBCC /R   Over/under turbo accelerator HC engines to above Mach 3.5 and 2D LH scramjets on the 1st stage

RBCC /R   LH/lox rocket engines to over Mach 2.5 and 2D LH scramjets on the first stage

V.   Modeling Approach

The most difficult aspect of a comparative analysis as broad as this is maintaining consistency between concepts. All assumptions must be scrutinized to ensure fair treatment of all concepts. A fair comparison between traditional multistage rockets and airbreathing concepts has been our principle concern.

We are currently using 3 different software products for modeling launch systems and their components. Our original RMLS rocket system models were developed in-house using Mathcad and TechnoSoft's AML software. Mathcad was used to develop and document many of the components before transcribing them into AML and later into Astrox Corp's SIDE software. More RMLS rocket model details and results can be found in **Reference 2**. Our airbreathing systems have been modeled by Astrox using SIDE. To ensure comparable results from both products our RMLS model was translated into SIDE and comparisons made to ensure consistent results. Many of the designs have been recently published by Astrox in **Reference 3**.

This was reasonably successful but some adjustments were still needed by the time the results were in. Astrox's SIDE models have scramjet weight models that were originally correlated to more advanced materials than was assumed for the rocket models. These were corrected for. Every attempt has been made to be as fair as possible. We believe we have a reasonably accurate comparison. Having said that, there is still plenty of room for improvement and the work continues.

Model Accuracy and Uncertainties

Our rocket models are relatively mature. The models estimate weights of over 50 items which make up the empty weight. The Weight Estimating Relationships (WERs) are from numerous sources. Some were developed in-house and are physics based. All were compared and correlated with shuttle and other launch vehicle data. Our airbreathing systems models are not as advanced, but we believe they are adequate to judge relative attributes of

systems. The airbreathing system models are currently undergoing refinement in the areas of integral conformal liquid hydrogen tanks and actively cooled engine structures.

Integral conformal hydrogen tanks form the bulk of the fuselage, and low weight tanks are critical. The shapes of both 2D and inward turning scramjet fuselages lead to tank shapes which are not particularly good pressure vessels. The best way to design these tanks, and how they compare to cylindrical rocket tanks, is a current area of investigation. For the purposes of this study all integral conformal hydrogen tanks were assumed to be 150% of the weight of a cylindrical tank of the same volume. Optimum pressures in these tanks have not been established but will be lower than in corresponding cylindrical tanks due to their non-circular shapes. We believe that the more curved tank shapes should be lighter, but no advantage has been taken of this possible reduction in weight.

Our models typically estimate the areas of up to 5 temperature regions (including actively cooled areas) and allow for the estimation of unique TPS weight and maintenance for each. The scramjet vehicles' actively cooled surface areas are (depending on the concept) 5-15 times greater than the TSTO rocket engines' area. Actively cooled panels have significant weight and maintenance. Weight and maintenance uncertainties are still high, but data is being collected and models are being constructed to improve our current estimates.

VI.   Model and Technology Assumptions

Rocket Engines

Figure 2 shows existing rocket motors and two square regions that represent the state-of-the-art for high pressure HC/lox and LH/lox rockets. Performance levels are more than adequate to achieve reasonable closures for TSTO optimally staged rocket systems. An elliptical region shows the projected performance of advanced long life methane/lox engines. Advanced methane engines appear to provide a number of design, development and maintenance related advantages which more than offset their reduced density impulse. Technology is needed to improve reliability, maintainability and life.
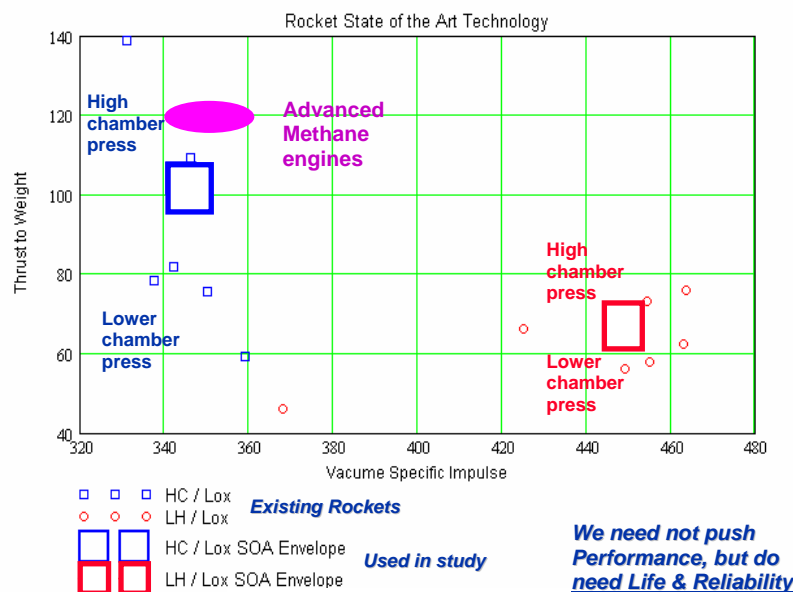

Figure 2. Rocket performance

Scramjet Engines

Two types of dual mode ram-scramjets were used in this study: 2D and Inward Turning. 2D scramjets have been extensively studied and evaluated for the last 15 years. A reasonable, but by no means complete, body of literature and data exists for them. Inward turning or streamlined traced scramjets are just as old but have not been studied to the same extent; however, this is starting to change. The Crown inlet scramjet research from the 1960's is a prime example of both an inward turning and streamlined traced design.

Adequate scramjet data and technology are still a few years in the future. The study is using what I would call nominal engine performance estimates. We did attempt to use conservative scramjet weight estimates to reflect use of existing materials. For the purposes of this study, actively cooled panel weight was assumed to be 8 lbs per square foot, and maintenance models were made sensitive to cooled area. No data exists on the probability of damage of these areas, so data on SSME rocket nozzle maintenance was used as a starting point. Our scramjet maintenance models are still emerging and only cursory results will be reported here.

Airframe Technology

Structure for the systems is assumed to be primarily Aluminum and Aluminum-Lithium alloys. An exception is the use of Inconel in some vehicles as noted. Both rockets and air-breathing systems assume integral tanks with TPS.

The impact of weight saving advanced structures is not being reported in this paper, but the assessment approach is explained in the results section. Graphite composites are being considered for tanks and other structures to save weight, and hot and warm structures are being examined to reduce TPS coverage and associated maintenance.

Thermal Protection Technology

The baseline TPS suite included technology consistent with shuttle TPS with the exception of extensive use of TUFI tiles in place of HRSI. Advanced Carbon Carbon is assumed for leading edges.
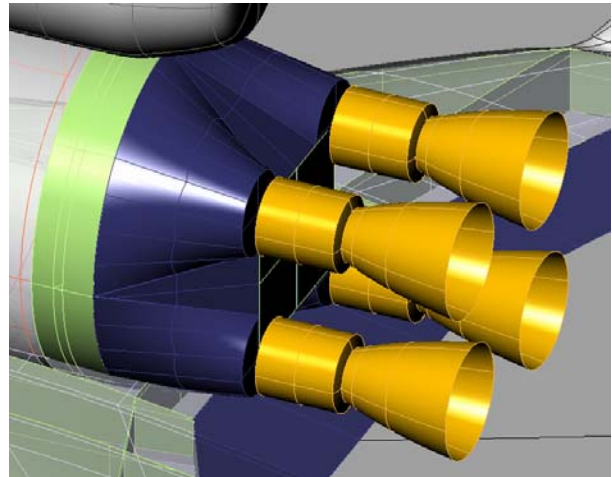
Figure 3: Nacelle Concept for Engine/Vehicle Interface

Fluid Related Subsystems

The subsystems for the baseline systems are similar to those of the Space Shuttle, just fewer of them. The ATS includes numerous advances. Autogenous RCS, OMS, APU and main propellant pressurization systems are assumed. Hydraulic and helium systems are eliminated. Fluid types are reduced down to lox, liquid methane (or similar), liquid nitrogen, and water.

Maintenance Operations

Baseline maintenance actions are derived from the Shuttle database and the knowledgeable people at Kennedy Space Flight Center who do its maintenance. They are derived from the Shuttle, but they are not Shuttle numbers. They reflect the same kinds of activities, but on a much simplified system. ATS features include numerous design improvements such as discussed above and shown in **Figure 3.** A ventilated rocket nacelle concept should significantly reduce engine removal and replacement maintenance. Maintenance assumptions are covered extensively in **Ref 1**.

VII. Study Results

The SSTO Rockets could not be sized with SOA or the ATS used, but their trend lines are shown in **figures 4-9** for completeness. The weights shown were estimated using SOA weight estimating relationships. Weight savings due to advanced technologies can be easily estimated using the graphs and the weight statements for the systems in question.

Graph Notation

The circles are the final solution weights. Plotted along with most circles are lines which indicate the empty weight uncertainty for the system. The solution circles are conservative, so they are on the high end of the uncertainty lines. Blue lines are used for systems that contain only LH and lox. Red lines are used for any system that uses RP1 in some segment of its flight. Magenta is used for the systems with methane. The different fuels show slightly different trends.

Uncertainty

Probabilistic (Monte Carlo) simulations show that the uncertainty for the rocket models is in the neighborhood of 4% of the vehicle empty weight fraction, so that value has been used for every rocket system plotted. The uncertainties in the airbreathing models are greater, but not well quantified. A 6% band is assumed for all of them and seems reasonable, if not optimistic, given the state of our airbreathing models. The resulting length of the line is caused by the uncertainty and the growth factor of the system being modeled. Systems which are harder to close (i.e. have less margin) will have higher growth factors. If the system concept is beyond the reach of the technology,

asymptotic weight growth occurs and no closure is possible at any weight. Green regions indicate reasonably good solutions.

Gross Weight Trends

Figure 4 shows gross weight trends plotted versus empty weight for the different systems

Gross weight trends are frequently given, but don't indicate whether the weight is propellant or structure. Most of the gross weight for rocket systems is in the form of inexpensive propellants, primarily lox. For Airbreathing systems a much higher percentage of the gross weight is in structures and propulsion. All of the vertically launched systems, both rockets and airbreathers, have considerably lower empty weights than the horizontally launched systems, with the exception of the SSTO rocket which did not achieve closure, i.e. could not be sized.

An examination of the details shows that there is a large weight penalty associated with the larger takeoff wing and gear needed for the horizontally launched systems. The wing and gear weight is much lighter for the vertically launched systems, which only need the wing for high speed flight and the gear and wing for landing while nearly empty. Also, rocket engines weigh little, so installed thrust-to-weight ratios above one do not impose much penalty. In the end, the weight penalty for increasing the size of rocket engines and associated structure is less than for increasing the size of wings and gear.
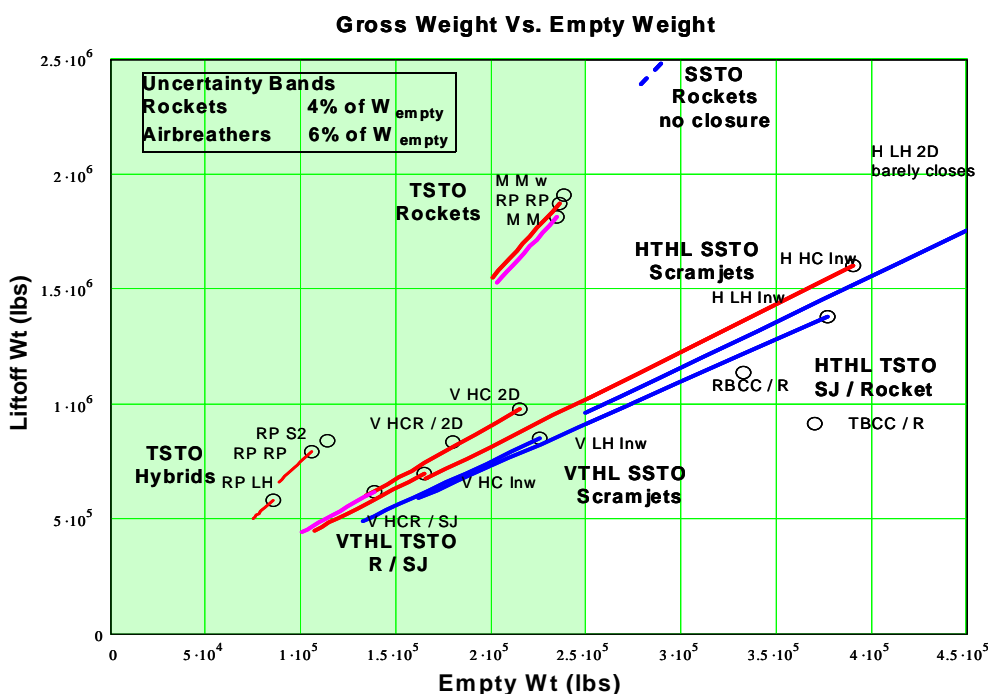
Figure 4.   Liftoff Weight vs. Empty Weight in (lbs)

Empty Weight Trends

In **figure 5,** empty weights are plotted against the empty weight fractions. This chart clearly shows how the uncertainty in empty weight fractions affects the various systems. Notice the extreme effect uncertainty has on the HTHL SSTO launched systems. This indicates that they have less inherent design margin.

This chart can also be used to show the impact of weight saving technology on the empty weight of the systems. First, you have to estimate how much the advanced technology will reduce the weight of the components. Then, for each specific design, determine what fraction the effected components are of the empty weight fraction. For example, let us consider the impact of graphite composite technology on the advanced methane design. If graphite composite tank technology decreases tank weight by 15%, and the tanks make up 10% of the empty wt, and the systems empty weight fraction is 12%, then the technology will reduce the empty weight fraction to:

$$(1-.15*.1).12 = .1182$$

7
American Institute of Aeronautics and Astronautics

42

The "M M" methane system with SOA WERs weighs about 240k lbs. If we reduce its empty weight fraction to .1182 it will weigh about 220,000 lbs.
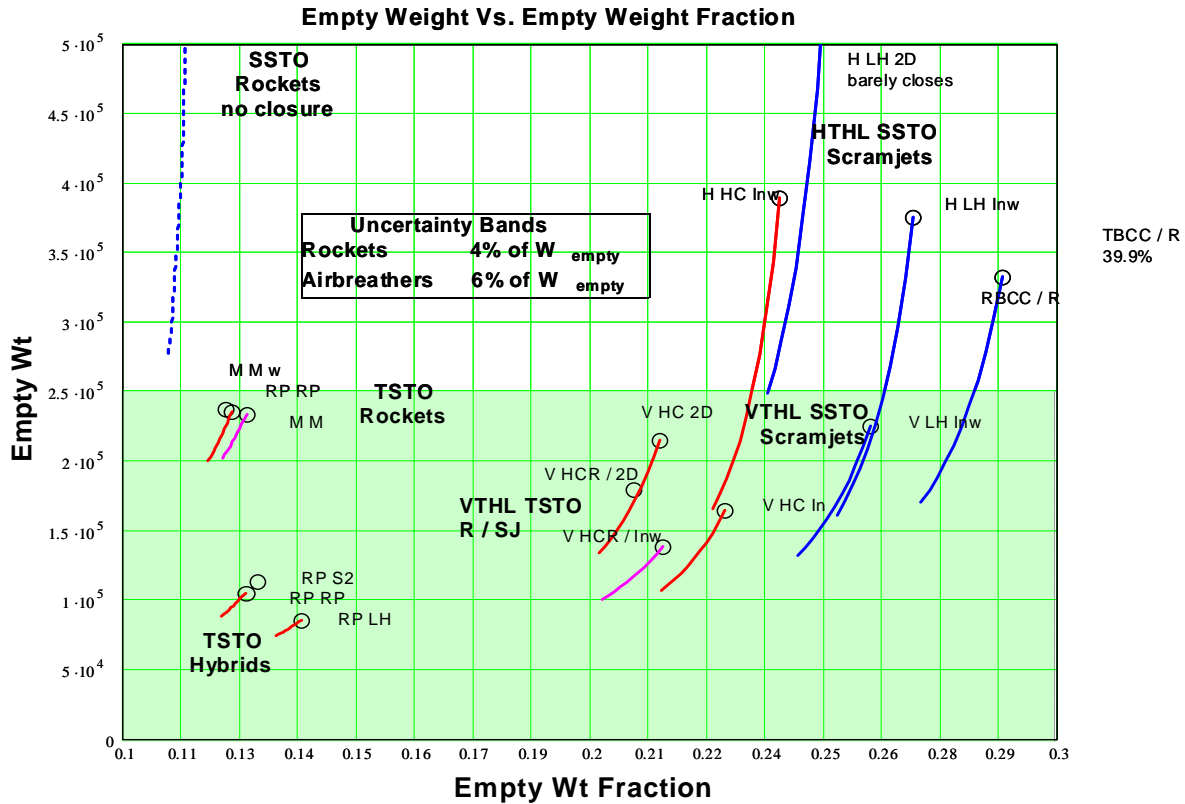

Figure 5. Total Empty Weight (lbs) vs. Empty Weight Fraction

Growth Factors Trends

Figure 6 shows a plot of Empty Weight Growth factors vs. Empty Weight. The growth factor is the derivative of the empty weight with respect to a change in the "scaling empty weight" of the vehicle. It measures how sensitive the design is to empty weight uncertainty. As can be seen, the large empty weight uncertainty bands are associated with systems with high growth factors or high uncertainties or both. All of our rocket designs are plotted with 4% empty weight fraction uncertainty and the airbreathers with 6%.

Examination of the following system sizing equation illustrates the general nature of the trend lines. W_g is gross weight, w_{pyld} is payload weight, $w_{fx.n}$ is fixed weight items and f_s and f_p are the scaling and propellant weights divided by gross weight. For a given system, the payload and fixed weight items are constant by definition. The scaling empty weight fraction is assumed to be constant for a given design concept as is the propellant fraction. In practice these are very good assumptions in a neighborhood around the solution point. As the sum of the scaling empty weight fraction and propellant fraction approach unity, the gross weight grows asymptotically large.

$$W_g = \frac{w_{pyld} + w_{fx}}{1 - f_s - f_p}$$

$$dW_{e\_dws} = \frac{w_{pyld} + w_{fx.n}}{\left[1 - \left(1 + \frac{\Delta ws}{w_s}\right) \cdot f_s - f_p\right]^2 \cdot w_s} \cdot f_s^2$$

In reality the fractions are not exactly constant, but they are very close to constant. A small correction factor was introduced, and this equation was used to nicely curve fit the results of our computer models. The empty weight growth factor equation is then derived as shown.
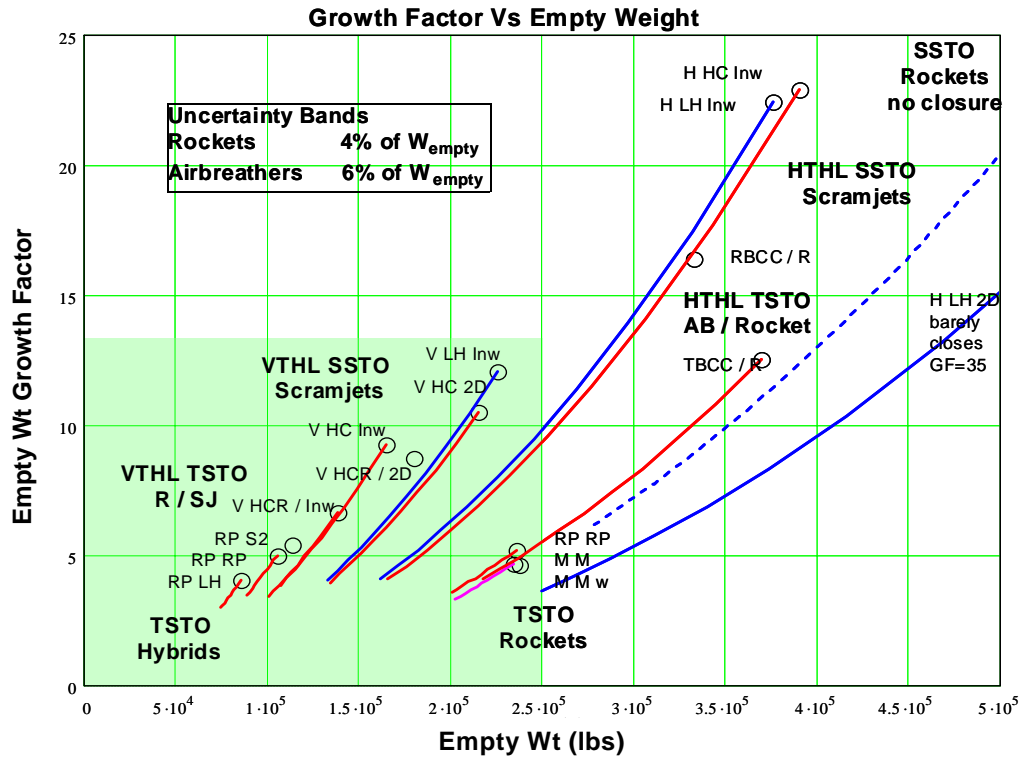
Growth Factor Vs Empty Weight

Figure 6. Growth Factor vs. Total Empty Weight (lbs)
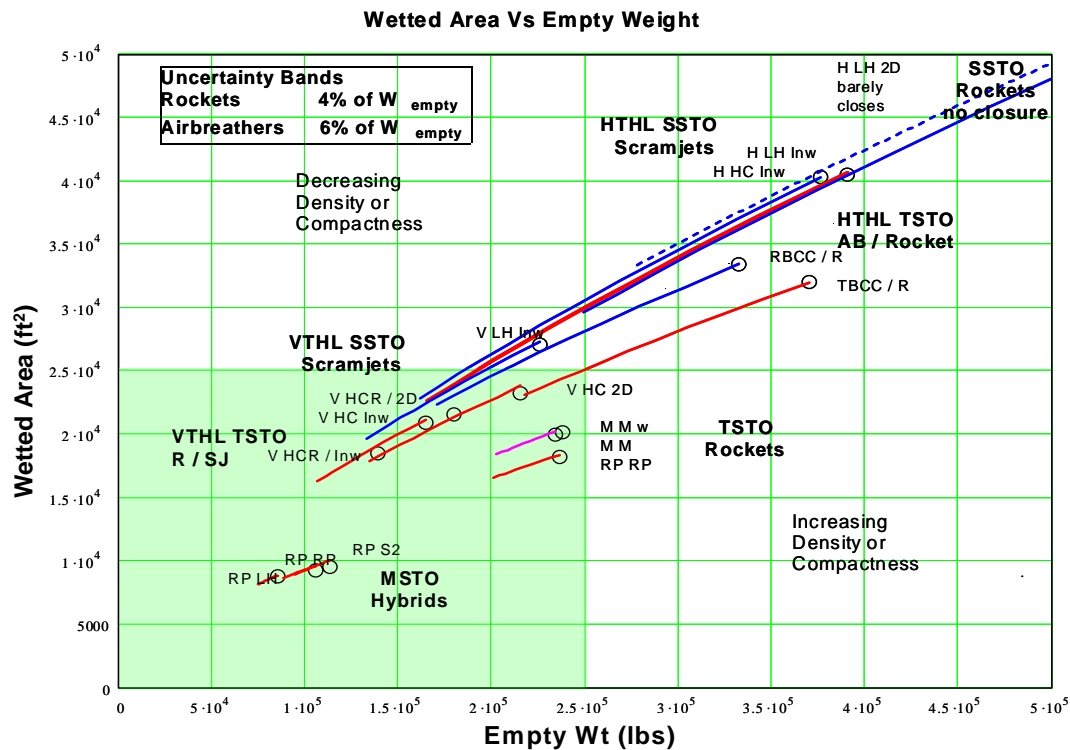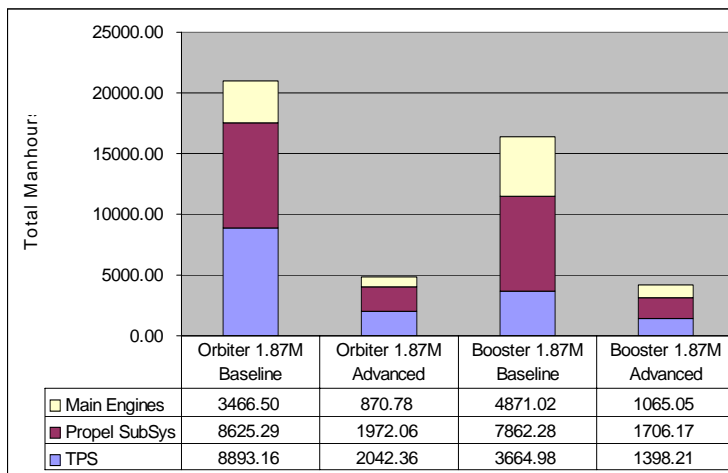
Wetted Area Vs Empty Weight

Figure 7. Wetted Area (ft^2) vs. Total Empty Weight (lbs)
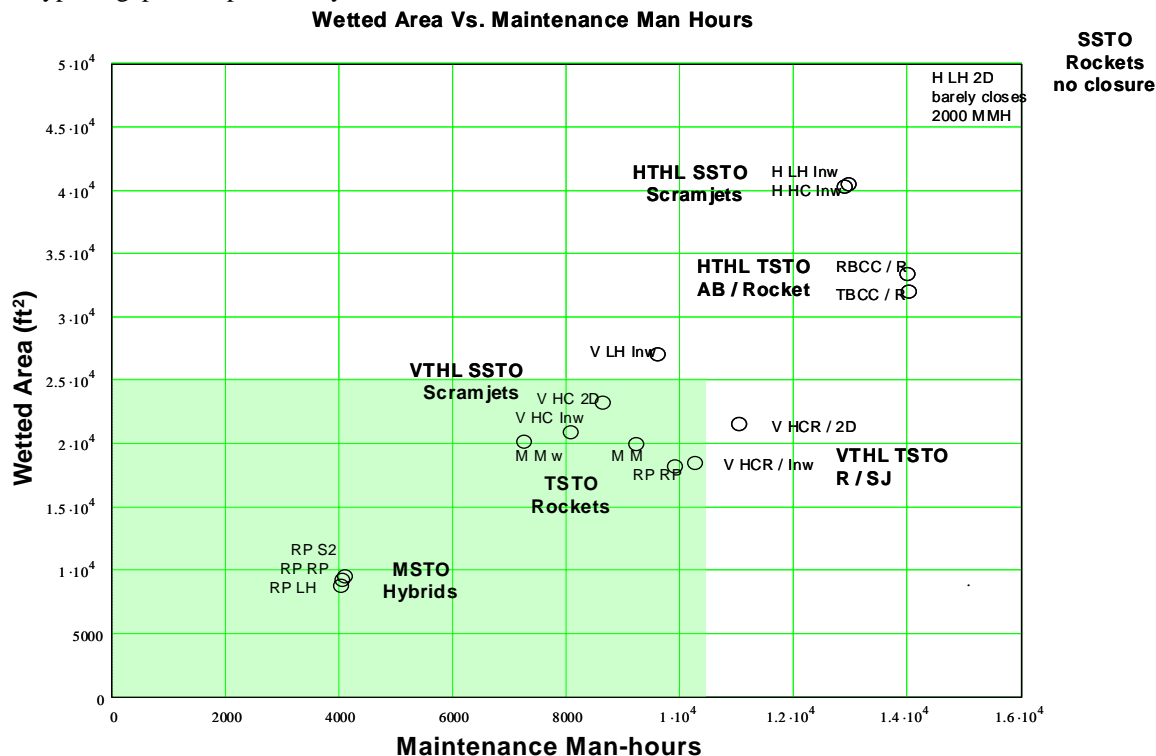
Wetted Area Trends

Figure 7 plots Wetted Area vs. Empty Weight. You can see the nonlinear variation of the wetted area with size. The wetted areas are nearly proportional to the empty weight to the 2/3 power as would be expected with scaling which is nearly, but not quite geometric. You can clearly see the effect of the horizontal takeoff requirement. The wetted areas are two or more times larger than for the vertical systems. Some of this can be removed by increasing the takeoff velocity. HTVL systems also have the lower density LH fuel to contend with, and when one tries to increase the density by using HC during the early boost phase one just drives up the wing size, with the net result being no gain. The effect of HC during the early boost phase is completely different for the vertical takeoff systems. The use of HC always reduces the wetted area for vertical launched systems.

Maintenance Trends

The RMLS operations and maintenance model (**Reference 1**) is being developed to provide design and technology sensitive parametric estimates of man-hours and clock-time needed to support and maintain different types of launch systems. It builds up estimates of failure probabilities and maintenance man-hours from low level component failure modes and associated maintenance actions. Parametric, probabilistic models of these "maintenance actions" are developed and made sensitive to design, technology, and development parameters. For example, TPS tile maintenance is sensitive to total area covered, average tile size, type of gap seals, probability of

	Orbiter 1.87M Baseline	Orbiter 1.87M Advanced	Booster 1.87M Baseline	Booster 1.87M Advanced
Main Engines	3466.50	870.78	4871.02	1065.05
Propel SubSys	8625.29	1972.06	7862.28	1706.17
TPS	8893.16	2042.36	3664.98	1398.21

Figure 8. Man hours for SOA 'RP RP' and ATS 'M M'

Figure 9. Wetted Area (ft^2) vs. Maintenance Man-Hours

10
American Institute of Aeronautics and Astronautics

damage, location on vehicle, type of attachment and water proofing needs. Some parameters are adjusted for vehicle design differences, such as TPS area, others for technology improvements such as more durable TPS, which would reduce the probability of damage.

Statistical models for main engines, fluid related subsystems, and TPS have been built up. These account for most of the maintenance actions. Fluid related subsystems include: all pressurization systems, RCS, OMS, APU and cooling systems. The 'main engine' and 'fluid related subsystems' models are primarily sensitive to their number, type and quality, and not as sensitive to their size. Conversely, the TPS maintenance is directly related to wetted area as well as to its type and quality. **Figure 8** shows an example of a comparison between a SOA RP1/lox (RP RP) system and an ATS methane/lox (M M) system. The ATS system has a range of improvements in technology, design and development. Advances in TPS, fluid related subsystems, engines, integration all contribute to the large reductions in maintenance.

The maintenance models for the airbreathing components have been defined, but as noted earlier, there is little data with which to correlate our models. Work is ongoing, but some initial estimates can be made. If we assume that each of the systems contains similar advanced rockets and subsystems, they should have similar maintenance hours for each stage for these items. There are two exceptions, the 'TBCC / R', with its more complex booster, and the hybrids with expendable upper stages. We are currently tracking about 2,800 average man-hours per sortie to maintain the main engines and the fluid related subsystems for each advanced TSTO rocket 'M M' stage. I have used this as an estimate for all advanced Methane stages and 3300 man-hours for advanced RP stages. To account for airbreathing systems' TPS and scramjet maintenance, we are currently assuming that most of the scramjet maintenance will be related to its actively cooled panel area. The actively cooled panels, seals and actuator maintenance should all be strong functions of cooled area. The scramjet systems' TPS heating load is more severe than the rocket systems', and they have 5 to 15 times the amount of active cooling. The maintenance per square foot will certainly be worse than the rocket systems, but by how much is hard to say. As an initial estimate, we are assuming 0.25 man-hours per square foot for all the scramjet vehicles. This is about what our advanced orbital maintenance is, so this estimate is optimistic.

Figure 9 shows that the systems with the lowest maintenance are the hybrids. They only have one small booster to maintain; however, many millions of dollars worth of upper stage hardware are thrown away per launch. SSTO vertical takeoff scramjets and TSTO rockets still appear to be favored if fully reusable systems are desired.

VIII. Promising Concepts and Future Work

RMLS 102 is our current baseline reusable system concept. It is an optimally staged TSTO VTHL System. It has serial burn HC/lox rockets on both stages. It is designed to be able to lose an engine on either stage at any time during the launch and still make the mission. RP1 and other hydrocarbons have been investigated. Cryogenic hydrocarbon fuels look attractive for their ability to simplify fuel related subsystems and operations. We will be looking at methane very closely for all of our HC rockets. We will further investigate the complete removal of high pressure hydraulic and helium subsystems through the use of autogenous pressurization and electric actuators. We will be trying to get down to 4 fluids: methane (or similar), lox, water and liquid nitrogen. We will further investigate the use of warm and hot structures for aero surfaces in order to minimize TPS maintenance. RMLS 102 is one of the smallest and simplest of the fully reusable system concepts investigated to date.

RMLS 107 is our hybrid system concept. The reusable booster is a smaller version of our RMLS 102. This system concept seems to be a rational step between expendable and fully reusable systems.

RMLS 401 is a SSTO VTHL HC/lox rocket boosted LH Scramjet system. It transitions to scramjet mode at about Mach 4 or slightly higher. The scramjet has minimal variable geometry and should be capable of Mach 4 to 14. It features an inward turning semicircular or kidney bean shaped Busemann Inlet. A 2D scramjet will be carried along as well. A large portion of the vehicle fuselage skin is designed to be in tension to minimize structural weight and simplify construction. Integral LH tanks are used. A LH/lox rocket is used to finish acceleration into orbit. This is an RBCC with the rockets integrated into the scramjet nozzle just downstream of the combustor. They are stored flush when not used. The RMLS 401 is the smallest, simplest SSTO airbreathing concept investigated to date, and it appears to be competitive with TSTO Rocket systems.

RMLS 304 is a TSTO VTHL HC/lox rocket boosted Scramjet system. The upper stage is a nearer term technology version of the 401. It is staged at about Mach 4. The booster glides back to base, perhaps with a small amount of

"boost back". The scramjet is assumed to be less capable: Mach 4+ to 12+. If the 304 is designed around the hybrid booster, it would be able to launch a payload of greater than 15,000 lbs.

IX.   Conclusions

- **Numerous reusable and partially reusable rocket systems are attractive and technically achievable now**, but sufficient numbers of annual missions and reduced costs are needed to justify their development. They are all two or more staged systems, and are vertically launched. The partially reusable systems are comprised of a reusable booster with expendable upper stages. Vehicle turn times of one to two weeks appear to be achievable with existing technology by using "ops-focused" design and development practices. The desired time of 24-48 hours (to be more "aircraft like") is beyond the state of the art but is within reach with a reasonable level of, again, "ops-focused" technology investment. Further reductions of turn time and operations costs will require technical advances to support development of durable, operable thermal protection systems, rocket engines, and fluid related subsystems. Maintenance and turn time is dominated by these subsystems.

- **Technology development, design and system development must be focused on operability**. A thorough (more aircraft like) development program will be necessary to obtain the levels of operability desired. Such a program could easily extend up to 10 years. Systems with considerable design margin make development easier. To this end, it is paramount that we keep our requirements lean, focus on simple systems and optimize them for high operability.

- **Horizontal launch does not improve the turn time of launch systems, it increases it.** This is due to the increased maintenance associated with their larger size. Times to mate, transport and fuel should be similar for both horizontal and vertical launch, while vertical launch pad mating, erection and fueling can be made small relative to the maintenance times of large horizontally launched systems. Systems such as Zenit have shown launch times of a few hours by automating the procedures.

- **"Aircraft-like" operations for "access to space" should not necessarily imply turbine based horizontal takeoff systems.** Conventional wisdom is sometimes wrong. These launch systems fare very poorly against vertically launched rocket and combined rocket/scramjet based systems. Horizontally launched TBCC/rocket systems are among the worst, being larger, having heavier empty weights and much greater wetted areas, including extensive amounts of actively cooled area. They are more complex, contain three different types of engines, and will have significantly larger amounts of maintenance. Having said all of this, there are hypersonic cruise missions where TBCC may be the engine of choice, but not for pure access to space.

- **Airbreathing propulsion for "access to space" should focus on vertically launched rocket/scramjet systems with an eye to SSTO.** Good scramjet performance in the Mach 10-15 régime, light weight integral tanks and advanced thermal protection systems are critical in achieving this goal. It is very difficult for a TSTO airbreathing concept to compete with a TSTO rocket system; having said that, a TSTO rocket boosted scramjet would be a lower risk first step towards SSTO. This system could launch considerable payload using the small hybrid class booster, and pave the way for SSTO. Above all we need to keep these scramjet designs as simple as possible without giving up too much margin.

Acknowledgments

References

[1]Rooney, B. and Hartong, A., "A Discrete-Event Simulation of Turnaround Time and Manpower of Military RLVs", AIAA-2004-6111, *AIAA Space 2004 Conference*, AIAA, Washington, DC, 2004.
[2]Hartong, A. and Rooney, B., "Near-Term RLV Options", AIAA-2004-5947, *AIAA Space 2004 Conference*, AIAA, Washington, DC, 2004.
[3]Dissle, A., Kothari, A. and Lewis, M, "Comparison of HTHL and VTHL Air-Breathing and Rocket Systems for Access to Space", AIAA-2004-5947, *AIAA Joint Propulsion 2004 Conference*, AIAA, Washington, DC, 2004.

APPENDIX E

Cost Comparison of Expendable, Hybrid, and Reusable Launch Vehicles

Greg J. Gstattenbauer[*] and Milton E. Franke[†]
Air Force Institute of Technology, Wright-Patterson AFB, OH 45433

John W. Livingston[‡]
Aeronautical Systems Center, Wright-Patterson AFB, OH 45433

This paper compares developmental, production, and maintenance costs (DPM) of two-stage-to-orbit expendable, hybrid, and reusable launch vehicles. This comparison was accomplished using top level mass and cost estimating relationships. Mass estimating relationships were correlated to existing launch system data and ongoing launch system studies. Cost estimating relationships were derived from Dr. Dietrich Koelle's "Handbook of Cost Engineering for Space Transportation Systems: Transcost 7.1". Hybrid launch vehicles appear to be preferable if current or modest increases in launch rates are projected while reusable launch vehicles appear preferable for large projected increases in launch rates.

Nomenclature

AOA	=	Analysis of Alternatives
CER	=	Cost Estimating Relationship
DOC	=	Direct Operating Cost
DPM	=	Development, Production, and Maintenance
ELV	=	Expendable Launch Vehicle
FUPC	=	First Unit Production Cost
HLV	=	Hybrid Launch Vehicle
LCC	=	Life Cycle Costs
MER	=	Mass Estimating Relationship
MYr	=	Man Year
RLV	=	Reusable Launch Vehicle
RMLS	=	Reusable Military Launch System
TPS	=	Thermal Protection System
TSTO	=	Two-Stage-To-Orbit

I. Introduction

THE United States space launch market requires low cost access to space. The argument over whether an expendable, hybrid, or reusable launch system should be used remains an ongoing debate. All current launch platforms (other than the Space Shuttle) are expendable launch vehicles (ELVs). ELVs are less expensive and are economically lower risk to develop. However, the total life cycle cost (LCC) for ELVs rises dramatically for increasing launch rates.

---

[*] 1st Lieutenant, U.S. Air Force, currently, Ground System Engineer, SMC Det 12, Space Vehicle Operations, 3548 Aberdeen Ave SE, Kirtland AFB, NM.

[†] Professor of Aerospace Engineering, Department of Aeronautics and Astronautics, 2950 Hobson Way, Wright-Patterson AFB, OH, AIAA Associate Fellow.

[‡] Aerospace Engineer, Aeronautical Systems Center, XREC, 1970 Monahan Way, Wright-Patterson AFB, OH, AIAA Member.

The views expressed herein are those of the authors and do not reflect the official policy or position of the U.S. Air Force, Department of Defense, or the U.S. government.

Hybrid launch vehicles (HLVs) are defined in this paper to be a first-stage reusable, second-stage expendable, launch system. HLV development costs are higher than those of ELVs due to fact that the first-stage booster is reusable. HLVs offer higher reliability than ELVs due to airframe robustness and system efficiency. The analysis of alternatives (AOA) performed by Aerospace Corporation concluded that the HLV is the preferred option based on current launch needs.[1]

The last alternative is reusable launch vehicles (RLVs). RLVs will be significantly more expensive to develop than HLVs or ELVs. However, RLVs provide the capability to meet both current and future needs of U.S. space launch vehicles.[1] RLVs can be designed to be more flexible than expendable counterparts, providing aircraft-like operations from military installations.

The purpose of this paper is to compare the developmental, production, and maintenance costs (DPM) of expendable, hybrid, and reusable launch vehicles. This comparison was accomplished using top level mass and cost estimating relations (MERs, CERs). Mass estimating relations were correlated to existing launch vehicle data and ongoing launch vehicle studies. Cost estimating relations were derived from data and existing CERs provided by Dr. Dietrich Koelle's "Handbook of Cost Engineering for Space Transportations Systems: Transcost 7.1".[2]

II. Research Focus

For this study, each launch vehicle is a two-stage-to-orbit (TSTO), hydrocarbon fueled, vertically launched system. The HLV and RLV are both horizontal landing vehicles and therefore control surfaces and landing gear. The maximum vehicle life for the reusable vehicles is set at 200 launches and the total system life is 20 years. Development and first unit production costs are functions of stage dry mass. Maintenance cost is a function of wetted area and engine dry mass. Maintenance relations were developed by the Aeronautical Systems Center (ASC).[3]

III. Methodology

A. Mass Estimating Relationships

Assumptions[4] were made for the total change in velocity (delta V) required by the launch vehicle to reach low Earth orbit to be 30,000 ft/s. This assumed delta V accounts for aero, gravity, and back pressures losses experienced during launch. Because the vehicles are hydrocarbon fueled, the assumed ELV first and second stage Isp values are 300s and 320s respectively. The ELV stage Isp values used are consistent with current expendable engines. The RLV Isp values were 320s and 350s for first and second stages while HLV used 320s Isp for both stages. HLV first stage and both RLV stages can afford using a more efficient engine due to their reusability. A structural mass fraction of 0.045 was used for ELVs, while the HLV and RLV structural mass fractions were approximated via summarizing the mass fractions for wings, stack, and thermal protection system (TPS). The MER model approximates stage dry mass using basic rocket sizing relationships.

Figures[5] 1, 2, and 3, illustrate the MER model's prediction of dry mass with respect to payload mass. The blue lines in each figure describe the predicted total dry mass, while the red lines describe the predicted dry mass of
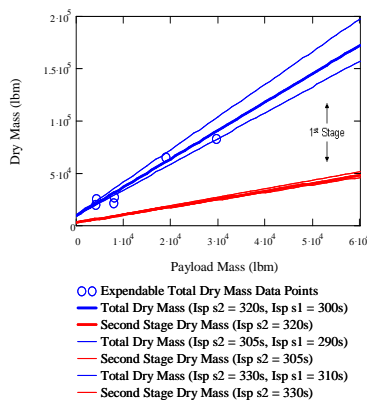

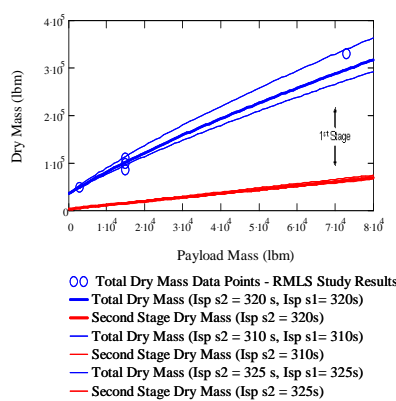**Figure 1. ELV total dry mass versus payload**

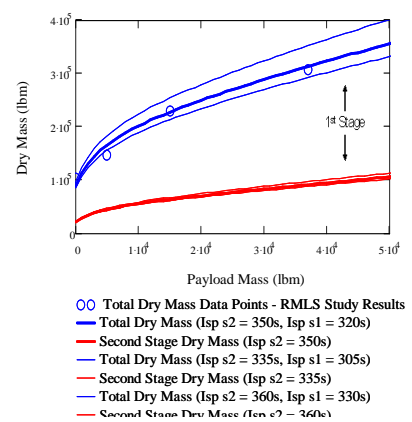**Figure 2. HLV total dry mass versus payload**

Figure 3. RLV total dry mass versus payload

the second stage. First stage dry mass can be found by subtracting the second stage dry mass (red line) from the total dry mass (blue line). The MER models were correlated to existing ELVs used by industry or Reusable Military Launch System (RMLS) studies performed by government. The sharp decrease in hybrid and reusable launch vehicle dry masses at small payloads is due to the square-cubed relation of TPS. At very high payloads, the TPS mass fraction becomes smaller.

B. Cost Estimating Relationships

The following sections cover the cost estimating relations for development, first unit production, and maintenance costs of ELV, HLV, and RLV airframes and engines. Costs from the CER model were outputted in Man Years (MYrs) but can be converted to present dollars; one MYr was approximately $230,000 in 2004[4]. Figure 4 details the different dollar equivalent of one MYr for the past 60 years.
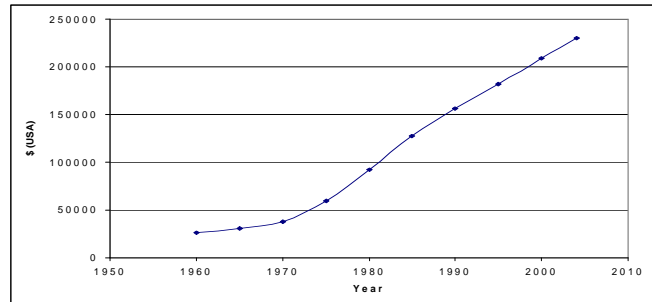
Figure 4. Man year costs over the past 60 years

1. *Airframe Development CER*

Airframe development CERs were derived from best fit of data provided by Koelle. Airframe development is a function of stage dry mass. The expendable and reusable airframe development CERs used in this study differ from Koelle. When compared, the reusable and expendable airframe development CERs developed by Koelle showed an inconsistent trend for increasing stage dry mass. The difference between the reusable and expendable airframe development CERs decreased as stage dry mass increased. For this reason, two new curves were generated that better approximate development effort as a function of dry mass.[5] HLV development costs are calculated using the same RLV first stage and ELV second stage development CERs. The reason for this is because of the definition of HLVs used in this study. HLVs are defined to have a first stage reusable booster and second stage expendable orbiter.

2. *Airframe First Unit Production CER*

Airframe first unit production costs (FUPC) were determined via the same method as airframe development costs. Existing FUPC data were correlated with a best fit power curve. Similar to the airframe development, the reusable airframe FUPC CER developed by Koelle was found to be inconsistent with the expendable FUPC CER. Comparison of the two CERs on the same graph revealed that Koelle's predicted reusable airframe production was less than expendable vehicles with the same stage dry mass for low sizes. This was incomplete due to the increase in system and airframe robustness required by reusable vehicles. To correct for this discrepancy, a new best fit curve was developed.[5]

3. *Vehicle Maintenance CER*

Vehicle maintenance includes airframe, engine, and subsystems for the reusable and hybrid launch vehicles. Since the HLV first stage and RLVs are launched more than once, the cost for turning the vehicle around must be included for DPM analysis. Also, vehicle maintenance is important when designing a military system. Maintenance time helps determine the fleet size required to carry out military-like operations with bomber-like sortie rates. The engine maintenance CER[5] was developed by Brendan Rooney of ASC/XRE. Subsystem maintenance was assumed to be 250 man hours for first stage booster and 500 man hours for the second stage orbiter. Airframe maintenance is related to wetted area of the vehicle. To calculate area maintenance, relationships of TPS area percentages were derived from calculated maintenance times from previous work done by Mr. Rooney. It is important to note that maintenance costs are very uncertain since no hybrid or reusable vehicles have been developed that provide accurate data. For this reason, maintenance costs must be viewed as being a best-guess estimate.

IV. Results and Analysis
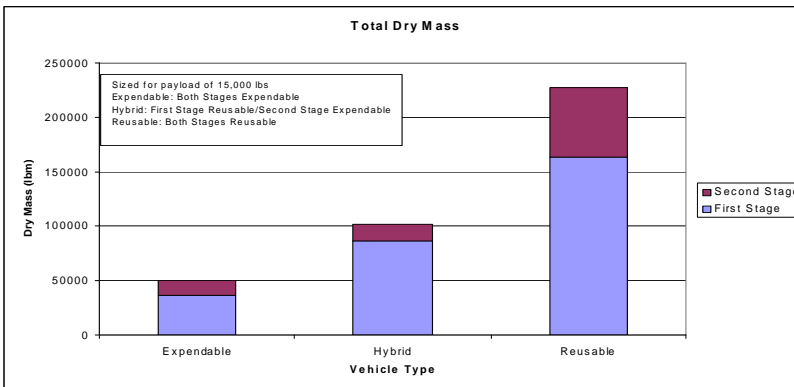
A. Vehicle Sizing

Vehicle size for each alternative was predicted using a MER model.   The MER model uses payload mass and stage Isp to calculate vehicle dry mass. The MER model correlates well to existing launch vehicle data from industry and RMLS data produced by government. Table 1 contains the stage Isp used for each vehicle alternative. Table 2 details predicted vehicle dry mass while Fig. 5 graphically displays predicted dry masses for each alternative sized for a payload mass of 15,000 lbs.

Table 1. Stage Isp for Each Vehicle Alternative

Vehicle Type	1st Stage (s) Isp	2nd Stage Isp (s)
Expendable	300	320
Hybrid	320	320
Reusable	320	350

Table 2. Vehicle Sizing @ Payload of 15,000 lbs

Vehicle Type	1st Stage Dry (lbm)	2nd Stage Dry (lbm)	Total Dry (lbm)
Expendable	35996	13950	49946
Hybrid	86273	15109	101382
Reusable	163551	63673	227224

Figure 5. Dry Mass for Each Vehicle Type

The HLV and RLV are both more massive than the expendable. The HLV is roughly two times, while the RLV over four times the mass of the ELV. The reason for the increased dry mass is due to the aero surfaces, TPS, and landing gear required by the first stage for the HLV and both stages for the RLV.

B. Airframe Development Effort

The development efforts for vehicles sized with a payload mass of 15,000 lbs are found in Table 3. Development effort was calculated using the CER model. The ELV development effort converted to 2004 U.S. currency is $8.7 billion. The HLV is roughly twice and the RLV is about 3.5 times that of the ELV alternative. Figure 6 illustrates the predicted airframe development versus payload mass.
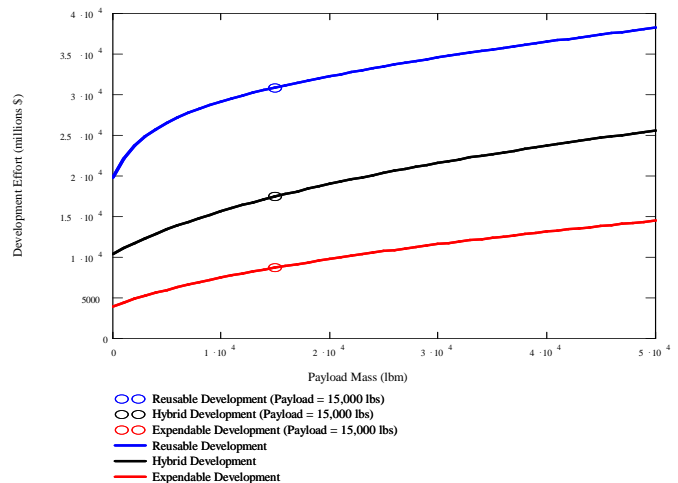
Figure 6. Developmental costs vs. payload mass for each vehicle option

Table 3. Airframe development effort @ payload of 15,000 lbs

Vehicle Type	Airframe Development Cost (2004 $)
Expendable	8.7 billion
Hybrid	17.4 billion
Reusable	30.8 billion

C. Airframe First Unit Production Costs

First unit production costs are the price tag of building the first deliverable. Production costs decrease as more vehicles are manufactured through application of a production learning factor. A production learning factor is significant for an expendable vehicle due to the requirement of a new vehicle for each launch. The CER model predicts an ELV airframe cost of $167 million. For a learning factor of 95%, the production cost will decrease to 71% of the FUPC after the 100th vehicle is produced. A Delta IV Medium launch vehicle delivers an equivalent payload for a launch cost of roughly $130 million in 2004 dollars.[6] With the application of a learning curve, the CER model predicts a similar production cost. The learning factor also applies to the second stage of the HLV since that stage is expendable. Figure 7 illustrates predicted FUPC versus payload mass. Table 4 contains the FUPC estimates for the different vehicle options sized for a payload of 15,000 lbs.
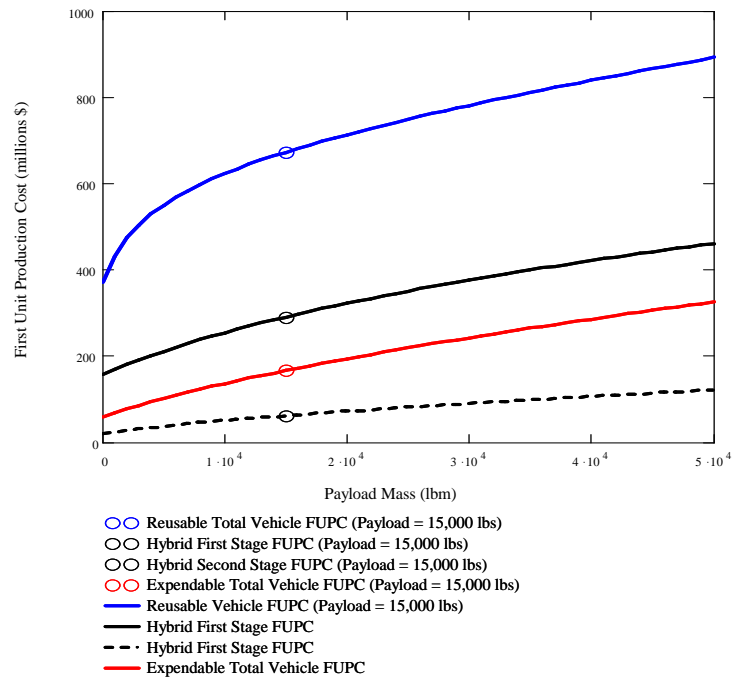
Figure 7. First Unit Production Costs vs. Payload Mass for Each Vehicle Option

Table 4. Airframe FUPCs @ payload of 15,000 lbs

Vehicle Type	First Unit Production Cost (2004 $)
Expendable: Total	167 million
Hybrid: First Stage	290 million
Hybrid: Second Stage	62 million
Reusable: Total	673 million

D. Engine Development Effort

Engine development effort is related to the size of the engines. A launch vehicle can use smaller engines which cost less to develop but will require more engines per stage, increasing production costs. Table 5 contains the engine sizing inputs used for this study. The number of engines was determined through discussion with individuals from ASC. Engine thrust was calculated from vehicle gross mass and the number of engines used per stage. Table 6 is the predicted engine development effort for each vehicle alternative. Figure 9 illustrates the total engine development required for each alternative.

5
American Institute of Aeronautics and Astronautics

Table 5. Engine size @ payload of 15,000 lbs

Vehicle Type	Number of Engines First Stage	First Stage Engine Thrust (lbf)	Number of Engines Second Stage	Second Stage Engine Thrust (lbf)
Expendable	1	1079433	1	182100
Hybrid	4	320248	1	63130
Reusable	4	682726	3	142055

Table 6. Engine development costs @ payload of 15,000 lbs

Vehicle Type	First Stage Engine Development (2004 $)	Second Stage Engine Development (2004 $)	Total Engine Development (2004 $)
Expendable	3.68 billion	1.75 billion	5.43 billion
Hybrid	3.33 billion	1.78 billion	5.11 billion
Reusable	4.56 billion	2.37 billion	6.93 billion
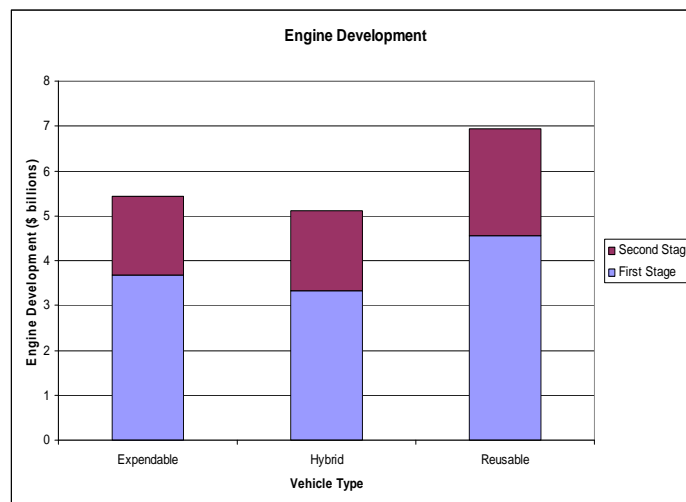
Figure 8. Engine Development for Payload Mass of 15,000 lbs

E. Maintenance Costs

Maintenance costs were included in the examination of DPM cost. The maintenance calculated using the comparison model to service the vehicles for launch was found to be minimal, around $1 million for the reusable and $270,000 for the hybrid. These costs corresponded to 6,000 and 1,330 hours respectively. Figure 9 shows the minuscule impact of varying maintenance time on DPM. To understand the impact of maintenance, a high approximation of 10,000 hours per launch for the reusable and 3,800 hours per launch for the hybrid were used for the comparison. The total cost for the 10,000 hour maximum maintenance time equated to $80 million dollars after 400 launches for the reusable launch vehicle. This is pennies compared to the total cost of the system. However, as stated earlier, maintenance time does affect fleet size. For military applications, during a surge in launch requirement, fleet size will need to be increased to provide the required sortie rates. The following example illustrates how maintenance time impacts fleet size.

A reusable vehicle sized for a payload mass of 15,000 lbs is estimated to require a total of 6,000 hours of maintenance time after each flight. If the maximum number of people able to work on the vehicle at any one time was limited to 50 individuals, then a vehicle could be ready for flight after a minimum of 120 hours. This would include vehicle and engine inspection, replacing broken TPS panels, and other activities. If surge operations dictated launch rates of 1-3 launches per day, then a small fleet size of 3 vehicles would be insufficient to

accomplish mission needs. Instead fleet size would need to consist of 5-20 vehicles since each vehicle would be under maintenance for roughly 5 days and therefore, unable to launch.
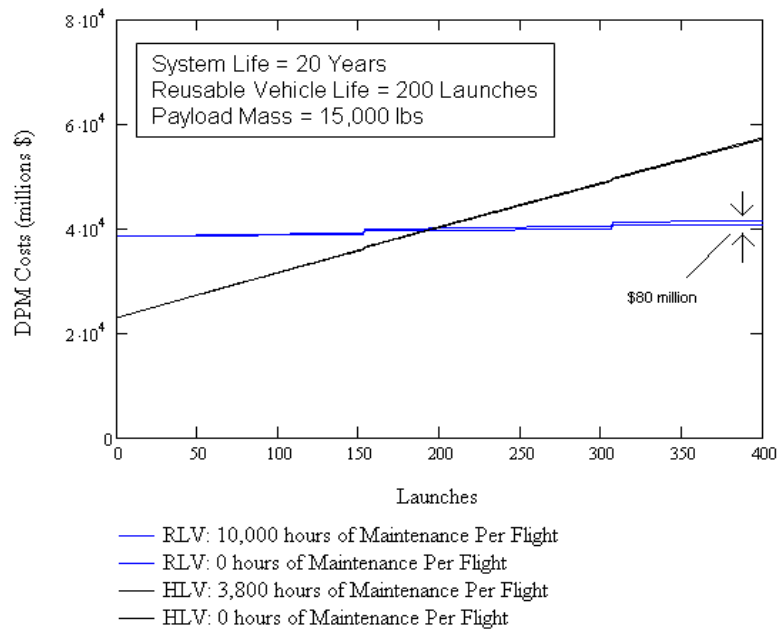

Figure 9. Effect of maintenance on DPM costs

F. Cost Analysis: Total DPM Comparison

The following analysis compares DPM costs if each vehicle alternative were to undergo complete development and production for an assumed system life of 20 years. Figure 10 illustrates the DPM comparison and the preferential launch regions for each vehicle alternative. Figure 11 includes the same information; however, DPM is plotted against an average launch rate per year. Figures 10 and 11 were generated via summarizing DPM costs over the total system life. As stated earlier the HLV first-stage and both RLV stages have a maximum life of 200 launches.
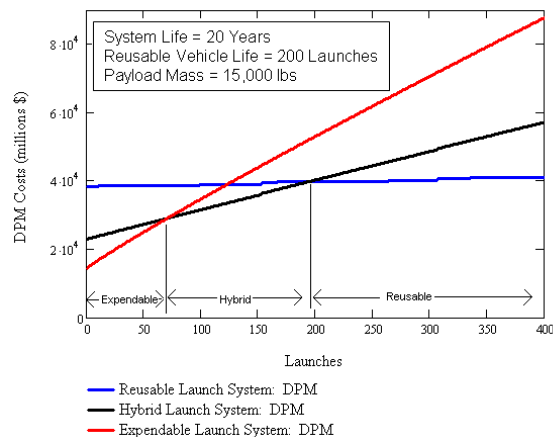
Figure 10. Total DPM costs vs. number of launches
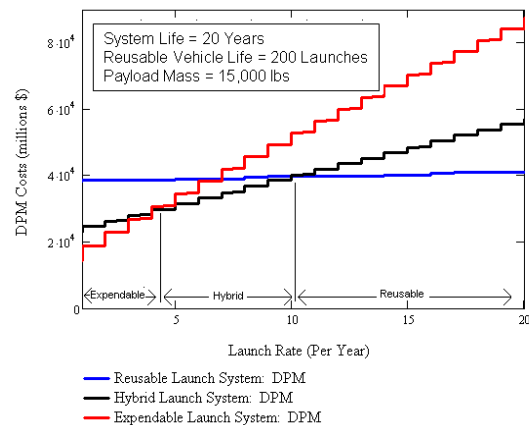
Figure 11. Total DPM costs vs. average launch rate per year

If each vehicle underwent complete development and production then the expendable vehicle would be preferable for lower than 75 launches over a 20 year system life. The hybrid vehicle would be preferable for 75 –

200 launches and the RLV preferred for launches greater than 200 launches over 20 years. The slopes of alternative in Fig. 10 and step sizes in Fig. 11 describe the cost for each additional launch. ELVs have lower development costs compared to hybrid and reusable vehicles but require new vehicles for each launch. Nonetheless, as the number of launches over the system life increase, the higher production costs outweigh the lower development costs after an average of 5 launches per year. Similarly, the lower development cost of the HLV compared to the RLV is outweighed by the production costs for average launch rates greater than 10 per year. The RLV curve consists of maintenance costs and new vehicle production amortized over the vehicle life of 200 launches, therefore the slope is close to linear. This comparison is valid only if each system undergoes total DPM. However, since expendable vehicles currently exist, no new expendable development needs to be completed. Therefore, further analysis will compare the different vehicle alternatives for a real world scenario.

G. Cost Analysis: Payload Size Impact for Total DPM

Figure 12 illustrates how total DPM is affected by varying payload mass for a lifetime of 400 launches over 20 years. As payload mass increases, the vehicle dry mass increases and subsequently, so do development, production, and maintenance costs. Figure 12 shows how the number of launches required for an HLV or RLV system to be preferred decreases as payload mass increases. Simply put, large payloads favor HLVs and RLVs sooner compared to expendable vehicles when each alternative undergoes complete development and production.
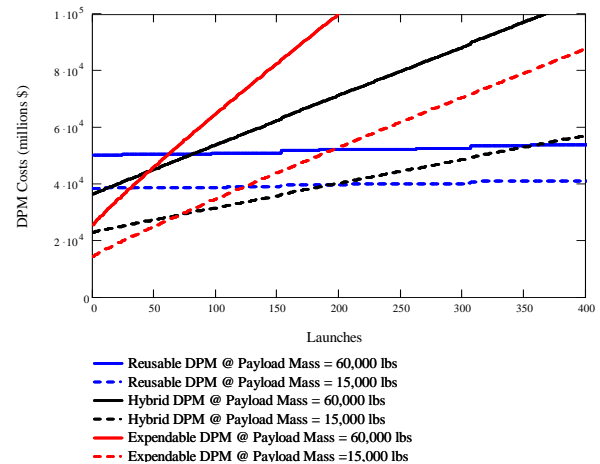
Figure 12. Total DPM for increasing payload size

H. Real World Scenario: DPM Comparison

As described earlier, ELVs are currently in use today and therefore do not require further development. Also, the hybrid vehicle is planned to use existing second stage engines and require minimal second stage airframe development due to use of an expendable second stage. For these reasons, a comparison of current expendables was completed against a reusable vehicle and the hybrid vehicle being designed by the U.S. Air Force. Figures 13 and 14 detail the preferential launch regions for the real world scenario.
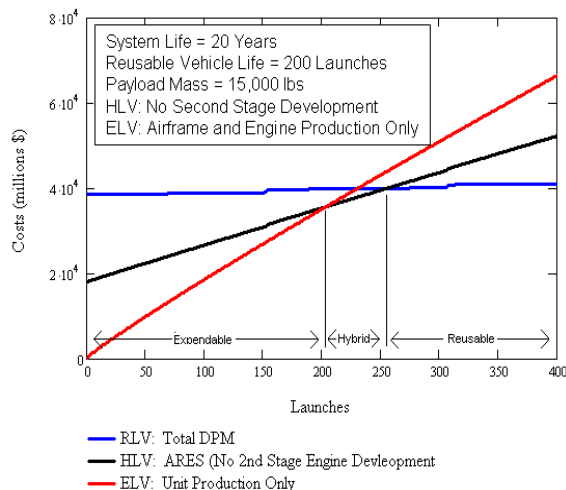
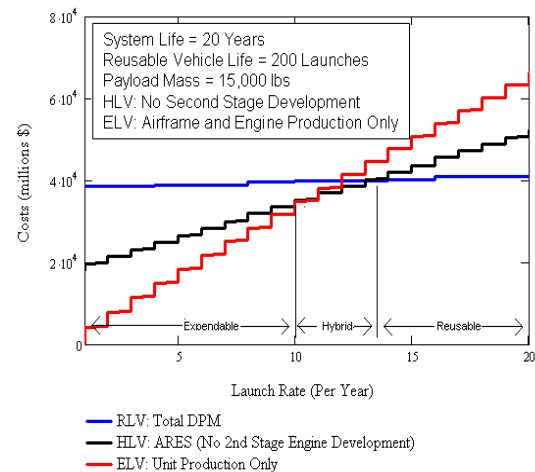**Figure 13. Real world DPM comparison vs. number of launches**

Figure 14. Real World DPM Comparison vs. Average Launch Rate Per Year

American Institute of Aeronautics and Astronautics

On the basis of DPM costs, HLVs are preferable for 200 – 260 launches, or roughly 10 – 13 launches per year over 20 years. The RLV, with its lower cost per launch, dominates the hybrid for launches greater than 260 over 20 years and current expendable systems for launches greater than 225 over 20 years. Again, this real world scenario includes limited development for the hybrid vehicle. If complete development were to take place, then the hybrid launch vehicle would not be preferable against the expendable or reusable launch vehicle. Being said, both the hybrid and reusable systems have lower direct operating costs (DOC) than the expendable alternative. Analysis of DOC will be further discussed in a later section. The following section will address total cost-per-pound of payload for the real world scenario.

I. Real World Scenario: Cost-Per-Pound of Payload

Figure 15 describes how the total cost-per-pound of payload decreases as the number of launches during the system lifetime increases. The DPM costs for the real world scenario were amortized over the amount of payload lifted to low Earth orbit. The blue oval corresponds to current world launch costs of $12,000 per pound of payload for the U.S. and $6,000 per pound for non western countries. The oval was plotted for 120 launches. This number of launches corresponds to the six missions the U.S. military carried out in 2005.

The expendable cost-per-pound of payload trend predicts that current launch costs well. Figure 15 illustrates low cost-per-pound of payload requires a large number of missions for hybrid and reusable vehicles. The HLV and RLV systems included development and therefore a larger number of launches needs take place before the total cost-per-pound of payload falls below current expendables.
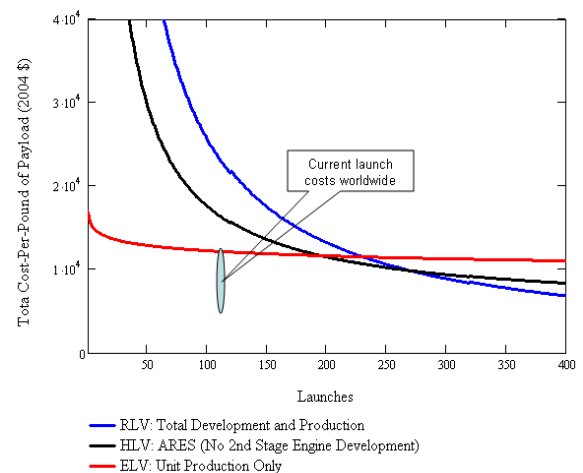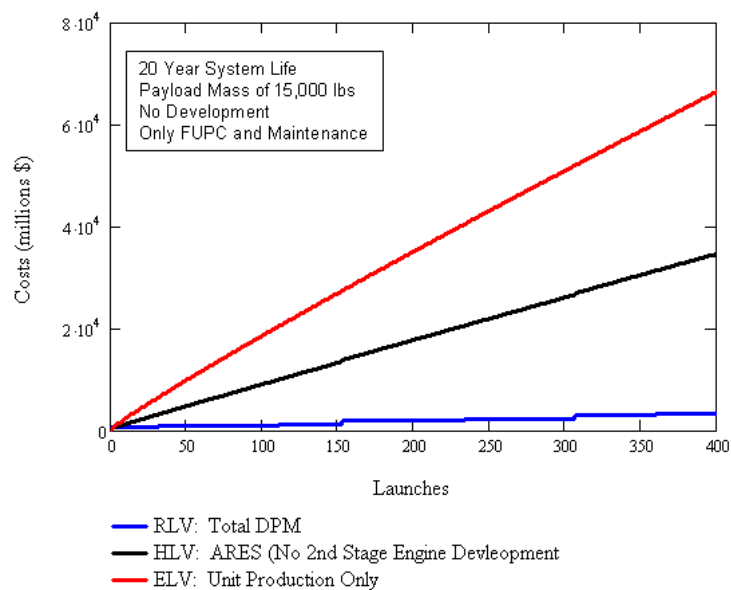

Figure 15. Total Cost-Per-Pound of Payload for Real World Scenario

J. Direct Operating Costs

Development is an indirect cost while production and maintenance are direct costs. It is the direct costs that affect an organization's operating budget. Therefore production and maintenance are known as direct operating costs (DOC). Figure 16 displays the DOCs trends for the different launch vehicles alternatives. Figure 16 was generated by summarizing production and maintenance costs for each alternative and plotting them against the number of launches.

The direct operating costs for expendable and hybrid vehicles rise dramatically for increasing number of launches. Each launch requires the production of a new ELV or HLV second stage. The DOC for the RLV remains almost flat consisting of maintenance costs and RLV vehicle production costs amortized over the vehicle life of 200 launches.

Figure 16. Direct Operating Costs vs. Number of Launches

Lower DOC allows for greater mission flexibility. A decision maker can afford to send multiple sorties using RLVs to complete a mission and still spend less than one launch using a current ELV. For that reason, RLV allows for greatest mission flexibility of the three alternatives. HLVs are ranked second best with a DOC of roughly half of ELVs.

K. DOC: Cost-Per-Pound of Payload

If the government were willing to pick up the development costs for a hybrid or reusable launch vehicles, then industry would see launch costs similar to those found in Fig. 17. An analogy for a situation where industry profited from government developed system is the Boeing 707 spin off from the KC-135. Boeing was able to save billions in development by using the design of the KC-135 when developing the Boeing 707 and subsequent aircraft.

Figure 17 details how the U.S. space industry would be able to offer launch costs on the order of $1,000 per pound of payload for RLVs and $6,000 per pound of payload for HLVs. This reduction in launch costs would make the U.S. competitive with other nations in the space launch market. HLV launch costs of $6,000 per pound of payload would be similar to those offered by non-western nations using current expendable vehicles. However, the RLV launch costs of $1,000 per pound would allow the U.S. to recapture of the world launch market. Not only would the cost-per-pound be lower than current

Figure 17. Direct Operating Costs vs. Number of Launches

worldwide expendable systems, but the vehicles would be more reliable due to flight testing and maintenance. This decrease in launch costs would open the space market to any who could afford a payload.
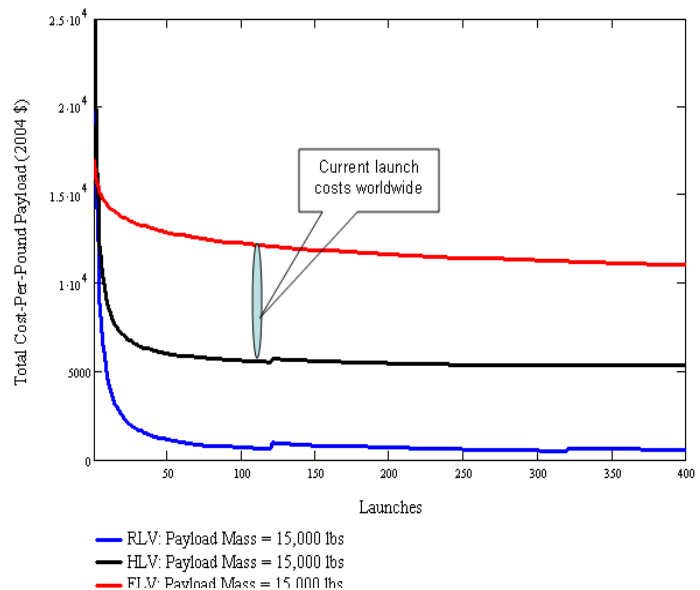
V. Conclusion

A. Expendable Launch Vehicles

Expendable launch systems have relatively low development costs and are well understood. Except for the Space Shuttle, all other current launch vehicles are expendable systems. ELVs can be designed to launch in a few hours, but have high direct operating costs and long production times that limit their ability to take on more missions if needs develop. In the case of a surge in launch requirements, it is necessary to have a stockpile of complete systems available which to draw from. Expendable systems are preferable for predictable, low launch rate missions, but will have trouble responding to higher launch rates.

B. Hybrid Launch Vehicles

Hybrid launch systems will cost roughly twice as much to develop due to the complexity and cost of the reusable booster. A hybrid system is well within current technology. Development risks are slightly higher than expendable systems, but direct operating costs are lower, by about half, due to the reusable first stage. Additional development effort is needed to insure that the booster is sufficiently reliable and that the system as a whole is more responsive. Unlike the expendable system, only upperstages need to be stockpiled for surge requirements. Hybrid systems are preferable over expendables for current or modest increases in predicted launch rates.

C. Reusable Launch Vehicles

Reusable launch systems have the highest development costs and technical risks of the three alternatives analyzed in this research due to booster and orbiter complexity, but the technology is within current state of the art. The extremely low direct operating costs quickly outweigh the high development costs for launch rates above about 20 per year. A reusable system is the more flexible system due to their extremely low direct operating costs. They require only stockpiling of payloads to support surge operations. Reusable launch systems are the systems of choice if it is believed that future launch rates will increase significantly and will require responsive and flexible launch capabilities.

References

[1] Department of the Air Force, Mission Need Statement for Operationally Responsive Spacelift, AFSPC 001-01, HQ, AFSPC/DRS, United State Air Force, 20 December 2001.

[2] Koelle, Dietrich, *Handbook of Cost Engineering for Space Transportation Systems.* Germany: TCS-TransCostSystems, 2003.

[3] Rooney, Brendan D., "Hybrid Launch System Vehicles: Ground Facilities and Operations Integration," Aeronautical Systems Center's Capability Integration Directorate, Design, and Analysis Division, Wright-Patterson AFB, AIAA

[4] Humble, Ronald W., Henry, Gary N. and Larson, Wiley J., *Space Propulsion Analysis and Design,* McGraw-Hill Publishing Company, New York, 1995.

[5] Gstattenbauer, Greg J., "Cost Comparison of Expendable, Hybrid, and Reusable Launch Vehicles," M.S. Thesis, AFIT/GSS/ENY/06-M06, Air Force Institute of Technology, Wright-Patterson AFB, Mar 2006

[6] Futron Corporartion, "Space Transportation Costs: Trends in Price Per Pound to Orbit 1990-2000," September 6, 2002.

APPENDIX F

A Discrete-Event Simulation of Turnaround Time and Manpower of Military RLVs

Brendan D. Rooney[*] and Alicia Hartong.[†]
United States Air Force, WPAFB, Ohio, 45433

Abstract

The effect of design and technologies on the ground operations of a reusable launch vehicle is required to make space access affordable. A gap in turnaround time exists between the reality of the Space Shuttle and the goals of a military reusable launch vehicle. A discrete-event simulation is in development to find ways to reduce this gap in turnaround time. Manpower and component failure data from past aerospace systems are used to define root causes and times of maintenance actions. Stochastic models are developed to simulate the component failures and repair times for these maintenance actions. Finally the Arena discrete-event simulation uses the maintenance information to evaluate turnaround time and manpower effects of various designs and technologies.

Nomenclature

AFRSI	=	Advanced Flexible Reusable Surface Insulation
FRSI	=	Flexible Reusable Surface Insulation
GSE	=	Ground Support Equipment
HRSI	=	High-temperature Reusable Surface Insulation
M_h	=	length of time complete one maintenance action
NF_{RR}	=	number of tiles needing removal and replacement per mission
OMS	=	Orbital Maneuvering System
pTileRR	=	probability of removal for each tile
RCC	=	Reinforced Carbon-Carbon
RCS	=	Reaction Control System
RLV	=	Reusable Launch Vehicle
RSATS	=	Responsive Space Advanced Technology Study
TA	=	Total Tile area on the vehicle
$TileSize$	=	individual tile size
TM_h	=	total man-hours required per mission
TPS	=	Thermal Protection System

I.   Introduction

THE purpose of a Air Force Reusable Launch Vehicle (RLV) is to deliver payloads to low earth orbit. The Space Shuttle was originally designed to accomplish this in a timely and cost effective manner, but fell short in this regard. The Air Force needs to design a launch vehicle to achieve a fast turnaround time at low cost. The key to having fast turnaround in an RLV is a design that has a small logistical footprint. A low maintenance RLV reduces cost and turnaround time. The RLV design must be assessed with respect to maintainability. A computer model using conceptual design inputs was developed for this purpose. The paper will explain the research, the modeling approach, the vehicle systems modeled thus far, some results, and future potential for the project.

---

[*] Aerospace Engineer, Aerospace Systems Design and Analysis, WPAFB,OH, and AIAA Member.
[†] Aerospace Engineer, Aerospace Systems Design and Analysis, WPAFB,OH, and AIAA Member.
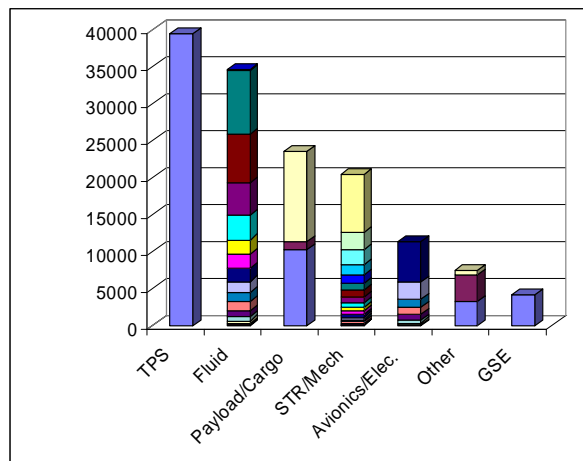
II.   Basic Approach

In order to properly assess an aircraft or space plane for maintainability the background on historical vehicles must be known. What areas on a vehicle cause the greatest maintenance headaches? What are the causes or failure modes of the maintenance? How long does the maintenance take to complete? These are the questions that were asked at the beginning of the project. The vehicle systems with the most maintenance must be known in order to guide the technology programs in achieving maximum maintenance man-hour reduction using limited resources. Knowledge of failure modes which caused each maintenance action can be used to redesign the vehicle or use advanced technology to eliminate or reduce maintenance actions. The length of time to complete a maintenance action will then help with determining total maintenance man-hours or the amount of work required for each subsystem. Research in answering these questions started with looking at the Space Shuttle, however other vehicles and subsystems were also researched. Experts working on the Space Shuttle are a good source for determining maintenance causes that can not be learned anywhere else. Numerous research papers on each subsystem provided information to help fill in gaps about failure modes and maintenance times. All of the information was then used to determine the modeling approach for each subsystem.

Once the initial research was completed a Pareto chart of the maintenance man-hours of the Space Shuttle was analyzed. The thermal protection systems (TPS) require the most amount of maintenance man-hours per mission. The TPS require modeling high temperature tile, leading edge protection, advanced blankets, low temperature blankets, and seals. Due to the large amount of maintenance man-hours, the thermal protection systems were the first to be modeled.   The modeling process consists of three main steps:

1) Develop probability distributions[1] of failures and maintenance actions.
2) Monte Carlo simulations.
3) Discrete event simulation.

The probability distributions calculate the number of maintenance actions or failed parts for a particular component or system. Probability distributions also calculate the time to complete a maintenance action. Monte Carlo simulations, which "roll-up" the distributions

Figure 1. Man Hours in the Orbiter Processing Facility.
Space Shuttle STS-85 Man-hours Courtesy Edgar Zapata NASA KSC

into higher level statistics, provide total maintenance man-hours for that maintenance action, i.e. total man-hours for tile removal and replacement. The discrete event simulation uses all this information, queuing time, and resources to calculate total turnaround time and man-hours and allows for exploration of ground operations optimizations.

A.   Development of Probability Distributions

The objective of the models is to identify failure modes, predict failures of components, estimate the duration of maintenance actions, and make all of these sensitive to design choices and technology. The modeling approach primarily uses probability models, i.e. involving statistical distributions, to calculate the quantity and types of failed parts and the time required for maintenance. The type of distribution needed for each calculation depends on the total quantity of parts that might need the maintenance action. For the TPS models a Poisson distribution is used because of the high number of tiles (20,000) and blankets. The objective for each system using the Poisson distribution is to calculate the average number of parts needing the operation. The calculated average will give the number of parts failed during the mission. To have a good understanding why parts are failing the failure modes for the maintenance actions must be known. If there are different failure modes the Poisson distribution calculations are repeated for each and added together. The Poisson distribution works well for design parameters such as TPS area or seal length. For smaller part quantities that use metric design parameters a binomial distribution is used. The

2
American Institute of Aeronautics and Astronautics

general format for determining the average parts failed is explained below. The number of tiles that need removal is given as an example. The model must be sensitive to Tile Area (TA) to be useful as a design tool. The tile size and probability of removal and replacement (Failure Rate) are unique for the black tile and are assumed constant.

$$Average\_Parts\_Failed \equiv \frac{TA}{TileSize} * Failure\_Rate \tag{1}$$

Once the failure modes are known the contribution for each can be calculated using the following type of equation.

$$Average\_Parts\_Failed \equiv \frac{TA}{TileSize} * F * Failure\_Rate \tag{2}$$

The F symbol represents the fraction of parts that are subject to that failure mode. A Poisson distribution uses a "roll of the dice probability" between 0 and 1 with the average number of parts failed. A generic version of the calculation used for many of the systems on the vehicle is shown. The equation is an inverse cumulative probability distribution.

$$Number\_of\_Parts\_Failed \equiv qPoisson(random\_probability, average\_\#\_failed) \tag{3}$$

In the cases for scheduled operations, such as leak and functional checkouts, the number of failed parts requiring service, e.g. engines, thrusters, do not need to be calculated. However, the frequency of the scheduled operation is entered into the model.

The time to complete the maintenance actions are then determined using a probabilistic model. The triangular distribution was chosen to represent man-hours because of the simplicity of the inputs. Three inputs of minimum, most likely, and maximum duration are all that is needed. A historical minimum and maximum based on percentage of the most likely value is used, i.e. 80% to 150% of the most likely value. Some operations have insufficient data in regards to minimum and maximum values, so an educated estimate based on percentages for similar systems fills in the gap. Several of the operations have a fixed most likely value based on averages. However, where information is available and physics allow, a most likely value can be calculated from a baseline using a design parameter. For example, thrust levels of an engine determine the most likely value for engine removal. Since engine size can be changed in conceptual design models, the time to remove an engine should change due to a larger size or complexity in removal. Time to remove the engine is expected to vary non-linearly with engine size. The following equation helps explain the concept.

$$MostLikely\_Value \equiv Setup\_Time + reference\_value * (Thrust / Thrust\_reference)^{0.8}$$
$$Minimum\_Value \equiv MostLikely\_Value * Historical\_Percentage \tag{4}$$
$$Maximum\_Value \equiv MostLikely\_Value * Historical\_Percentage$$

After the three inputs are set the triangular distribution is defined.

$$Time\_To\_Complete\_Operation \equiv qTriangle(random\_probability, min, most, max) \tag{5}$$

One now has an engine removal model which is sensitive to size. Discussions with maintenance personnel and technologists can now be undertaken to determine the values one should use for specific engines and installation concepts.
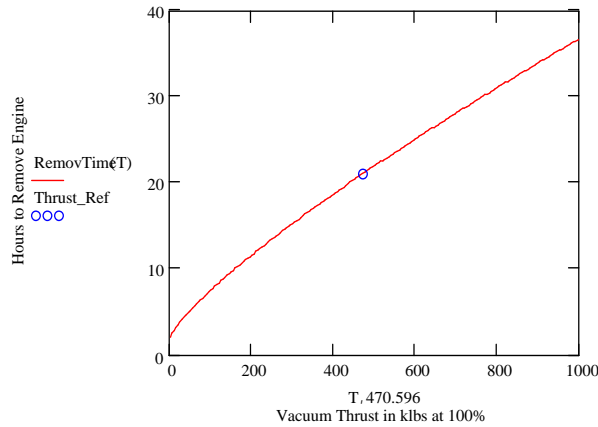
Figure 2. Plot of Engine Removal Time for Varying Thrust
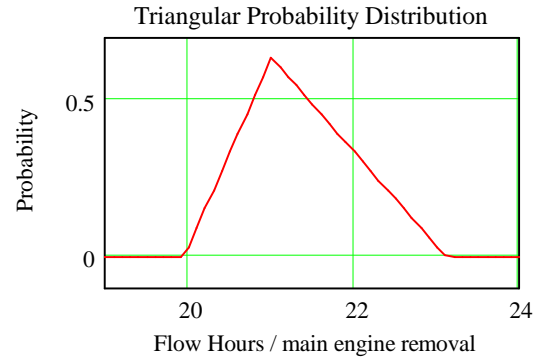
Figure 3. Example Distribution Duration to Complete Maintenance Action

B.   Monte Carlo Simulations

The objective of the Monte Carlo simulations is to predict the total maintenance man-hours for a subsystem and the variance. The Monte Carlo simulations use the probabilistic models to calculate the total man-hours. These types of calculations are useful in assessment of technology. A new advanced technology can be compared against an old technology. The assessments are particularly helpful in guiding technologists where to put limited funds if operability is a goal. The first step uses the probabilistic model for determining the quantity and type of repairs or service needed. Then for each maintenance action man-hours are calculated. The number of technicians needed for a maintenance action is based on historical data. The number of technicians needed is multiplied by the duration giving total maintenance man-hours for the parts. The steps are repeated for each maintenance action and totaled. The simulation is normally run 1000 times with a new random probability for each run in order to generate statistics. The Monte Carlo simulation, shown in figure 4, outputs statistics for the total man-hours. It is these maintenance man-hours that help assess the amount of work required for maintaining a particular system or technology.

As an example a statistical rollup model (curve fit) for the total number of HRSI tiles removed and replaced can be derived from the Monte Carlo simulations of all of the failure modes. The rollup model matches the results of the simulation, but runs many times faster. Use of the model will not require rerunning of the simulation of the separate root causes thus saving time. The model must be sensitive to Tile Area (TA) to be useful as a design tool. The tile size and probability of removal and replacement (pTileRR) are unique for the HRSI "black" tile and are constant.

$$TM_h(TileA) := \begin{vmatrix} TM_h \leftarrow 0 \\ \text{for } i \in 1.. NF_{RR}(TileA) \\ \quad \begin{vmatrix} M_h \leftarrow qTriangle(rnd(1), mn, most, mx) \\ TM_h \leftarrow TM_h + M_h \end{vmatrix} \\ TM_h \end{vmatrix}$$

Figure 4. Monte Carlo Simulation.
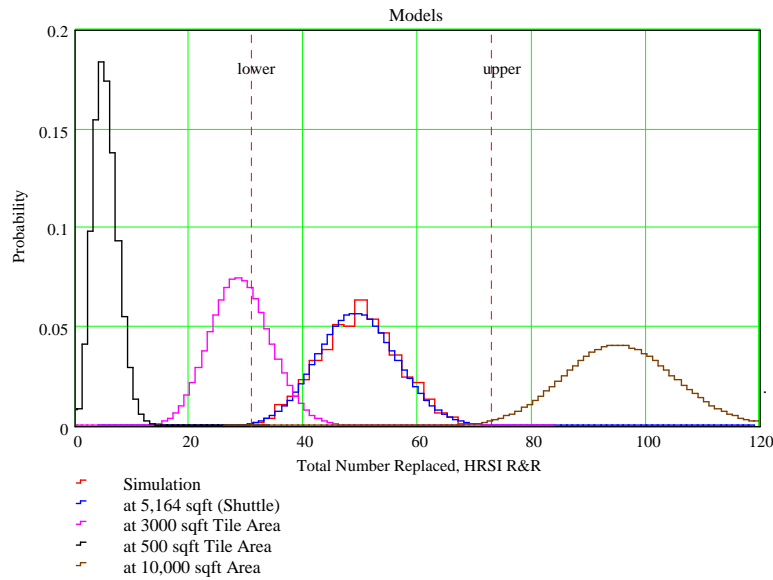*Mathcad[2] Equation for determining total Man-hours using total number of failures (NF$_{RR}$) and duration of each maintenance action (qTriangle).*

Inverse cumulative probability function

$$qNFRR(p,TA) \equiv qPoisson(p, \frac{TA}{TileSize} \cdot pTileRR) \tag{6}$$

Density probability function

$$dNFRR(x,TA) \equiv dPoisson(x, \frac{TA}{TileSize} \cdot pTileRR) \tag{7}$$

4
American Institute of Aeronautics and Astronautics

Figure 5. Tile Failures for Varying Tile Area.

The above Poisson distribution can be used when only the tile area changes in a design. If a different type of tile is used, or the designer thinks the effect of each failure mode needs changing, then the lower levels will need to be recalculated. This new equation can represent varying tile areas quickly as figure 5 shows. The same roll-up, shown in figure 6, for varying tile areas can be done for total man-hours to remove and replace all failed tiles as long as the underlying TPS system is the same. This approach allows us a lot of flexibility in providing the appropriate level of detail and or speed in our discrete event simulation models.
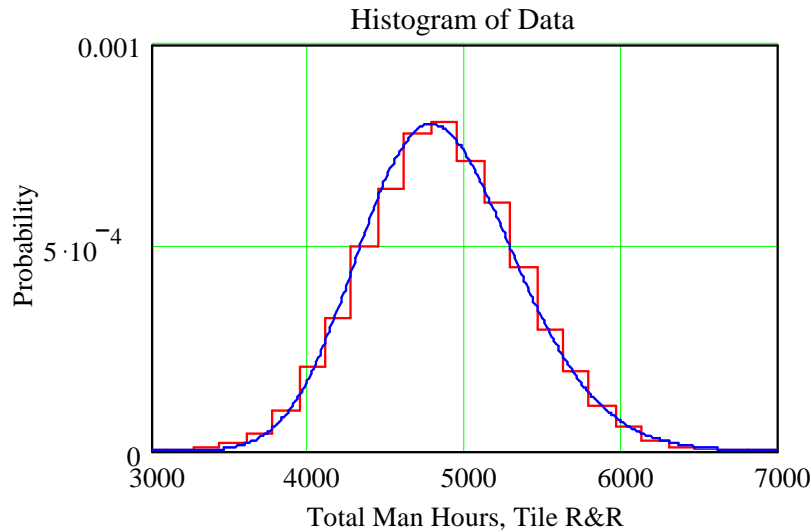
Figure 6. Total Man-hours Histogram Example.

C.   Discrete Event Simulation
The objective of the discrete event simulation is to predict how quickly the vehicle can launch again and the resources required.   In other words how many sorties can the user of the Reusable Launch Vehicle fly and how

5
American Institute of Aeronautics and Astronautics

much money will it cost? The parameters of interest are usually turnaround time, number of personnel, and other resources required to maintain a fleet. A discrete event simulation model has the ability to take the necessary inputs and calculate maintenance man-hours and turnaround time as a function of the number of resources and sequence of operations. The Arena[3] computer program is used for the flexibility and user interfaces the program offers. The visual basic application combined with Arena makes it easy to have a graphical user interface, shown in figure 7, or input files such as a spreadsheet.

Figure 7. Visual Basic Graphical User Interface.

With proper programming, design parameters taken from a conceptual design such as tile area and thermal barrier length are entered into the discrete event simulation along with number and types of resources and job flow sequencing information. The simulation outputs desired operability metrics to guide the designer, technologist, and the user of the Reusable Launch Vehicle.
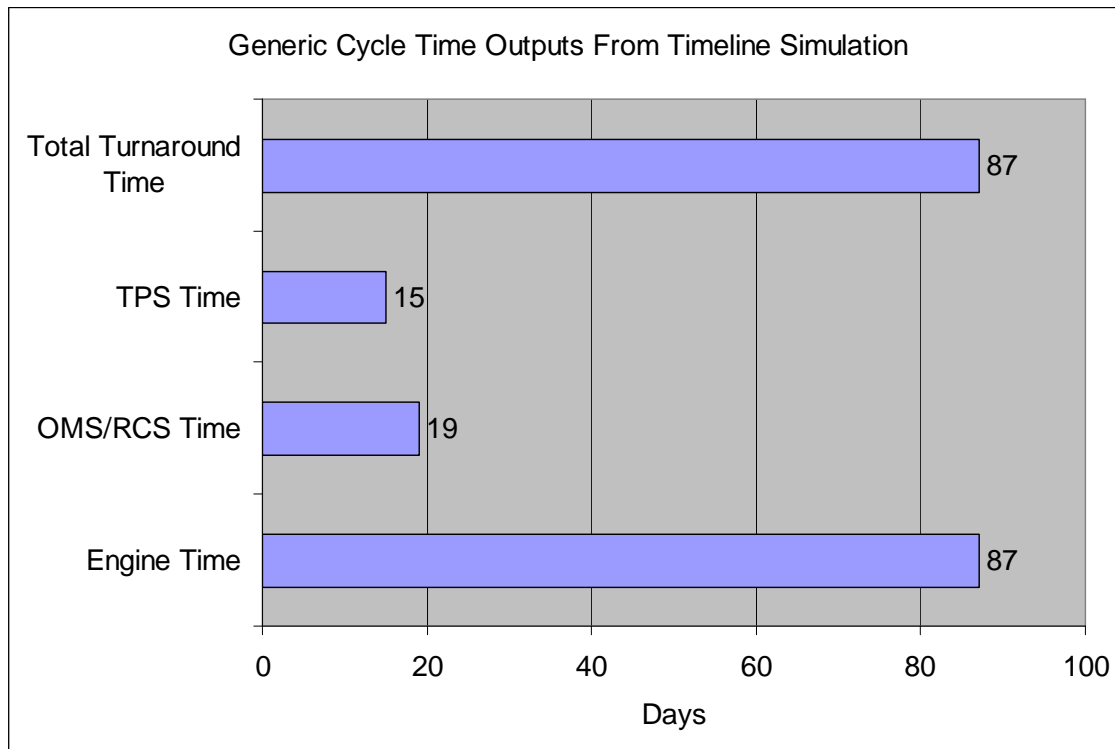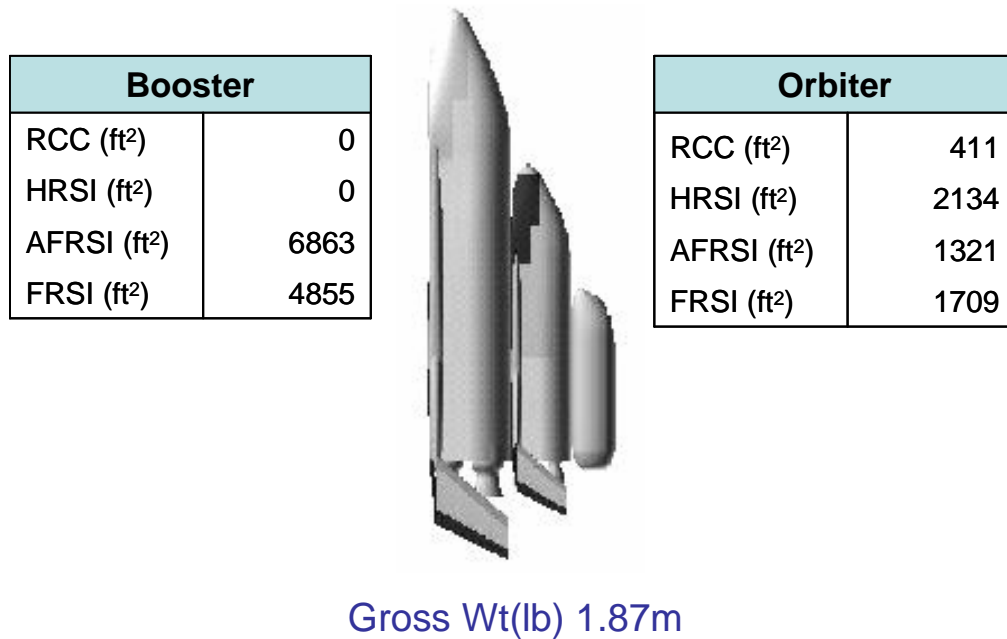
Figure 8. A Generic Output from the Discrete Event Simulation.

III.   Scope

The systems modeled for a reusable launch vehicle are Thermal Protections Systems or TPS, Main Engines, and Fluid Related Subsystems. Fluid Related Subsystems include main engine pressurization and feed system, Orbital Maneuvering System and Reaction Control Systems (OMS/RCS), the Auxiliary Power Units (APU), actuation system, and Active Thermal Control System (ATCS). The maintenance data[4,5,6] supplied to the models is based on Space Shuttle information. The scope of the project to date has been focused on unmanned vehicles. However there is enough information available to model a manned version. The current ground operations simulation configuration models the repair facility operations for the three vehicle areas mentioned. The landing, mating, and pad operations are not included as of the time of this writing. However, the repair facility operations are the largest with regards to man-hours and turnaround time. Each of the three systems models will be described in detail. A two stage to orbit vehicle, called RMLS102, capable of carrying 15,000 lbs to low earth orbit was designed. For each system the RMLS102 design inputs for two technology levels will be described. The first technology level is called a baseline design and only assumes current technology. The second technology level is an advanced design with assumptions about improved durable TPS, nontoxic propellants, etc. The advanced technology assumptions are considered conservative and just a first order of magnitude reduction. No assumptions are made about improvements in worker productivity, more efficient management, or less quality control personnel. These types of improvements will be part of an upgrade to the simulation.

RMLS102 Concept

Booster	
RCC (ft²)	0
HRSI (ft²)	0
AFRSI (ft²)	6863
FRSI (ft²)	4855

| Orbiter	
RCC (ft²)	411
HRSI (ft²)	2134
AFRSI (ft²)	1321
FRSI (ft²)	1709

Gross Wt(lb) 1.87m

Figure 9. A Military Reusable Launch Vehicle Design with TPS areas.
NOTE: Design Synthesis Performed by A. Hartong. Vehicle weight includes 15% margin.

IV.   Thermal Protection Systems Model Description

The TPS model contains several major models to provide part failure and man-hour data. The high temperature tile such as Space Shuttle HRSI has three maintenance models. The models are flexible enough to simulate different technologies such as metallic tiles. All models calculate the number of parts requiring a maintenance action then use the triangular distributions for man-hour calculations.
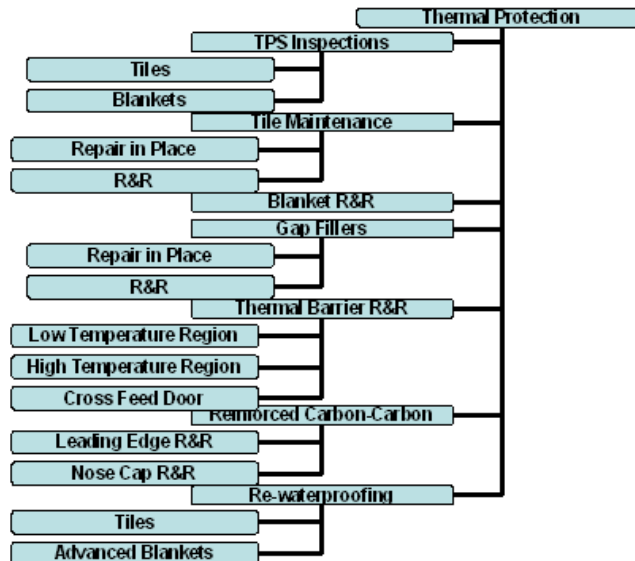
Figure 10.   Thermal Protection Systems Scope.
All possible maintenance intensive operations.

A. Tile maintenance models.

Tiles are removed due to five failure modes[7]:
1) The tiles are removed to gain access to failed parts under the TPS.
2) Debris can hit tiles any time during the flight (for shuttle mainly due to ice and foam from the external tank and kicked up debris by the engines at takeoff) causing damage bad enough to cause removal.
3) Ground handling damage to tiles is caused by technicians that need to repair TPS or other parts..
4) The environments the tiles are subjected to require that there be no misalignments on the vehicle, any tiles that fail the criteria for safe flight are removed.
5) Finally, tiles can be removed because of engineering modifications, but they are a small portion of the removals.

The second and third maintenance models involve repairing of the tiles while still on the vehicle. Chips are small impact damages with the coating and a minor amount of tile substrate missing. Gouges are larger impact damages but are similar in nature to chips. The three major failure modes for minor repairs are:
1) Debris hits from ice and foam
2) Hits on the heat shield area from engine plume recirculation
3) Cross feed door debris coming from protective Mylar

Equations for all three tile maintenance actions are made using individual tile size, total tile area, fraction of tile due to a failure mode, and probability of tile removal due to that failure mode. The equation creates a Poisson distribution of the number tiles, chips, or gouges needing repair or removal.

Baseline System for Tile Maintenance Models

The baseline design for the RMLS102 thermal protection system will be similar in technology to the Space Shuttle but will differ in a few key areas. The damage from debris hits is reduced drastically because there is no external tank foam falling and very little ice. The table compares the acreage for the Space Shuttle orbiter and both stages of the RMLS102.

	Space Shuttle	RMLS 102 Orbiter	RMLS 102 Booster
Windward TPS Area Sq ft	5164	2134	0
High Temp Blankets	1800	1321	6862
Low Temp Blankets	3581	1709	4855
RCC Wing Area	360	267	0
RCC Other	49	144	0

Table 1.   Comparison of RLV Thermal Protection areas.

Advanced System for Tile Maintenance Models

The advanced design primarily assumes a more durable TPS system. Most probabilities for tile maintenance are reduced to 1/6 of the original. The probability to remove a tile due to needing access to other parts is reduced to about 3/4 of the original. The time to replace a tile is reduced to an average of about 1/3 of the original time. If there is a need to remove a tile then there will still need to be time allocated for manufacturing or modifying the tile even if bonding time is reduced or attachments are used.

B. Advanced Blanket Subsystems Models

The advanced blankets are those that are similar in function to the AFRSI[8] blankets used on the Space Shuttle or another technology such as a tougher blanket. These blankets have replaced most of the white tiles that were used earlier in the Shuttle Program. The blanket removals are caused by two primary failure modes:
1) There is a drag chute used on the Space Shuttle during landing. The chute comes out of a door at the bottom of the vertical tail. The door must be protected by high temperature blankets. The drag chute door blankets are expended at the end of every flight and must be replaced.
2) Blankets also must be removed due to damage during flight.

There are also low temperature blankets called FRSI used on the leeward side of reusable launch vehicles. The FRSI type blanket removals are not modeled for now because the maintenance associated with these are very low, however the impact on inspection time is modeled.

Baseline System for Advanced Blanket Models

There are no drag chute blankets. This reduces advanced blanket man-hours.

Advanced System for Advanced Blanket Models

Blanket removal and replacement time is reduced to an average of about 2/3 of the original. The probability of removal is reduced by 1/2 due to a tougher blanket.

C. Gap Filler Maintenance Models

Gap Fillers are used in between tiles to prevent heat from entering in. They are normally made of Nextel fabric, Inconel foil and alumina batting[8]. Damages include lost coatings, frays, fabric breaching, tears, charring, and protruding or lost gap fillers. The failure modes are split into areas based on information that was available. Gap filler maintenance has two models: repairs in place and removals. The failure modes are split into primary areas of the vehicle:
1) Damage occurs on the vertical stabilizers
2) Near the wings
3) Forward fuselage area because of the high heat gradient
4) The aft area including the base heat shield.

The gap fillers needing maintenance are calculated based on the probability of repair or removal per square footage of tile area. The average number of gap fillers needing repair or removal per square foot is multiplied by the total area. This will change in the future to be sensitive to the individual tile size. The numbers that need repair or removal are based on the probability of repair or removal for each failure in the same way as the Tile R&R model.

Baseline System for Gap Filler Models

Gap Fillers are the same as Shuttle but less gap fillers are required because of smaller tile area.

Advanced System for Gap Filler Models

Gap filler maintenance time and probabilities are reduced by about 1/2 because the gap fillers are assumed to be more robust and easier to install.

D. Thermal Barrier Maintenance Models

Thermal barriers, a kind of seal, are used around openings into the vehicle and in the closeout areas between major components. Aerothermal seals are used on the control surface cavities. Aerothermal seals are not modeled because the maintenance is low compared to the barriers. The thermal barriers with the largest amount of maintenance were the focus of the project. These barriers protect the landing gear and cross feed doors penetrating into the windward side of the vehicle. The thermal barriers are split into the high temperature (nose gear door), low temperature (main gear door), and cross feed (external tank) door models. On the Shuttle, the high temperature area is on the windward surface in the nose landing gear door area. The high temperature region is approximately above 2000 degrees F. This area requires the most complicated thermal barriers. The low temperature region is for square door openings in regions below 2000 degrees F, the main landing gears on the Shuttle. These doors require much less complex barriers than the high temperature region. Therefore, the time to replace the barriers is much lower. The external tank doors on the shuttle are round but are similar in design to the main landing gear doors. The failure modes associated for the barriers include:
1) Gaining access to failed parts
2) Damage during opening for the gear doors and closing for the cross feed doors
3) Ground handling damage because of the high technician traffic around these doors.

The thermal barrier models calculate the number of thermal barriers needed based on the linear footage around the doors or penetrations needing thermal barriers. A probability of any barrier needing replacement is based on shuttle history for each failure mode. A binomial distribution uses the probability needing replacement, the fraction of barriers subject to a failure mode, and the perimeter length of the door to calculate the number of barriers needing replacement. The man-hours are calculated using the triangular distribution model.

Baseline System for Thermal Barrier Models

There are no cross feed doors and therefore no thermal barrier maintenance from the doors. Debris hits on tile from the Mylar associated with these doors are also eliminated.

Advanced System for Thermal Barrier Models

For the advanced design the probability to replace thermal barriers is reduced by 1/2. Durable barriers, perhaps metallic or stronger fabric, will be used. The time to replace the barriers is reduced by 1/2.

E. Reinforced Carbon-Carbon Maintenance Model

The Reinforced Carbon-Carbon (RCC) system does not have a large amount of maintenance except when the RCC needs to be recoated. The size of the nose cap does not greatly influence the chance of damage or the time to

remove it because it is one piece (two with chin panel). The nose cap has a chance of being removed every 8 flights for the Shuttle. The simple probability of removal determines whether or not the nose cap needs removal. The leading edge RCC is divided up into panels. The RCC wing area is used to calculate the number of leading edge panels needed. The panels are removed due to scheduled recoating or to flight damage.

Baseline System for RCC Models
Reinforced Carbon-Carbon is similar to Space Shuttle setup.
Advanced System for RCC Models
No improvements are assumed.

F. Inspections and Re-waterproofing Models

Quality assurance workers perform a micro-inspection on the TPS within the first three weeks of the repair facility flow[8]. A micro inspection looks for charred filler bar, hot spots, subsurface flow, thermal barrier discrepancies, missing parts, and gap filler damage. The micro inspection is very intensive because of the importance of having a perfect TPS system. Inspections of the blankets are modeled separately from tile inspections because tile inspections are more intensive. An estimate of how many man-hours are needed for each square foot is taken from Shuttle experience. The total duration of the inspections for each kind of TPS is based on how many technicians are available. Re-waterproofing is used to prevent water from absorbing into tiles and blankets on the shuttle. If the shuttle is not waterproofed the water adds extra weight. The waterproofing chemical called DMES degrades after each reentry and therefore needs to be reapplied. A simple calculation of time required to water-proof per tile and total area is used to calculate the total duration. The number of tiles is calculated from the total area and individual tile size. Total man-hours are then known from the number of injection technicians normally used on the Shuttle.

Baseline System for Inspections and Re-waterproofing
There will be less maintenance associated with inspections and re-waterproofing due to the smaller size of the RMLS102.
Advanced System for Inspections and Re-waterproofing
The inspections for the thermal protection system will be less intensive due to greater confidence in the system and so the inspections times are reduced by 1/2. The new windward TPS are assumed not to require re-waterproofing and the blanket re-waterproofing uses a non-toxic chemical.

V. Main Engines Model Description

This section of the model deals only with the main engines. The pressurization system, feed system, and other components commonly referred to as the Main Propulsion Subsystem are included in the Fluid Related Subsystems section. Some of the operations for the engines are scheduled and do not require a probability distribution. The complexity and number of engines dominate the man-hours that are calculated. Operations are either included or not performed depending on the type of engine or technology level chosen.
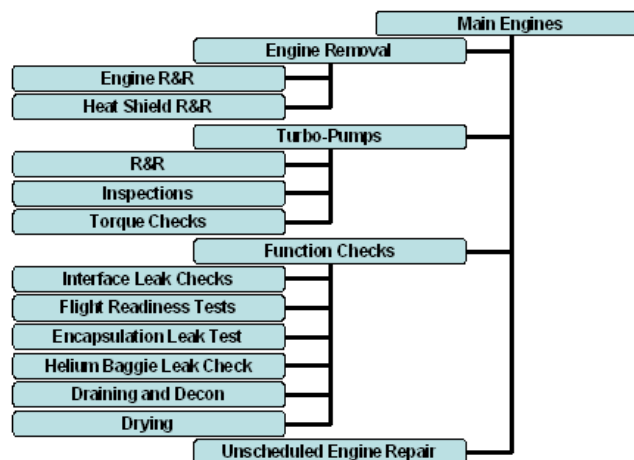
Figure 11.   Main Engines Scope
All possible maintenance intensive operations.

A. Engine Removal Model

Removal of the engine and heat shield is the one of most time consuming operations for the main engine[4]. The accessibility design of the heat shield and engine-vehicle interface will have an enormous impact on the man-hours required to remove the main engines from the vehicle[9]. A heat shield/engine removal model based on thrust of the engine portrays the complexity of the removal process. A minimum setup time is used for the heat shield removal and installation. Currently the frequency of removal for the engine and heat shield is based on component level part failures. The components that cause engine removal are:
1) Nozzle
2) Pre-burners
3) Hot Gas Manifold
4) Main Injector
5) Main Combustion Chamber
6) All pumps
7) Heat Exchanger
8) Other causes

Different concepts can be selected to reflect different operation times for these designs, while still varying with thrust level.

Baseline System for Engine Removal Model

The baseline engine used in the RMLS102 is a kerosene fueled engine similar to the RD-180. The engine design size can change with varying levels of 100% vacuum rated thrust. The booster engines have a 100% vacuum thrust of 855klbs and the orbiter has 185klbs. The engines use a shuttle style interface with the vehicle. The duration to remove and replace the engines is higher for the booster and lower for the orbiter because of the different thrust levels.

Advanced System for Engine Removal Model

The engine integration with the airframe is improved with a ventilated nacelle and aft compartment concept, shown in figure 12. The time estimated to remove and replace the insulation is about one-fifth the time of shuttle heat shield time. The engine removal portion is estimated to be one-third the shuttle engine remove and replace time. The nacelle allows for better access to engine parts and for inspections. Unscheduled removals due to part failure are all reduced to 1/2 of the baseline vehicle.
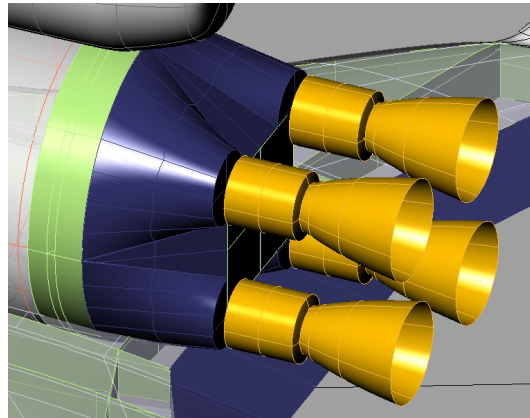
Figure 12.   Nacelle Concept for Engine/Vehicle Interface.

B. Turbo-Pump Maintenance Models

The turbo-pumps models normally include fuel and oxidizer high pressure turbo-pumps and low pressure or boost turbo-pumps. The high pressure turbo-pump inspection times are based on thrust level baselined to Shuttle times[4,5]. The frequency of pump inspections can vary depending on the concept chosen. A torque check operation can be performed to verify rotors are free to move. Turbo-pump leak checks are included in most engines and are primarily done to check for leakage through valves. Removal times of high-pressure pumps are also based on thrust level. The frequency of the removals depends upon unscheduled failure baselined to shuttle data and user-defined scheduled overhauls.

Baseline System for Turbo-Pump Models

The turbo-pumps require removal for overhaul every ten flights.

Advanced System for Turbo-Pump Models

For the turbo-pumps inspection times are reduced by 1/2 and performed every 10 flights instead of every flight. High pressure turbo-pumps are only removed for overhaul every 20 flights versus 10 flights for baseline, and removals due to unscheduled repairs are reduced to 1/4 of the baseline engine. No torque checks are performed because advanced bearings are assumed. Leak checks are reduced by 1/2 for the advanced system because of a better developed engine.

C. Engine Function Checks

This section deals with what are called engine function checks. These are operations[4] that are not specific to any one component but primarily effect the whole engine. Vehicle to engine interface leak checks are performed every time the engines are removed. Flight Readiness Testing involves leak checks and checkouts of the actuators of both the pneumatic and hydraulic systems. The encapsulation leak test is only performed if the engine is removed. However it is done because of the ability to detect leaks of less than one standard cubic inch/minute. A Helium Baggie Leak Check is only performed if the Shuttle engine is used in the design. One engine experienced a main combustion chamber manifold crack caused by a weld repair during initial fabrication. To preclude this type of leak from going undetected in the future, a "big-bag" leak check was developed[10]. For kerosene engines draining of the coolant jacket is required to prevent coking during post shutdown soak back. Decontamination involves clean-up of carbon deposit of chamber walls and injector face. Draining and decontamination are treated as one operation. Cryogenic fueled engines require drying. Drying out the bearings ensures all moisture is removed from the bearing area after flight. If moisture freezes, the ice can interfere with the bearing movement causing engine failure.

Baseline System for Engine Function Checks

The turbo-pumps require removal for overhaul every ten flights. There is no helium baggie leak check. The engine only requires draining and decontamination but no drying.

Advanced System for Engine Function Checks

The advanced engine is assumed to use methane and LOX propellants. The engine function checks have been improved. The main engines are now methane, so drying is needed instead of draining and decontamination. On-board purging is assumed, so a separate operation for drying is not required. Flight readiness testing will be reduced to one-third the time of the shuttle in part because the hydraulics are replaced with an electromechanical system. The encapsulation leak test and the engine-to-vehicle interface leak checks are only performed when the engine is removed and with the advanced engine are reduced to a third of the time as compared to the SSME. For the engine-to-orbiter gimbal checks improvements made with the advanced system do not require hydraulics, and so time to complete the operation is reduced to one-fifth.

VI.   Fluid Related Subsystems

As mentioned previously, the fluid related subsystems include:
1)   Main engine pressurization and feed system.
2)   Orbital Maneuvering System or OMS
3)   Reaction Control Systems or RCS
4)   Auxiliary power units
5)   Actuation system
6)   Active thermal control.

The feed and pressurization systems are defined as those components supporting the main engines that are part of the vehicle and not the removable engines. Most operations use shuttle experience for durations. The man-hours calculated depend on the number of engines, the concept chosen (shuttle or advanced), and the number of personnel involved.

A. Feed and Pressurization Systems Model

Valves and solenoids control propellant flow to the engines and require leak and functional checkout. Major maintenance of system components is required especially when high pressure helium flow can literally cut the seals apart. Helium is also a danger to personnel in confined areas. Functional verification is required for all regulators, isolation valves, and valve control solenoids. Leak checks and checkouts of the fuel and liquid oxygen systems are required because there are multiple interfaces where leaks can occur. Screens are used in the main propellant lines to filter out debris. The screens must be inspected to ensure
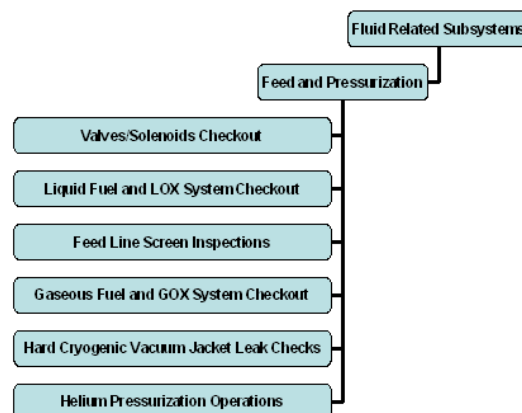
Figure 13.   Feed and Main Engine Pressurization Scope.
All possible maintenance intensive operations.

13

there is no catastrophic failure resulting from the debris. These include system anomaly retests to make sure the inspections did not miss anything. Detent rollers from the pre-valves generate debris in the system. A latch mechanism, used to prevent the flapper valve from closing during flow conditions, generates debris which can lodge on the pre-valve screens preventing closure. If a system uses a self pressurizing engine, the gaseous fuel and oxygen systems require checkout. If a hard cryogenic like hydrogen is used, vacuum jacket lines inspection would be required.   Kerosene and warmer cryogenic propellants, like methane, do not need vacuum jackets. Options are given as to type of system.

Baseline System for Feed and Pressurization

The RMLS102 baseline has subsystems very similar to the Shuttle subsystems. However the size and complexity of the subsystems are smaller. Helium is used in the pneumatic system for valve actuation. The helium option is based on shuttle man-hours. For pressurization, the vehicles use helium because of the kerosene propellant. This system will be larger than the helium system used for the main propellant valves and solenoids but will be modeled after them. The kerosene tank pressurization, valves, and solenoids require extra maintenance actions because of the helium usage.

Advanced System for Feed and Pressurization

The main engines use methane and liquid oxygen as propellants. The gaseous system is used to pressurize the main tanks for the autogenously pressurized system.   Hence, no maintenance intensive helium operations are required. Gaseous methane and gaseous oxygen systems will require checkout but are simpler than helium systems. Nitrogen is used to drive the valves and solenoids instead of helium, also reducing helium related maintenance. The feed lines require inspection, however the complexity of the operations is reduced drastically. The feed line screen inspections are reduced to 2 people and 2 hours per engine. This reduction is possible with better development in parts, reducing debris in the system.

B.   Orbital Maneuvering and Reactions Control Systems

An orbital maneuvering system (OMS) and reaction control system (RCS) have many components. The model uses the number of engines, thrusters, and propellant type to determine man-hours for the system[11]. Hydrogen/Ox, Methane/Ox, Ethanol/Ox, and MMH/NTO are the propellant options.   Removal and replacement of the orbital maneuvering engines is not a planned operation. However, the OMS removal occurs due to needed repair on items inside the OMS (like helium system components). Due to the toxic propellants, a pod concept was adopted for the Space Shuttle so repairs could be performed in a separate facility.   For new vehicle designs without a pod, engines will still need removal for unexpected repairs and are modeled after the pod removal times. Probabilities of engine removal after each flight, the duration of removal, and numbers of personnel determine the total man-hours required.   An interface leak check is required for every OMS engine removal. Trickle purges are performed separately for the OMS and RCS but are the same operation. Trickle purges are needed to remove the toxic propellants from the OMS and the RCS, hence trickle purge operations are eliminated for a non-toxic system. The high pressure helium valves are a major component in checking out the helium subsystem, and calculations are based on the number of RCS thrusters or OMS pods. The helium subsystem checkout is only required for a helium pressurized system. The shuttle OMS engines use ball valves for propellant delivery. The toxicity of the system requires that these valves be drained to prevent corrosion. This operation is not required for non-toxic systems. Quick disconnects are used for servicing while the vehicle is on the pad. More information is required to separate out RCS
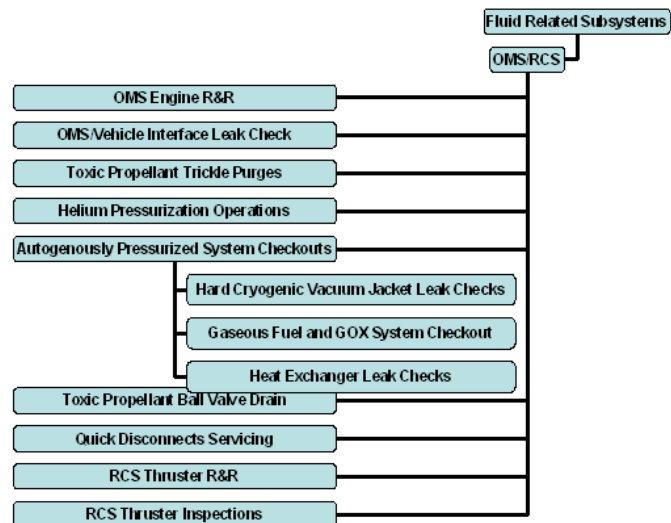
Figure 14.   Orbital Maneuvering and Reaction Control Systems Scope.
All possible maintenance intensive operations.

connections from the OMS so the amount of work involved can be adjusted to the quantity of thrusters or OMS engines. RCS thrusters are removed due to three failure modes[12]:

1) The oxidizer valve becomes corroded. The nitrate oxidizer contaminates the valve over time and causes leakage. The oxidizer valve failure mode is eliminated with a non-toxic system.
2) Over time the fuel valve Teflon seat wears out and so requires RCS replacement.
3) Thrusters are damaged from human handling and other ground mishaps.

A binomial distribution uses failure mode fraction, probability of failure, and number of thrusters to calculate the number of thrusters needing removal and replacement. Inspections are needed for the RCS thrusters because of potential damage due to Nitrate corrosion. After a Space Shuttle mission, technicians thoroughly inspect the vehicle for wear and tear, looking for the minute chips and hairline fractures that can result from supersonic impacts or from the plastic expansion and contraction of materials in the orbiter. To detect any chipping, inspectors currently take impressions of the thrusters using a silicon-based rubber and then section and inspect these molds to determine the surface area and depth of chips. But this manual process is time-consuming and subjective, and it risks leaving residue in the thruster.

Baseline System for Orbital OMS/RCS

The RMLS102 OMS and RCS will use the same toxic system that the Space Shuttle uses. However there are only 12 RCS thrusters instead of 38 for each stage and one OMS engine on the orbiter.

Advanced System for the OMS/RCS

The OMS and RCS use liquid methane and oxygen for propellants. For the OMS/RCS system the trickle purges, ball valve drain, RCS thruster removal due to nitrate corrosion, and RCS inspections are all eliminated because the propellants are non-toxic. A self-pressurized OMS/RCS that uses a propellant like methane will still require maintenance. The operations for the methane systems are based on the main engine pressurization system but are assumed to require 1/2 the time and 1/2 the technicians. A heat exchanger for the self-pressurized system is added for the larger OMS engine. Heat exchanger leak checks are performed and based on the heat exchanger used for the Space Shuttle main engines. An electric heater is used for the smaller self-pressurized RCS system, but no maintenance is added.

C. Auxiliary Power Units and Actuators

The APU supplies power to the actuators and the avionics in the vehicle. Maintenance Operations for these systems assume a triangular distribution for calculating man-hours. Operations for the APU are scaled with the number of APUs using shuttle durations as a point of reference. Hydrogen/Ox, Methane/Ox, Ethanol/Ox, and hydrazine are the propellant options. In the Space Shuttle, APU lube oil is used in the hydraulic pump gearbox assembly of the APU. There is a seal cavity with drain and purge ports between the fuel pump and gear box. Leakage occurs across the seals with hydrazine and lube oil mixing together. The reaction between the oil and hydrazine makes a waxy substance which clogs the oil filter and drain passage[13]. Flushing of the oil system is required after each flight to prevent the clogging. After the oil is removed the system is purged with nitrogen. The lube oil servicing model is used when a

Figure 15.   Auxiliary Power Units Scope
All possible maintenance intensive operations.

hydraulic pump gearbox is required. For the Space Shuttle, catch bottle drain operations are also time consuming and required modeling. The fuel pump reduction gear is located in the lube oil system gearbox, and a shaft from the reduction gear drives the fuel pump. Seals are installed on the shaft to contain any leakage of fuel or lube oil. If leakage occurs through the seals, it is directed to a drain line that runs to a 500-cubic-centimeter catch bottle for each. If the catch bottle were overfilled, it would relieve overboard at approximately 28 psia through a drain port. The maintenance operation involves venting APU fuel tanks and fuel manifolds, draining APU cavity drain system catch bottles, and performing a functional test of catch bottle relief valves and alcohol-flush cavity drain system. A

leak and functional check is performed for the APU in addition to the lube and catch bottle drain servicing. The leak and functional tests are performed because of potential leaks between any of the seals. Due to hydrazine toxicity these checks are very important. The Space Shuttle uses all hydraulic actuation and there are two major operations. Inspections for the hydraulic systems on the Shuttle involve looking for leaks of hydraulic fluid. Inspections are required to prevent contamination of fluid to other parts. The hydraulic systems are similar to any large aircraft hydraulics and therefore can be modeled in a similar fashion. Bleeding the hydraulic lines and the filling is treated as one operation. Manual verification of air intrusion into hydraulic lines is a possibility requiring bleeding of the lines.

Baseline System for APUs and Actuators

The hydraulic actuators and APU system are setup similar to the Shuttle except there are only 2 sets instead of 3 and they have electrical generators built in as well as the hydraulic pump. The electric generators supply electricity to the avionics and batteries for the short duration flights this vehicle is assumed to make.

Advanced System for APUs and Actuators

As an alternative to a traditional toxic APU, the bipropellant gas generator electric APU model uses methane and liquid oxygen. The gas generator is modeled similar to the advanced orbital maneuvering system. This system replaces the hydrazine hydraulic/electric APU with an all electric system.. All operation times for the bipropellant gas generator are assumed to be 1/2 of the OMS engine times. The lube oil servicing is eliminated because there is no hydraulic gearbox needed. The catch bottle drain is not needed.. The hydraulic bleed, fill and inspections are eliminated with the electric system.
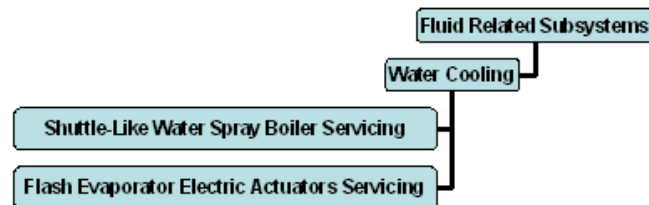
D. Water Cooling

A water cooling system is required to cool bays and internal items which generate heat or are subject to heating and are not cooled or purged by nitrogen. This includes the actuators, the APUs, and may include other subsystems such as avionics, though these may be cooled by nitrogen.

Baseline System for Water Cooling

The Space Shuttle water cooling system is used. However there are 2 instead of 3 boilers.
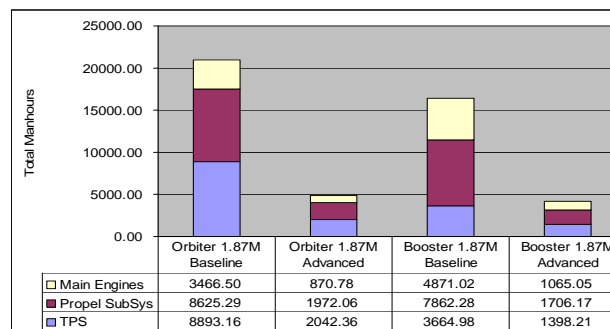
Advanced System for Water Cooling

Since there is no hydraulic fluid to cool the actuators, water cooling is needed for each actuator. The electric actuators are insulated and incorporate an open loop water flash evaporator for cooling. The low pressure water lines and central water source are much easier to maintain than the hydraulic lines of the baseline system. A simple flash evaporator requires simple leak checks and servicing. The size of the system is not known so the maintenance is only an estimate based on the shuttle evaporator.

Figure 16.   Water Cooling and Actuators Scope
*All possible maintenance intensive operations.*

VII.   Conclusion

The capabilities provided by the research, the developed Monte Carlo modeling, and the discrete event simulation done in Arena all work to provide information that help determine a Reusable Launch Vehicle's sortie rate and man-hours required to send payloads into orbit. The discrete event simulation developed allows the designer, technologist, and user of the RLV the flexibility to evaluate the effect of different designs and technologies. As discussed, the assessments are not possible without knowledge of the launch vehicle systems involved and the failure mechanisms that drive maintenance. The model can incorporate new knowledge about

	Orbiter 1.87M Baseline	Orbiter 1.87M Advanced	Booster 1.87M Baseline	Booster 1.87M Advanced
Main Engines	3466.50	870.78	4871.02	1065.05
Propel SubSys	8625.29	1972.06	7862.28	1706.17
TPS	8893.16	2042.36	3664.98	1398.21

Figure 17.   Maintenance Man-hours for RMLS102.

16
American Institute of Aeronautics and Astronautics

systems to improve the accuracy of assessments. Upgrades to the model will also include areas outside the repair facility such as landing, mating, pad time, and launch. The RMLS102 design, a two-stage-to-orbit system, was assessed for man-hours for use in a technology assessment study as shown in Figure 17. Man-hours required for technology assessment do not include the queuing time involved in discrete event simulations. Only the amount of physical work involved in performing operations is required to assess a technology. The results provided assess the baseline RMLS102 design versus the advanced system of the RMLS102.

A further breakdown of maintenance man-hours helps explain the improvements gained for each system. Figure 18 reveals what improvements have been made and improvements that can still be made for the thermal protection systems. For example, a lot of focus has been put on making thermal protection easy to remove and replace, which is an important part of reducing man-hours. However, the other parts or systems still need attention as figure 18 shows. For example, the gap filler maintenance shows up as a long pole after other areas are improved. Improved gap fillers or a design that requires no gap fillers might be considered. The main engine and fluid related subsystems areas have similar results.
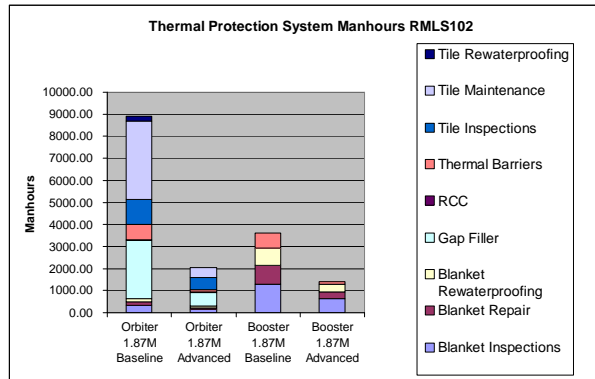
Figure 18.   Maintenance Man-hours for RMLS 102.
For thermal protection work performed in the repair facility only

The modeling approach will be applied to other systems that comprise a reusable launch vehicle. Other areas might include structure, avionics and ground support equipment. The cycle time is not presented nor was it needed for the study at this time. The cycle time simulation is in the process of improvement to represent more realistic processing. Many operations will be changed to parallel, serial, or processed in different sequences. The next stage in model development will include critical path analysis to reduce turnaround time from months in the case of the Space Shuttle to hours or days for a military reusable launch vehicle.

References

[1]Crow, Edwin L.; Davis, Frances A.; Maxfield, Margaret W., "Statistics Manual" – Dover Publications 1960.

[2]Mathcad, Engineering Modeling, Software Package, Ver. 11, Mathsoft, 2002.

[3]ARENA, Discrete Event Simulation, Software Package, Ver. 7.00.00, Rockwell Software, 2002.

[4]Christensen, R. L., and Komar, D. R., "Reusable Rocket Engine Operability Modeling and Analysis," NASA TP-1998-208530, 1998

[5]Byrd R.J., "Operationally Efficient Propulsion System Study (OEPSS) Data Book," Rockwell International., RI/RD 90-149-1.

[6]Scholz, A. L., Hart, D., and Lowry, D. J., "Shuttle Ground Operations Efficiencies/Technologies Study," Boeing Aerospace Operations, NASA CR-180582, 1987.

[7]Dominguez, X., "Mission STS-98 OV-104 Flight 23 Thermal Protection System Post-Flight Assessment," The Boeing Company, June 2001.

[8]Gordon, M., "Space Shuttle Orbiter Thermal Protection System Processing Assessment Final Report – Non-Proprietary Appendix Sections" – Rockwell, May 1995.

[9]Craddock, J., Buchert, N., Rodriguez, Jr., H., and Cosgrove, M., "Main Propulsion System Maintainability Issues for the Future Shuttle," The Boeing Company, AIAA 2002-3756, Huntington Beach, CA, 2002.

[10]Klatt, F. P., Buchert, N., Rodriguez, Jr., H., and Cosgrove, M., "Cost Effective Launch Operations of the SSME," Rockwell International, Canoga Park, CA, 2002.

[11]Rehagen, R., and Rodriguez, H., "Space Shuttle Orbital Maneuvering System/Reaction Control System Improvements for the Future Shuttle," The Boeing Company, AIAA 2002-4326, Huntington Beach, CA, 2002.

[12]Roshan-Zamir, S., Schick, T. D., Reistle, B., Etchells, M., Dyer, E., "Space Shuttle Analysis Report: Reaction Control System (RCS) Primary Thruster Reliability & Maintenance Analysis and Assessment," SAIC, NAS9-19180, 1999.

[13]McKenna, R., Hagemann, D., Loken, G., and Jonakin, J., Sundstrand Corp., Baughmann, J., Rockwell International, Lance, R., NASA-JSC "An Improved APU for the Space Shuttle Orbiter," AIAA 85-1481, 1985.

APPENDIX G

THERMAL-BASED COMPARISON BETWEEN ROCKET BOOST-BACK AND JET FLY-BACK BOOSTER RECOVERY APPROACHES

Gregory E. Moster, Captain David Callaway, and Amarshi Bhungalia
Air Force Research Laboratory
Air Vehicles Directorate
Wright-Patterson AFB, Ohio 45433

ABSTRACT
The Air Force Research Laboratory has been exploring approaches that may be considered for a quick turn-time booster research demonstrator for possible utilization on a full scale such as the Affordable Responsive Space (ARES) system. Part of this effort includes the evaluation and comparison of a wide variety of operating approaches that may yield significant variations in aerodynamic heating, material selection, design-space expansion, and maintenance approaches. One approach that has been under investigation by AFRL since 2001 is Rocket Boost-Back. This approach replaces the fly-back hardware (Thermal Protection System (TPS) and the jet engines) used to fly back to the launch site area (common in the most widely publicized systems) with additional rocket fuel and uses rocket motors to "boost" the system back within gliding range of the launch site. Eliminating the need for TPS opens up the design space and may allow a larger variety of wing and tail configurations than the limited Space Shuttle looking concepts. This paper will compare the relative size, weight, and thermal implications of the rocket boost-back and jet engine fly-back (AFRL baseline system) concepts at a high level in order to identify where additional effort may be desired.

INTRODUCTION
The Air Force is currently in the process of considering the development a low turn-time (measured in hours instead of weeks) reusable first stage to support affordable rapid access to space. In order to achieve this challenging objective, all options must be considered and a thorough understanding of the challenges must be known. Reusable Military Launch System (RMLS) team members have worked closely with NASA Kennedy Space Center (KSC) and NASA Johnson Space Center (JSC) maintenance and flight operations personnel for the last five years in order to increase their understanding of this challenging task. From their work and collaboration with jet aircraft operators and maintainers, a straight forward conclusion appears to be that the greatest difficulty lies in reducing or eliminating flight operations and maintenance actions that make the system vulnerable to catastrophic failure mechanisms. Catastrophic failure mechanisms are undesirable because they can cause a loss of vehicle (and possibly life). This looming possibility forces operators and maintainers to expend significant resources. It also causes the military to expend valuable resources (personnel, money, and hardware) needed to support the US during conflicts. A rough idea of effort involved can be seen in figure 1 that captures NASA KSC's estimate of the man-hours used to maintain the Space Shuttle in the Orbiter Processing Facility (OPF). It can be seen here that TPS maintenance is a very large part of the maintenance effort. Part of this effort can be tied to how NASA fly's or operates the vehicle. For example, when the Space Shuttle lands the gear doors are opened. Opening the gear doors breaks a high temperature seal. When this critical seal is broken maintenance must be performed. Seal maintenance is a time consuming and critical task that demands highly skilled
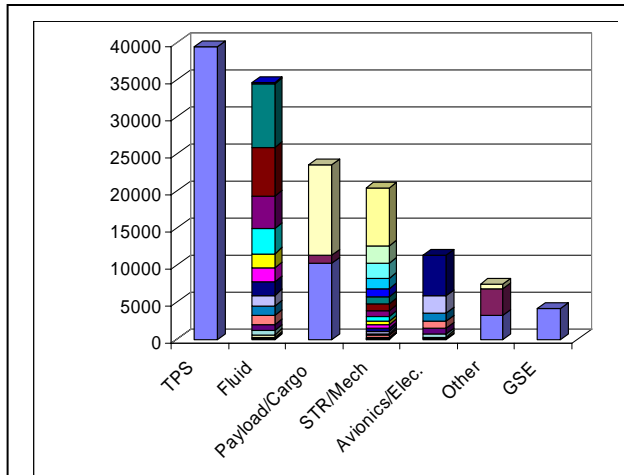
Figure 1. Man Hours in the OPF
Space Shuttle STS-85 Man-hours Courtesy of Edgar Zapata NASA KSC

technicians and a robust verification process, because if the seals are not "perfect", a catastrophic event like the Columbia may occur. Therefore, the question may not be "how do we make better seals"; it may be "how do we avoid the seals entirely". These types of questions and considerations pushed the RMLS team to consider options that may enable future Air Force boosters to recover by avoiding the high thermal environment encountered during normal reentry. The rocket boost-back approach is one of these approaches being considered.

The rocket boost-back approach uses the rocket engines (not necessarily the main engines) to decelerate the booster after staging to a velocity where either non-critical TPS or no TPS is required. This trading of thermal energy for fuel can be accomplished in a variety of ways. The approach presented here simply turns the booster around after staging until the vehicle is parallel with the Earth's surface with the engines burning and pointed in the general flight path direction (figure 2). The design and thermal analysis of this approach will be compared to the baseline system that reenters similar to the Space Shuttle before employing jet engines for the return to launch site flight segment. This paper will describe analysis software, sizing assumptions, and present the results (size, aerodynamic, trajectory, and thermal loading) of the baseline fly-back and rocket boost-back approaches.
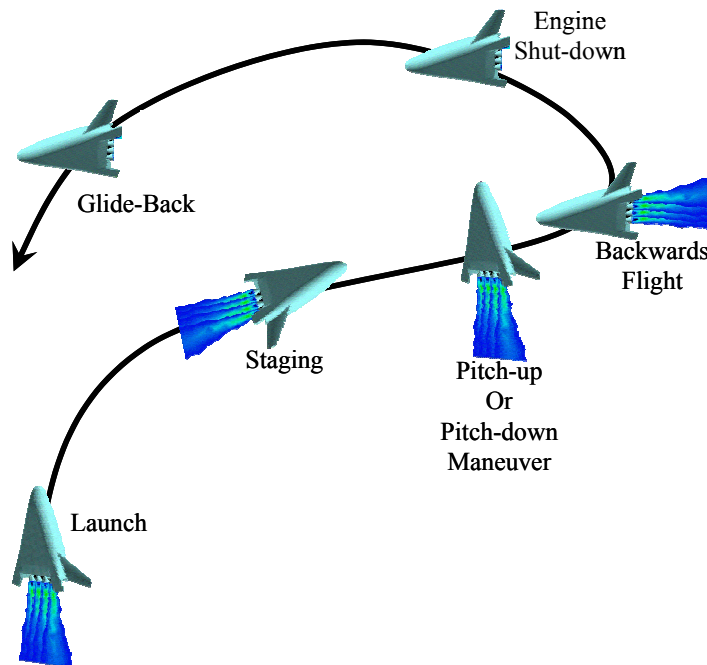
Figure 2. Rocket Boost-Back Concept

ANALYSIS SOFTWARE

System sizing was accomplished using the Integrated Propulsion Analysis Tool (IPAT) developed by the Air Force Research Laboratory (Air Vehicles and Propulsion directorates) which was heavily based upon the RMLS sizing software co-developed with the Air Force Aeronautical Systems Center (ASC). This software utilizes TechnoSoft Inc. Adaptive Modeling Language (AML) as the core software for managing the parametric design process. AML has links into several analysis codes that provide the required sizing information. These include aerodynamics, trajectories, and thermal analysis. Lift and drag coefficients were obtained using Missile Dat Com developed by AFRL. Trajectories were simulated using the Program to Optimize Simulated Trajectories (POST II) developed by NASA Langley Research Center (LaRC). Thermal analysis was accomplished using MINIVER also developed by NASA LaRC. These are the same tools utilized by the Air Force during NASA's Second Generation Launch Initiative (SGLI) and Next Generation Launch Technology (NGLT) study efforts and verified with NASA and industry.

ASSUMPTIONS

In order to level the analysis playing field as much as possible, common assumptions and models were used for both assessments. The rocket boost-back sizing was performed using the baseline jet fly-back model with the TPS and fly-back systems removed. We assume that leading edge heating can be handled by high temperature metallic materials with minimal to no insulation.

Common Conditions

Payload	58,279 lb
Launch Thrust to Weight	1.3
Engine ISP	290 seconds
None throttling of rocket engines	
Staging velocity	7,000 feet per second
Staging flight-path angle	20 degrees
Wing loading	74.7 pounds per square foot
Aspect Ratio	2.4 (approximately)
Maximum dynamic pressure	700 pounds per square foot
Maximum normal wing loading	2.5 g's
Maximum axial loading	6.0 g's
Cruise and glide lift over drag	5 to 6
Return-To-Launch-Site Altitude	Pass over the field at 30,000 feet or more
Standard day conditions	

Fly-Back Specific

Fly's 15 minutes past launch site to account for cruise condition winds

Rocket Boost-Back

After staging keep two out of four engines ignited at full throttle (50% of full-throttle used to boost back)

RESULTS

The results of the comparison follow in figures 3 through 11. The rocket boost-back has a higher fuel fraction and is 31% heaver at launch than the jet fly-back system; however, it has a 27% lower empty weight. Staging altitude was not constrained and both approaches staged at nearly 145,000 ft. Figures 10 and 11 show an estimate of the nose stagnation temperature using MINIVER. This preliminary estimate may not be accurate due to uncertainties in the input file and with the use of a two foot radius nose. Work will be accomplished to improve these estimates as the Air Force activities continue. The trend should be correct because only the trajectories varied between the two analyses.

Description	Fly-Back	Boost-Back
Fuel Fraction	0.6878	0.8122
Launch Weight	423,122 lb	615,726 lb
Landing Weight	70,714 lb	52,940 lb
Empty Weight	69,240 lb	50,841 lb
Fuselage Length	81 ft	97 ft
Fuselage Diameter	14 ft	16 ft
Time Back Over Field	84 minutes	11 minutes
Cross-range	94 nm	0 nm

Figure 3. Fly-Back (left) and Boost-Back (right)
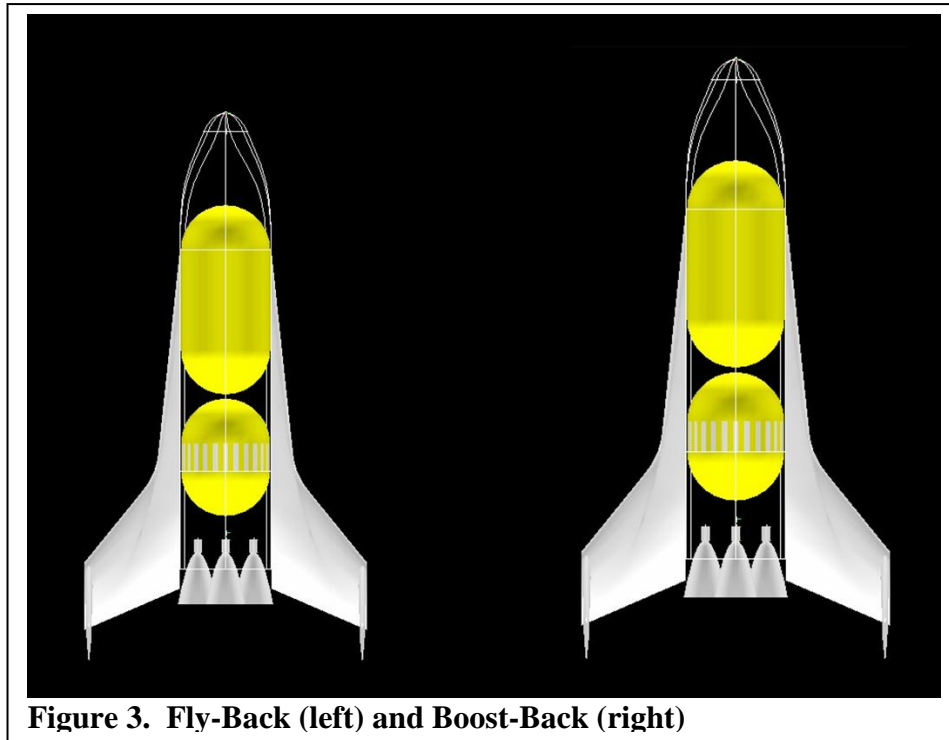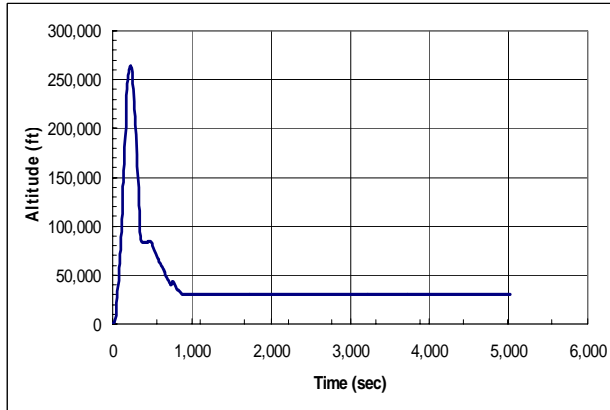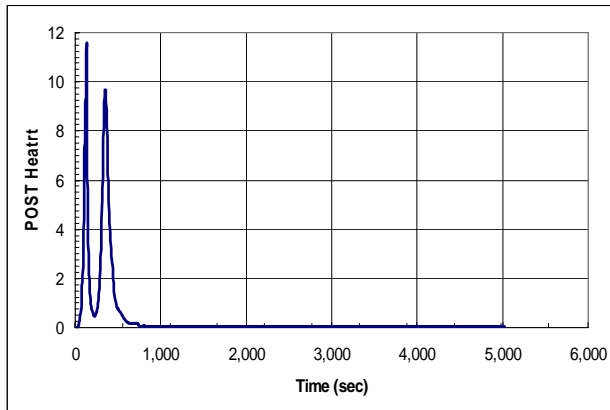
Figure 4. Fly-Back: Time vs altitude
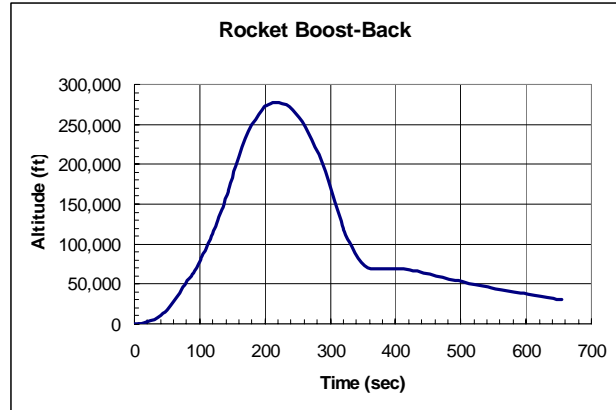
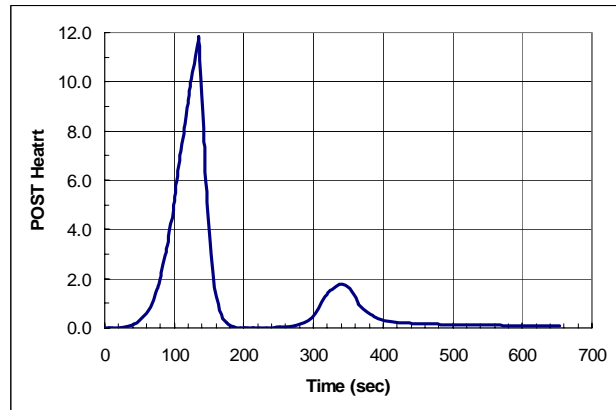**Figure 5. Boost-Back: Time vs altitude**
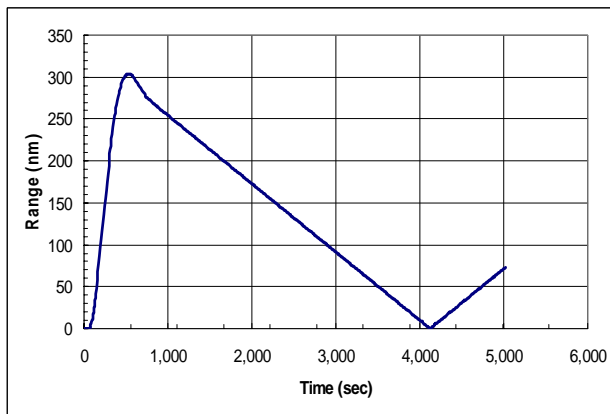
Figure 6. Fly-Back: Time vs range to field
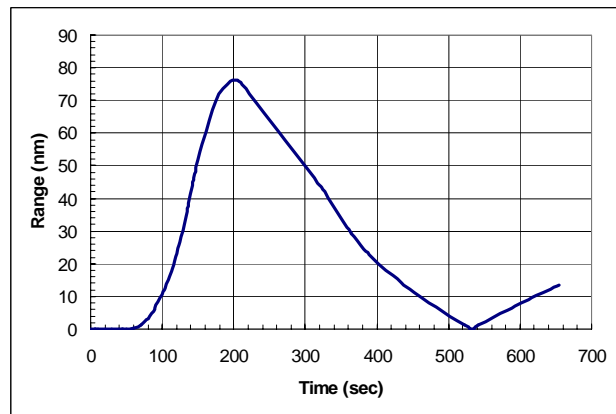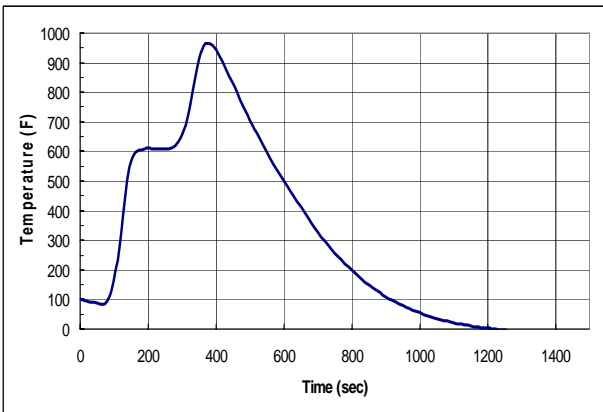

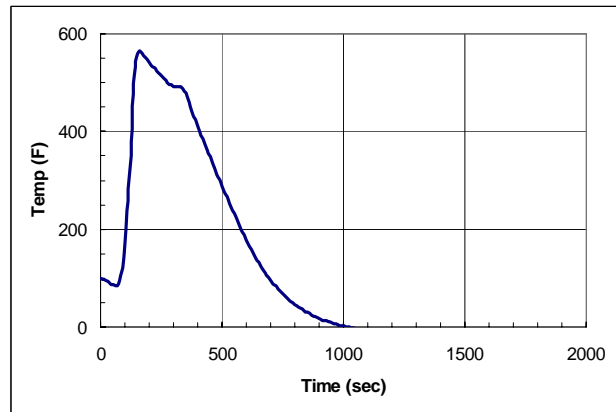**Figure 7. Boost-Back: Time vs range to field**

Figure 8. Fly-Back: Time vs heat rate

Figure 9. Boost-Back: Times vs heat rate

Figure 10. Fly-Back: Time versus nose stag. temp

Figure 11. Boost-Back: Time versus nose stag. temp

CONCLUSIONS

The jet engine fly-back booster is smaller both in size and launch weight than the rocket engine boost-back booster, but not in empty weight. Typically, empty weight is considered the acquisition cost driver, so the rocket boost-back booster would normally be expected to be cheaper. The cost savings is compounded by the possibilities of using normal aircraft materials without TPS and not requiring jet engines. Eliminating the TPS and jet engines combined with normal aircraft materials may drive the cost of the rocket boost-back system down to half of the fly-back booster and make the option selection straightforward. The simplicity of the larger boost-back may more than make up for it's larger size with operations cost and turn-time reductions too. For example, large and simple airline transports and Air Force refueling aircraft have very short turn-times and are very reliable; however, more complex fighter and bomber aircraft take considerably more time and resources to maintain and return to use. Therefore, the rocket boost-back approach looks extremely promising, but needs further exploration to verify these results and determine how it compares to the typical jet fly-back systems being currently proposed to the Air Force and NASA.

REFERENCES

1. Rooney, Brendan; Hartong, Alicia, "A Discrete-Event Simulation of Turn-Around Time and Manpower of Military RLV's", AIAA 2004-6111, 2004.

ACKNOWLEDGEMENTS

APPENDIX H

Thermal Protection System (TPS) Optimization

Amarshi A. Bhungalia, Lt Carrie Clewett, Harold Croop and David A Brown

Air Force Research Laboratory, Air Vehicles Directorate, Structures Division, Wright-Patterson AFB OH 45433

The Air Vehicles Directorate of the Air Force Research Laboratory conducts research in a broad range of technical disciplines to support emerging and next generation capabilities. One major focus area is Operationally Responsive Spacelift (ORS) and the technologies required to enable effective and affordable space access vehicles. As part of our planning and program decision-making, technology assessments and trades are often desired. These assessments provide quantifiable measures to support and guide the planning decisions. A recent in-house technology assessment was done to provide technical rationale that aids in the planning and resource allocation related to near-term and far-term ORS technologies. This paper will describe the Thermal Protection System (TPS) technology assessments that were made as part of this in-house effort. The desire was to make comparable assessments of numerous TPS concepts against a baseline shuttle-like acreage, windward tile. These concepts exist in various stages of maturity, each with its own set of distinct advantages and disadvantages. The results of this technology trade are documented in this paper.

Nomenclature

AML	Adaptive Modeling Language
CEAC	Combined Environment Acoustic Chamber
MINIVER	MINIature VERsion aero-thermal analysis program
TPS	Thermal Protection System
TSTO	Two Stage To Orbit

I. Introduction

The Shuttle thermal protection system consists of various materials applied externally to the outer structural skin of the orbiter to maintain the skin within acceptable temperatures, primarily during the entry phase of the mission. The orbiter's outer structural skin is constructed primarily of aluminum and graphite epoxy. During entry, the TPS materials protect the orbiter outer skin from temperatures above 350 F. In addition, they are normally reusable for 100 missions with refurbishment and maintenance. These materials perform in temperature ranges from minus 250 F in the cold soak of space to entry temperatures that reach nearly 3,000 F. The TPS also sustains the forces induced by deflections of the orbiter airframe as it responds to the various external environments. Because the thermal protection system is installed on the outside of the orbiter skin, it establishes the aerodynamics over the vehicle in addition to acting as the heat sink.

Orbiter interior temperatures also are controlled by internal insulation, heaters and purging techniques in the various phases of the mission. The TPS is a passive system consisting of materials selected for stability at high temperatures and weight efficiency. Some of these materials are discussed below.

Reinforced carbon-carbon (RCC) is used on the wing leading edges; the nose cap, including an area immediately aft of the nose cap on the lower surface (chine panel); and the immediate area around the forward orbiter/external tank structural attachment. RCC protects areas where temperatures exceed 2,300 F during entry.

Black high-temperature reusable surface insulation (HRSI) tiles are used in areas on the upper forward fuselage, including around the forward fuselage windows; the entire underside of the vehicle where RCC is not used; portions

1

of the orbital maneuvering system and reaction control system pods; the leading and trailing edges of the vertical stabilizer; wing glove areas; elevon trailing edges; adjacent to the RCC on the upper wing surface; the base heat shield; the interface with wing leading edge RCC; and the upper body flap surface. The HRSI tiles protect areas where temperatures are below 2,300 F. These tiles have a black surface coating necessary for entry emittance.

Black tiles called fibrous refractory composite insulation (FRCI) were developed later in the thermal protection system program. FRCI tiles replace some of the HRSI tiles in selected areas of the orbiter.

Low-temperature reusable surface insulation white tiles are used in selected areas of the forward, mid-, and aft fuselages; vertical tail; upper wing; and OMS/RCS pods. These tiles protect areas where temperatures are below 1,200 F. These tiles have a white surface coating to provide better thermal characteristics on orbit. [1], [2], [3]

II.   In-House Study

To meet requirements for the anticipated military environment, the Air Force has been leveraging Shuttle tile and blanket technology to develop TPS designs which are more operable and which have enhanced robustness. To improve operability, the Air Force has been focusing on mechanical attachments for easier TPS removal and replacement. To improve robustness, the focus has been on use of CMC as a wrap over tile or just as a tile outer-moldline skin. These developments are represented in the designs that were compared in this study.

In order to make assessments, a notional baseline two-stage-to-orbit (TSTO) vehicle with its geometry, weight, and mission profile was used to size and compare the different TPS concepts with respect to weight, reliability, and turn-around time. A baseline vehicle configuration with the associated mission details is imperative to performing meaningful trades, because the baseline vehicle and mission profile set exterior environmental conditions, geometry, physical configurations, and a maintenance context. These conditions allow the various concepts to be viewed in a meaningful comparative context.

A baseline and five alternate TPS concepts were modeled. The MINIature VERsion (MINIVER) [4] aero-thermal analysis program was used to size TPS layer thickness, allowing sizing and weight trades to be made. In addition, qualitative and quantitative operability and maintainability assessments were made using NASA shuttle data and trends that have emerged from the TPS concepts development.

This paper presents the results of the TPS weights analysis and a brief comparison of TPS operability issues. Specifically, it presents the acreage, windward TPS weight comparisons of the 6 concepts and the basic advantages and disadvantages associated with each concept.

III.   Miniature Version Aerothermal Analysis Program

MINIVER is a versatile engineering code that uses various well-known approximate heating methods together with simplified flow fields and geometric shapes to model the vehicle. Post-shock and local flow properties based on normal-shock or sharp-cone entropy conditions are determined in MINIVER through user selection of the various shock shape and pressure options. Angle-of-attack (AOA) effects are simulated either through the use of an equivalent tangent-cone or an approximate cross flow option. The flow can be calculated for either two- or three-dimensional surfaces. However, the three-dimensional effects are available only through the use of the Mangler transformation for flat-plate to sharp-cone conditions.

MINIVER has been used extensively as a preliminary design tool in government and industry and has demonstrated excellent agreement with more detailed solutions for stagnation and windward acreage areas on a wide variety of vehicle configurations, including the Space Shuttle orbiter, HL-20, X33 (winged body, lifting body, and vertical

2

Lander), X34, X37, X43 and NASP. The principle advantage of this engineering code over some of the more detailed methods is the speed with which the analyses can be performed for each flow condition along a trajectory. Its strength lies in its ability to quickly provide the time-dependent thermal environments required for TPS analysis and sizing.

MINIVER is an interactive computer software program, which is used both to predict the aero-thermal environments and to perform simple TPS sizing for aerospace vehicles that operate in the hypersonic flight regime. Three subprograms comprise the MINIVER code: PREMIN, the preprocessor used to set up the input parameters required to run the next subprogram, LANMIN (LANgley MINiver) [5], which is used to compute the aero-thermal environments, and EXITS [6], which is used to predict the thermal response of the TPS.

IV. The Adaptive Modeling Language

The MINIVER code is integrated with an Adaptive Modeling Language (AML) [7] to enhance pre and post processing of the MINIVER code. Specifically, AML assists to formulate PREMIN data rapidly. If we do not use AML integration, it may take 2 to 3 days to formulate analysis for one point. Use of AML integration saves 2.75 days for only one point analysis, and we have a total of 30 points for one vehicle on just the windward side. Without the use of AML, if you make even one change in any parameter, the process has to start from the beginning. MINIVER is very sensitive to any mistakes, and it will not give any indication of where your mistakes are. It will simply stop running, and you will not get any results. You would then have to go through all your data piece by piece, make the appropriate corrections, and hope MINIVER will cooperate. However, by using the AML integration process, the mistakes you need to correct show up in a tabular form. You do not have to start the entire problem over from the beginning. All data is retained in the tables, and only the changes are reflected in the input file.

AML integration also allows PREMIN, LANMIN, and EXITS data preparation at the same time as input for combined aero-thermal analysis. The LANMIN module output gives flow condition and thermal data for the outer surface of the vehicle. The LANMIN output, along with some other data, creates the needed input data such as number of layers, material thickness, and material properties for EXITS. The Exits output data consist of transient temperature, radiation heat flux, convection heat flux and TPS weight per square feet surface area. The vehicle configuration office (ASD) provided the surface areas as shown in figure 1 and figure 2.
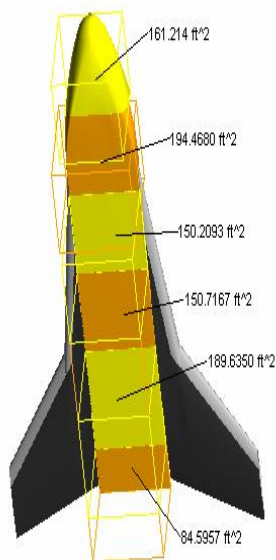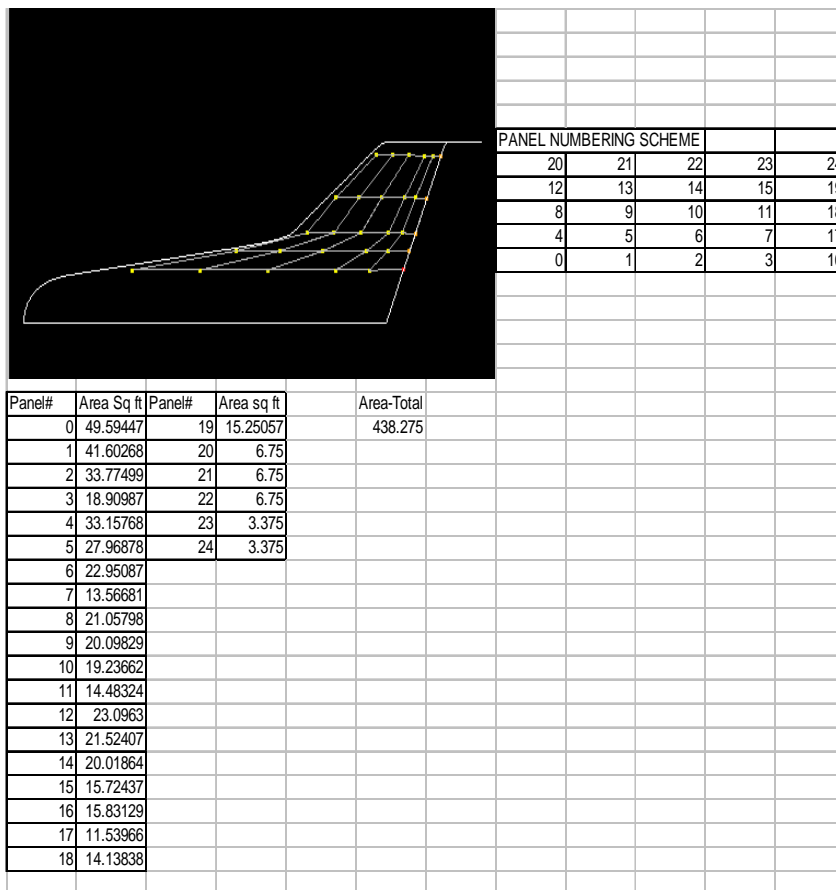

Figure 1 – Windward Zone areas for Fuselage

PANEL NUMBERING SCHEME

20	21	22	23	24
12	13	14	15	19
8	9	10	11	18
4	5	6	7	17
0	1	2	3	16

Panel#	Area Sq ft	Panel#	Area sq ft	Area-Total
0	49.59447	19	15.25057	438.275
1	41.60268	20	6.75	
2	33.77499	21	6.75	
3	18.90987	22	6.75	
4	33.15768	23	3.375	
5	27.96878	24	3.375	
6	22.95087			
7	13.56681			
8	21.05798			
9	20.09829			
10	19.23662			
11	14.48324			
12	23.0963			
13	21.52407			
14	20.01864			
15	15.72437			
16	15.83129			
17	11.53966			
18	14.13838			

Figure 2 – Windward Wing zone Areas

Multiple TPS concepts were included in this in-house study. The baseline concept, figure 3   was the traditional space shuttle HRSI TPS. The outer layer Reaction Cured Glass (RCG) Coating was modeled as 0.05 inch thick (minimum MINIVER thickness). [8] This material has a working temperature of 2300 deg F and has a density of 104 lb/ft3. The next layer is the HRSI Tile LI-900 insulation. This material has a working temperature of 2300 Deg F and a density of 9 lb/ft3 (This layer will be optimized). The next layer is adhesive, RTV-560. Other TPS concepts that were optimized include Alumina Enhanced Thermal Barrier (AETB) tile with TUFI coating, Ceramic Matrix Composite (CMC) Wrapped AETB Tile, and CMC Wrapped Tile with Aztex, Inc., X-CorTM through-thickness CMC pin reinforcement. Figure 3 shows CMC wrapped tile specimens that were successfully thermal-acoustic tested in the AFRL/VAS Subelement Facility (SEF) at WPAFB, OH. Figure 4 shows a 12" by 18" CMC faced tile TPS panel with X-CorTM reinforcement that was also successfully tested in the SEF.
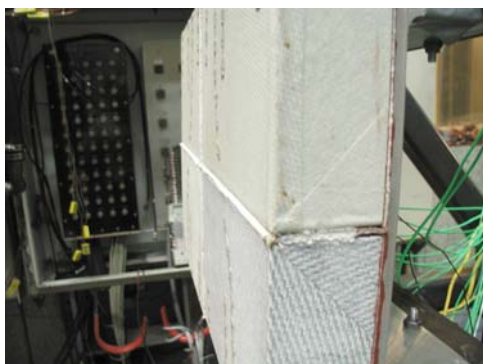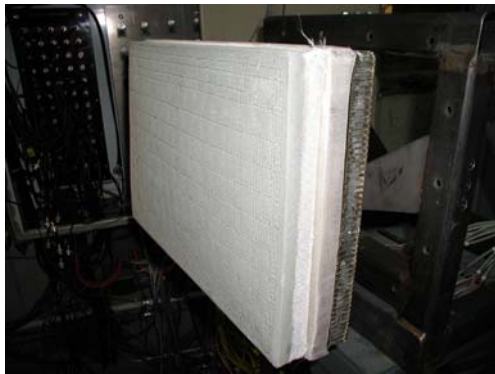
Figure 3: CMC Wrapped Tile TPS

4
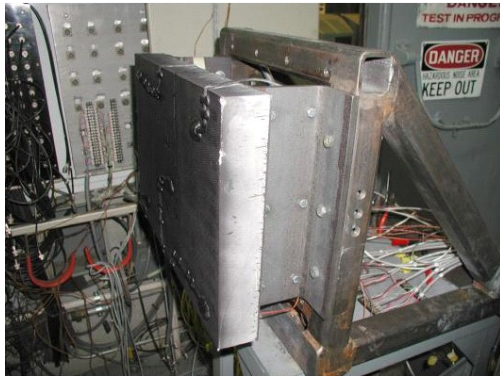
**Figure 4: CMC Faced Tile with X-Cor[TM]**

The remaining TPS concepts were Mechanically Attached Ceramic Blankets (no adhesive), and Mechanically Attached Metallic TPS (no adhesive). Figure 5 is an example of a 12" by 18" dual layer mechanically attached blanket test panel that has been successfully evaluated in the SEF.

Figure 5: Mechanically Attached Blanket TPS

AFRL/VA Reusable Military Launch System (RMLS) team was tasked to designed a notional space access vehicle. AML, a commercial software code was used for the RMLS vehicle configuration. This vehicle was chosen for baseline vehicle. Its length is 65 feet. The vehicle geometry, trajectory, and mission specifics came from a configuration designer from the Aeronautical Systems Center. The trajectory optimization was accomplished using the POST [9] software code and this was performed at AFRL/PR (west). The vehicle information and trajectory were used to get a temperature profile for the entire mission trajectory as shown in figure 14. A 35 degree constant angle of attack was used during reentry. A 350 degree F internal temperature was maintained at the last layer surface to drive the TPS thickness during optimization. The temperature at 5 points along the centerline of the fuselage was calculated, as well as temperature along 5 flow curves down the orbiter wing. See Figure 6, and figure 16.

The typical temperature vs time plot of fuselage center line flow curve is shown in figure 15. The temperature plots of wing flow curves are not shown in this paper, but maximum temperatures of the five wing and one fuselage flow curves as shown in figure 16. The right wing temperatures and TPS weights are assumed symmetrical as of the left wing. The leeward TPS design is not performed as a part of this in-house study. .
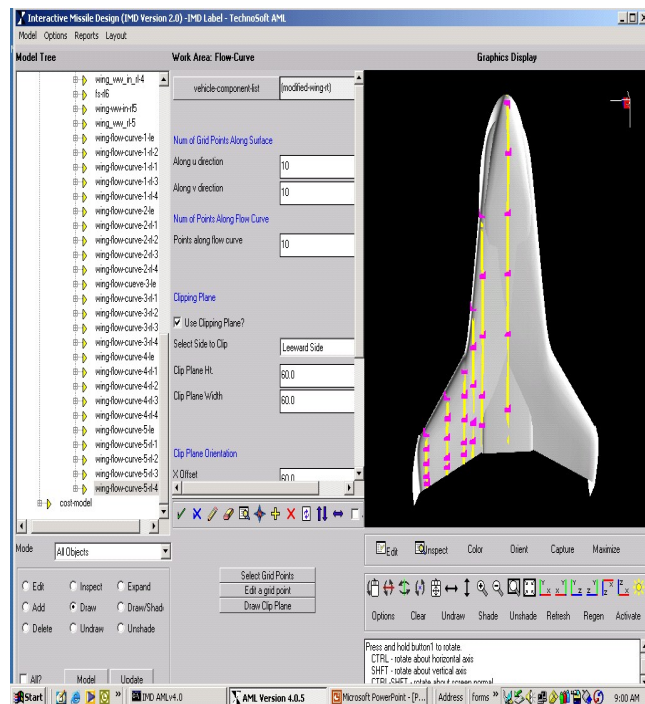
Figure 6: Fuselage and Wing Flow Curves

Leading edge and nose TPS was not included in this study. Max temp was about 2700 degrees F, and the resulting thickness of the TPS at that point was 5.31 inches. Adhesive was modeled as accurately as possible. The substrate was not modeled because some of the concepts were composite skin, while others were aluminum skin.

The six different concepts are summarized in figures 7 to figures 12. Summary of weight and maximum TPS thickness is shown in the table 1 and figure 13..

A. Abbreviations for the concepts:

High Temperature Reusable Surface Insulation (HRSI)

Reaction Cured Glass (RCG)

Toughened Unipiece Fibrous Insulation (TUFI)

Alumina Enhanced Thermal Barrier (AETB)

Ceramic Matrix Composite (CMC) Wrapped Tile

RCG Coating (0.005 in)
HRSI Tile (Optimized)
Adhesive (0.008 in)
Nomex Felt (0.16 in)
Adhesive (0.008 in)
Alum skin

Figure 7 - Concept No. 1 Shuttle Baseline

Concept No. 1 is based on the original bonded tile configuration for the Shuttle Orbiter windward surfaces. It requires two layers of adhesive with an intervening strain isolation layer to decouple tile and skin strains for aluminum based structure. This concept was chosen as the baseline since it is a flight proven system in use today

for the world's only reusable space launch vehicle. The design is lightweight but is susceptible to damage from debris impacts.

RCG Coating (0.005 in)
TUFI Tile (0.1 in)
AETB Tile (Optimized)
Adhesive (0.008 in)
Nomex Felt (0.16 in)
Adhesive (0.008 in)
Aluminum Skin

Figure 8 - Concept No. 2 Upgrade Ceramic Tile

Concept No. 2 is the upgraded, TUFI coated tile design developed for the Shuttle. This design has been proven in ground testing and in flight, for selected locations on the Orbiter, to offer superior damage resistance versus tiles without TUFI. This concept is similar to Concept No. 1 in that it requires strain isolation for use on aluminum structure.

RCG Coating (0.005 in)
CMC Face sheet (0.05 in)
AETB Tile (Optimized)
RTV Adhesive (0.008 in)
Composite Skin

Figure 9 - Concept No. 3 CMC Wrapped Tile

The first developmental design selected was Concept No. 3. It utilizes a CMC facesheet to provide further resistance, versus Concept No. 2, to potentially damaging impact events. This concept was selected in conjunction with a graphite reinforced composite structural skin without any intervening strain isolation layer. Elimination of the strain isolation layer and one layer of adhesive reduces attachment weight. This concept has only been demonstrated to-date in ground testing. The CMC outer skin of the TPS adds weight, versus Concepts 1 and 2, but provides a more robust system for the military environment.

RCG Coating (0.005 in)
CMC Face sheet (0.05 in)
X-Cor^{TM} (Optimized)
RTV Adhesive (0.008 in)
Composite Skin)

Figure 10 - Concept No. 4 – CMC Wrapped Tile with X-Cor^{TM}

Concept No. 4 is a further iteration of tile technology and an extension of Concept No. 3. It uses the Aztex, Inc., X-Cor^{TM} concept to reinforce CMC skinned tile with through-thickness CMC reinforcing pins. This concept has also only been evaluated to-date in ground testing. The CMC reinforcing pins provide added resistance to CMC facesheet delamination that might result from thermal strain mismatch at the facesheet-to-tile interface or from debris impact events. This concept is also directly bonded to a composite skinned structure.

RCG Coating (0.005 in)
NEXTEL (0.1 in)
Saffil (Optimized)
Nextel (0.2 in)
Saffil (0.2 in)
Nextel (0.1 in)
Composite Skin

Figure 11 - Concept No. 5 Mechanical Attached Ceramic Blanket

Concept No. 5 is a derivative of Shuttle bonded blanket technology. In this concept, mechanical attachment replaces the adhesive bond, creating the possibility for a dual-layer blanket stack as evidenced in this design. Blankets are relatively cheap, and the dual-layer feature can increase total thickness beyond what is currently possible with a single blanket. The dual-layer can also be used to block direct line-of-sight of the structure at blanket-to-blanket joints. This design does not offer improved damage resistance, but it does offer improved operability via its easy remove/replace attribute. If used in less damage-prone areas, this concept can improve vehicle turn-times through easy TPS removal and replacement where frequent access to underlying structure or subsystems is required.

Inconel Honeycomb
Saffil Alumina Insulation
Titanium Foil
Titanium Honeycomb
Aluminum skin

Figure 12 - Concept No. 6 – Mechanically Attached Metallic TPS

Concept No. 6 is a mechanically attached, metallic TPS design. It offers the operability advantage of mechanical attachment, along with the ductility advantage of a metallic material versus a ceramic. The latter is advantageous for debris impacts where deformation of a metallic skin might occur versus fracturing for a ceramic based concept. The metallic concept, however, has a lower maximum use temperature versus ceramic materials and may be limited to non-windward surface areas for military vehicles.

Concept	FS Max. Thickness	Wing Max. Thickness	Total Weight
1	3.52 inches	3.84 Inches	4739 Lbs.
2	4.56 Inches	4.87 Inches	5880 Lbs.
3	4.81 Inches	4.94 Inches	6578 Lbs.
4	4.97 Inches	4.46 Inches	7475 Lbs.
5	4.89 Inches	5.31 Inches	5289 Lbs.
6	Too high Temp.	-	-

Table 1 - Total Vehicle TPS Thickness and Weight

B. Weight results Analysis

HRSI tiles (BASELINE - Concept 1)	4739 lbs	
Mech-attached ceramic blankets (Concept 5)	5289 lbs	12% heavier than baseline
TUFI/AETB tiles (Concept 2)	5880 lbs	24% heavier than baseline
CMC wrapped AETB tiles (Concept 3)	6578 lbs	39% heavier than baseline
CMC wrapped tile w/X-Cor[TM] pins (Concept 4)	7475 lbs	57% heavier than baseline

V.   Matrix For The Comparison Of Concepts

(On a scale of 1-5, 5 = The Best, 1 =The Worst)

	Concept 1	Concept 2	Concept 3	Concept 4	Concept 5
Weight	5	3	2	1	4
Reliability	2	3	4	No Data	No data
Turn Time	2	3	4	No Data	No Data
Durability	2	3	4	No Data	No Data
Affordability	4	3	2	No Data	No Data

The concepts 4 and concept 5 are fairly new so very limited data are available for the reasonable comparison. There is a trade off for each concept for weight, reliability, turn time, durability and affordability. This in-house study has assisted AFRL/VA in making educated decision for technology trade off. The assessment the data as of this in-hose study provided the Air Vehicle Directorate's space programs office a quantifiable measures to support and guide the new technology planning decision.

VI.   Follow-On Efforts

The analysis described in this paper has been useful in providing additional technical information needed to impact future research within AFRL. However, additional analysis is anticipated to expand the scope of this study to include integrated hot structures for the entire vehicle and to further address operability issues. The MINIVER material data base also needs to be updated with more modern materials to facilitate expanded research. This material data base was constructed in 1991. AFRL/VASD has added few additional materials in 2003 but there is a need to add more recent materials for completeness.

Acknowledgements

Authors would like to thank the following people for providing their support: Kathryn Wuster from NASA Langley for providing MINIVER support and technical guidance.   TechnoSoft Inc. for developing AML/MINIVER integration interface and providing technical assistance in order to use the new developed software tool, Ms. Alicia Hartong and John Livingston from ASD/EN for providing RMLS vehicle configuration data and zone areas for windward side of the vehicle, and Mr. Erik Paulson for providing the optimized trajectory data.

References

1.   Orbiter Thermal Protection System, KSC Release No. 11-89, February 1989
2.   NASA Facts, FS-2000-06-29-KSC, March 1997
3.   NASA Technical Memorandum 11-296, Development of Metallic Thermal Protection Systems for the Reusable Launch Vehicle, Max L. Blosser, Langley Research Center, Hampton, Virginia
4.   LANMIN User's Manual Volume 1; Carl D. Engel, Sarat C. praharaj; REMTECH Inc. ; August 1983
5.   LANMIN Input guide, Volume 2;Carl D. Engel, Craig P. Schmitz; RAMTECH Inc.; August 1983
6.   EXITS User's and Input guide; John E. Pond, Craig P. Schmitz; REMTECH Inc.; August 1983
7.   Adaptive Modeling Language (AML) Version 4.1, TechnoSoft Inc, Cincinnati, OH, October 2003
8.   Engineering Aero-thermal Analysis for X-34 Thermal Protection Design, Kathryn E. Wurster et. all, (AIAA 1997)
9.   Program to Optimize Simulated Trajectories (POST) Volume 2; R. W. Powell, D. E. Striepe, et. all NASA Langley Research Center, October 1997.
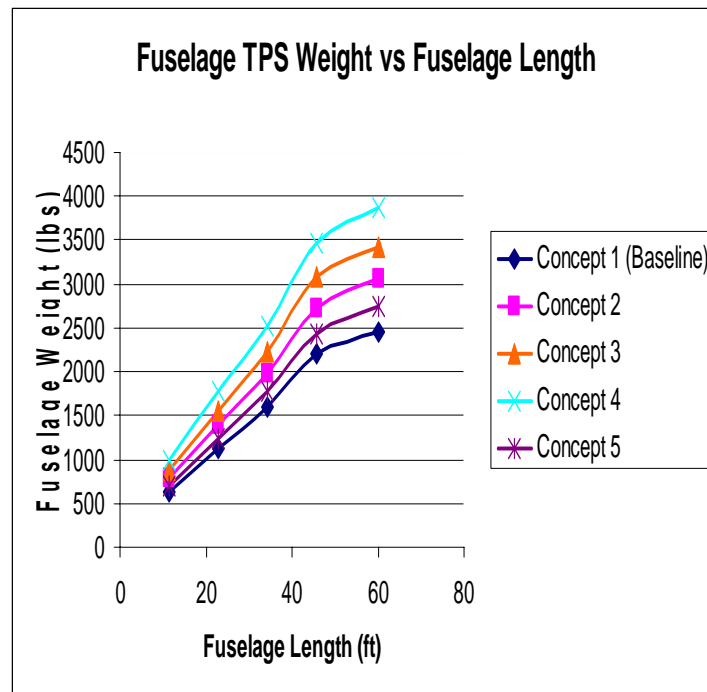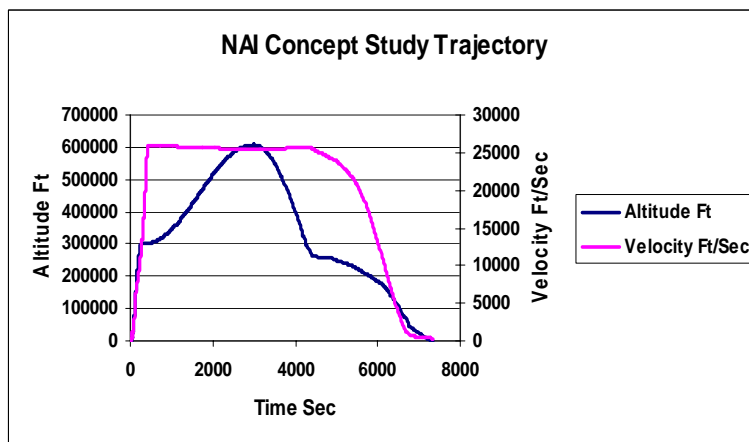
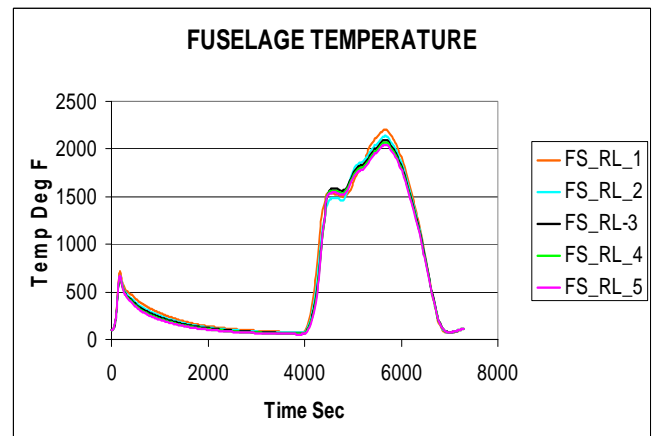**Figure 13 – FS TPS Weight VS FS length**

Figure 14 - Optimized Trajectory
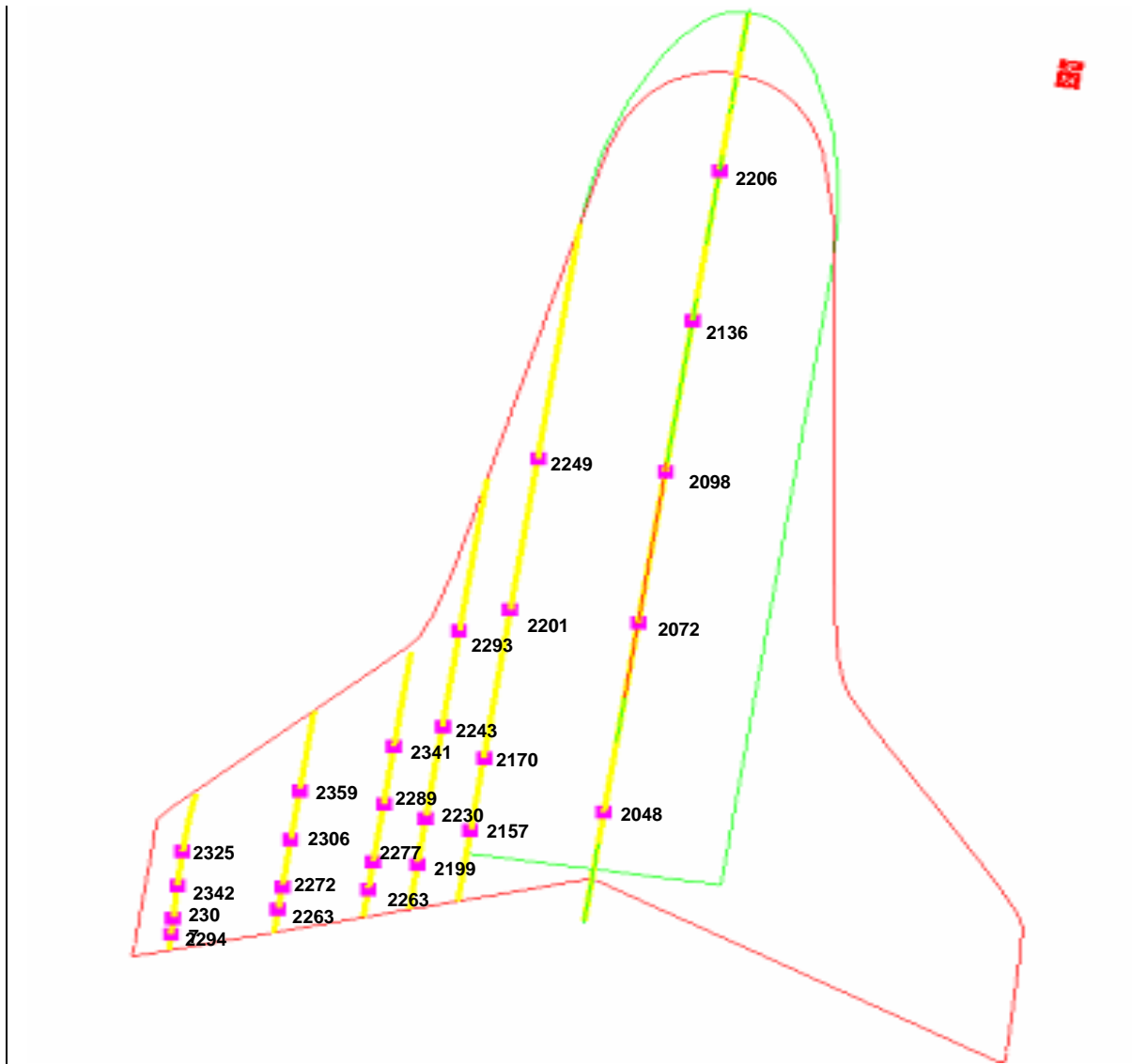

Figure 15 - FS Temperatures

Figure 16 - Typical Windward Max. Temperatures on FS and Wing for Concept 1

APPENDIX I

Noise Mitigation of Ducted Supersonic Jets for Launch Exhaust Management Systems

B.T. Vu
NASA-Kennedy Space Center
KSC, FL 32899

M. Kandula
Sierra Lobo, Inc. (USTDC)-Kennedy Space Center
KSC, FL 32899

ABSTRACT

The Launch Systems Testbed (LST) at the Kennedy Space Center (KSC) has conducted acoustic testing for passive mitigation of supersonic jet noise with exhaust ducts. Tests were performed with a cold nitrogen jet issuing from a nozzle of 1-inch exit diameter and an exit Mach number of 2.5. This report describes the existing cold jet simulation capability along with preliminary results on noise mitigation with closed and partially open ducts with rigid walls and an upstream J-deflector. Relative to the nozzle exit plane, the location of the duct inlet is va[*]ried at 10, 5 and –1 jet diameters. Farfield sound pressure levels were obtained at two levels (54 jet diameters and 10 jet diameters above ground) with the aid of 9 equally spaced acoustic sensors around a circular arc of radius equal to 80 jet diameters. Comparisons of the jet acoustic field were made with and without the duct.

INTRODUCTION

Air Force Research Laboratories (AFRL) has authorized NASA KSC to carry out a basic technology test program in support of developing clean launch pads for future launch vehicles incorporating passive sound mitigation techniques. These launch pad designs focus on reducing cost while enhancing safety and quick turnaround times. The overall goal of the program is to develop launch exhaust management systems, which effectively reduce the generated acoustic loads with innovative duct designs devoid of water injection systems. The preliminary series of tests are designed towards defining the jet acoustic load environment for closed duct and partially open duct (upper duct wall removed) configurations.

A major objective of LST is to establish a capability to simulate a small-scale launch vehicle environment for use in testing and evaluation of launch pad designs for future space vehicles. Scale model testing along with analytical methods is helpful in designing such systems as a means of predicting the full-scale acoustic environment [1-5]. In the initial phase of this study, the LST conducted cold jet tests with nitrogen gas issuing from an ideally expanded small-scale nozzle of 1-inch exit diameter with an exit Mach number of 2.5. Tests were conducted with free jets, jet passing through closed ducts and partially open ducts with an upstream J-type deflector.

EXPERIMENTAL SETUP

TEST FACILITY

The Trajectory Simulation Mechanism (TSM) located at the Launch Equipment Test Facility (LETF) in the KSC Industrial Area served as the primary facility for conducting these tests. It is designed to simulate **x-y** launch trajectories for nonstationary scaled acoustic load on the launch

---

1

vehicle, payload, and ground support equipment. TSM features a 1/10-scaled model of the Space Shuttle launch parameters. The simulation capability is available only for cold jets where the nozzle exit temperature is colder than the ambient temperature.

A schematic of TSM and related test setup is included in Fig. 1. The TSM facility is outfitted with a chamber and a supersonic nozzle held in vertical position. The chamber is fed from pressurized gaseous nitrogen bottles (8000 psi) in conjunction with two pressure regulators in series. The pneumatic system was modified to facilitate a continuous supply of nitrogen for the duration of the tests. The TSM facility also provides necessary instrumentation for measurement of the flow and the acoustic field.

The convergent-divergent nozzle was designed on the basis of a characteristic method and was made of stainless steel. The Mach 2.5 nozzle has an exit diameter of 1 inch. This dimension compares with 3 to 4 feet of nozzle exit diameter typical of large rocket engine nozzles. Typical chamber and nozzle conditions for the scale model test series considered here are displayed in Table 1. The nozzle is capable of generating an acoustic load in excess of 150 decibels (dB) near the nozzle exit.

A scaled aluminum exhaust duct with an upstream J-deflector (30-degree inclination to the vertical) was fabricated and installed under the nozzle. A photographic view of the actual jet/duct setup is displayed in Fig. 2. The cross section of the duct is 6 inch by 12 inch. The exhaust duct can be positioned at desired levels relative to the nozzle exit plane (NEP). Only static tests (with a stationary nozzle) are considered in the present investigation.

INSTRUMENTATION

The chamber conditions (pressure and temperature) are measured by a pressure gauge and thermocouple mounted on the chamber wall. From the measurement of the total pressure and the static pressure at the NEP, the exit Mach number is computed with the aid of Rayleigh's pitot tube formula [6].

The acoustic field surrounding the nozzle/duct configuration was measured by an array of acoustic transducers (microphones) placed azimuthally at 22.5-degree increments (Fig. 3). Bruel & Kjaer microphones of 0.5-inch diameter were used for recording the sound pressure. The sensors were placed azimuthally at 80 nozzle exit diameters from the NEP, thus representative of far-field condition.

DATA ACQUISITION

Time history measurements are made of chamber pressure, chamber temperature, and pitot and static pressures at the NEP. These measurements serve to indicate the time at which steady-state conditions are achieved. Generally, it takes about 60 seconds for steady conditions to prevail.

As soon as the flow becomes steady, acoustic data begin to be recorded. Pressure-time data from the microphones are processed by the data acquisition system. The data are sampled at a maximum rate of 125,000 samples/second. With the aid of LabVIEW software, the time domain data are processed in the form of narrowband spectra, 1/3-octave band sound pressure levels, and overall sound pressure levels (OASPL) at each location.

TEST PROCEDURE

The chamber and the nozzle are attached to a mounting plate on the TSM horizontal carriage. This carriage is placed in the "maintenance position" and retracted towards the TSM base for all static tests. For the duct testing, the exhaust duct is installed below the nozzle at the desired levels corresponding to one of the following configurations: 10 inches below the NEP (jet

2

core completely outside the duct; Fig. 4), 5 inches below the NEP (jet core partially outside the duct; Fig. 5), and jet core totally inside the duct (Fig. 6). Pre-test calibration of all the nine microphones is carried out. The B&K calibrator is used for this purpose, with 94 dB and 114 dB at 1 kHz.

First the pressure regulator (PR-1) is opened such that the downstream pressure is about 3000 psig. Subsequently, the second pressure regulator (PR-2) control valve is operated such that the chamber pressure (indicated by the digital readout placed close to the regulator) is at the desired value of 250 psia to ensure Mach 2.5 at the nozzle exit. At this time, the chamber pressure, the pitot pressure, and the pitot pressure at the nozzle exit begin recording. It generally takes about 60 seconds to reach a steady-state chamber pressure. Once the steady-state chamber pressure is achieved, as indicated by the real-time display in the control room, the acoustic data begins to be recorded. The acoustics data are taken over a period of about 4 seconds. Post-test calibration of the microphones is also carried out.

RESULTS AND DISCUSSION

OVERALL SOUND POWER

Fig. 7 shows a comparison of the OASPL for free jet with those of a jet passing through a closed duct, with the NEP located at different heights relative to the duct inlet. While there is axial symmetry of the OASPL for the free jet, there is considerable directivity of the OASPL in the presence of exhaust duct. For the nozzle to duct inlet distances of 5 inches and -1 inch (NEP inside the duct), the OASPL near 0 degree exceeds the value for the free jet case. When the NEP is held at 10 inches above the duct inlet, a reduction in OASPL of about 3 dB is achieved relative to the free jet case. These findings suggest that there is an optimum location of the NEP relative to the duct inlet plane, which results in the largest reduction in the OASPL.

In the case of partially open ducts (Fig. 8), trends are contrary to the closed duct case with regard to the OAPSL variation with the duct inlet to NEP distance. For the open duct, the OASPL increases as the distance between the NEP and the duct inlet plane increases. In general, the OASPL near the duct axis for partially open ducts are considerably higher than that for the free jet case. This result suggests that closed ducts are preferable to partially open ducts as far as sound mitigation is concerned.

SPECTRAL SOUND POWER

The spectral content of the sound power level for the free jet is depicted in Fig. 9. In this configuration, the spectral distribution is symmetric, independent of the azimuthal position of the microphone. A peak frequency of about 4 kHz is noted in this case and agrees well with the estimated value based on a Strouhal number ($St = f\, u_j\, /\, d_j$) of 0.2. Here f denotes the frequency, u_j the nozzle exit velocity, and d_j the nozzle exit diameter. In the closed duct case (Fig. 10) with duct inlet 10 inches below the NEP, the peak frequency near $\theta = 0$ deg. (corresponding to the duct axis) is about 4 kHz, which is close to the free jet value. However, the peak frequency increases as the angle from the jet axis is increased. Differences in the spectrum for various angles are observed over a wide range of frequencies (roughly 1.5 decades).

Fig. 11 presents the spectral distribution of sound power level for the partially open duct configuration, with the duct inlet 10 inches below the NEP. Notable differences in the spectral behavior are observed between the closed duct and the partially open duct case. In the case of the partially open duct, significant directivity effects persist even at much lower frequencies.

CONCLUSIONS

With the use of a closed duct the overall sound power of a Mach 2.5 supersonic jet is reduced by about 3 dB. The peak frequency is found to increase above the free jet value as the

3

angle from the jet axis is increased. The results also suggest that there is an optimum distance between the nozzle exit plane and the duct inlet for minimizing the sound power. The partially open duct results in increased sound levels near the duct axis relative to the free jet case. With regard to the closed duct, larger reductions in sound power may be realized by increasing the duct length, increasing duct cross section (adding a diffuser), and including absorbing liners on the duct walls.

ACKNOWLEDGEMENT

REFERENCES

1. McInerny, S., Rocket Noise - A Review, AIAA 90-3981, 13th Aeroacoustics Conference (1990).

2. Sutherland, L.C., Progress and Problems in Rocket Noise Prediction for Ground Facilities, AIAA Paper 93-4383, 15th Aeroacoustics Conference (1993).

3. Kandula, M. and Caimi, R., Simulation of Jet Noise with OVERFLOW CFD Code and Kirchhoff Surface Integral, AIAA 2002-2602, 8th AIAA/CEAS Aeroacoustics Conference, Breckenridge, Colorado (2002).

4. Kandula, M. and Vu, B., On the Scaling Laws for Jet Noise in Subsonic and Supersonic Flow, AIAA-2003-3288, 9h AIAA/CEAS Conference, Hilton Head, South Carolina (2003).

5. Vu, B.T., Kandula, M., Margasahayam, R., and Ford, D., "Launch Systems Testbed: An Innovative Approach to Design of Future Space Structures," Space Technology and Application International Forums, Albuquerque, NM, Feb. 2-6, 2003.

6. Shapiro, A.H., The Dynamics and Thermodynamics of Compressible Fluid Flow, Vol. 1 (John Wiley & Sons, New York, 1953).
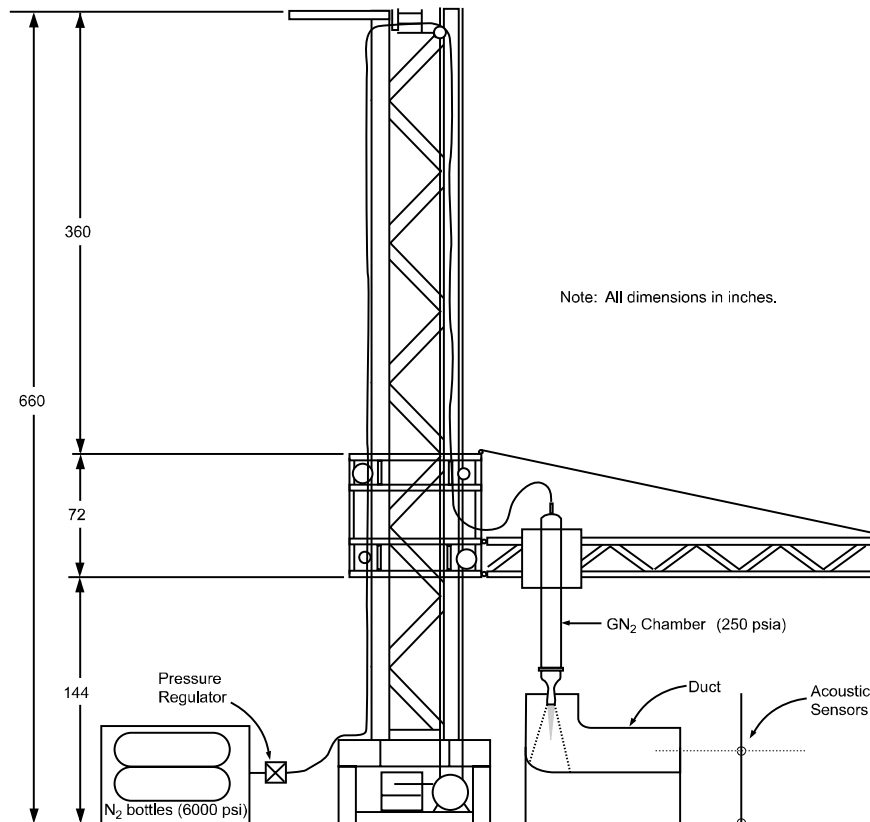
4

Figure 1. Overall Test Setup.

Table 1. Summary of Nozzle Parameters

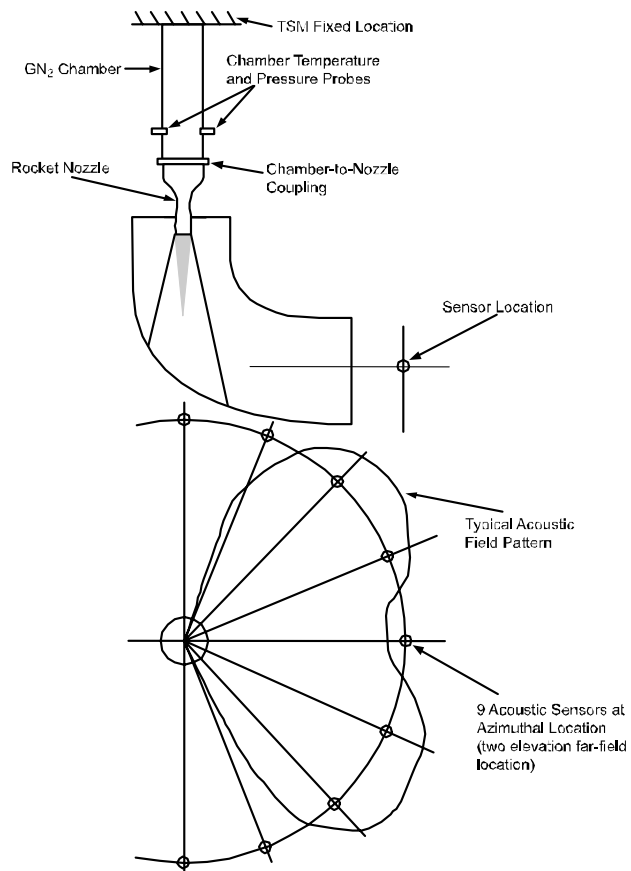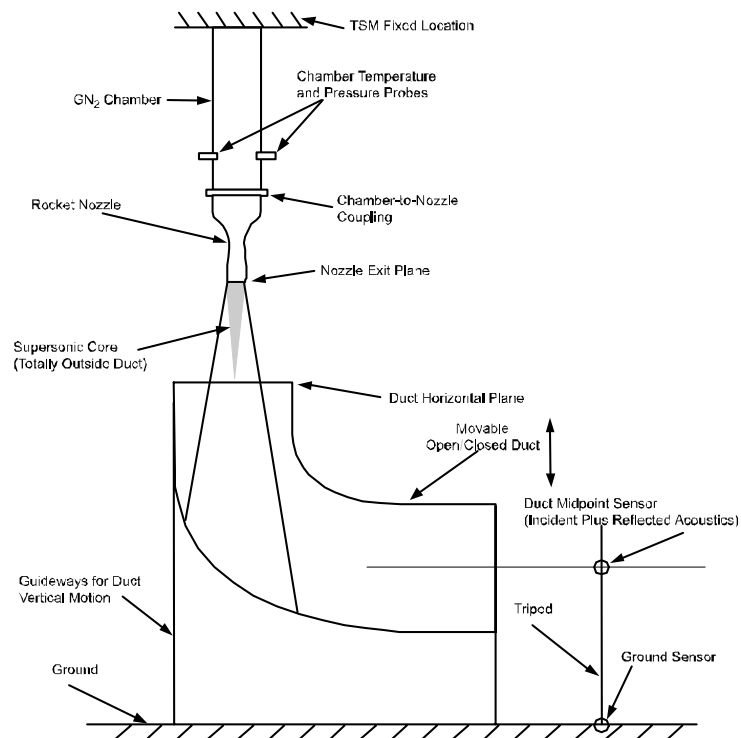| Parameter	Value
Stagnation pressure, psia	250
Stagnation temperature, °R	500
Nozzle mass flow rate, lbm/s	1.7
Nozzle exit diameter, inch	1.0
Exit pressure, psia	14.7
Exit temperature, °R	222
Exit velocity, ft/s	1,820
Nozzle exit Mach number	2.5
Jet exit Reynolds number	4×10^{6}

5

Figure 2. Jet/Duct Configuration

Figure 3. Microphone locations.

Figure 4. Duct inlet at 10 inches below the NEP.
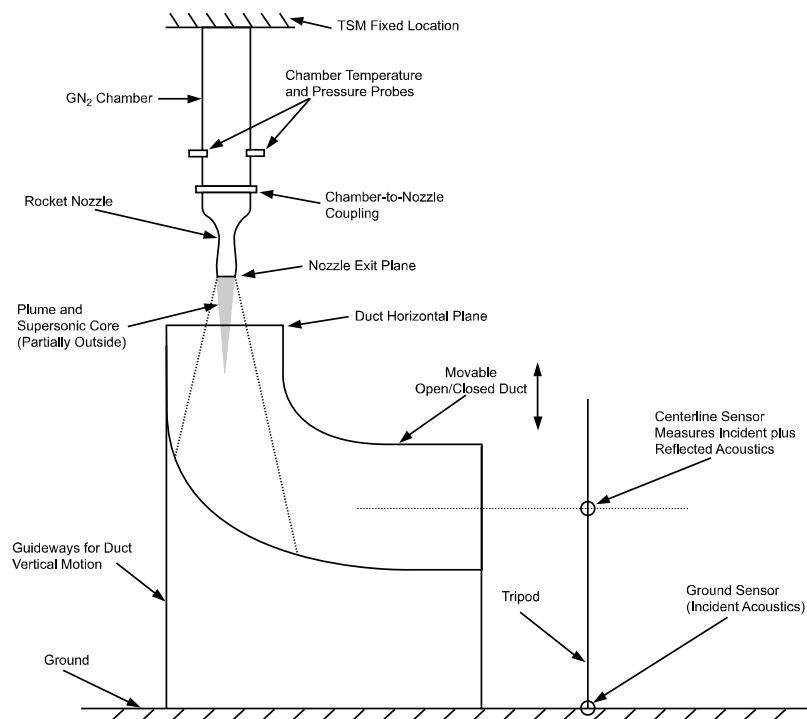
Figure 5. Duct inlet at 5 inches below the NEP.

7

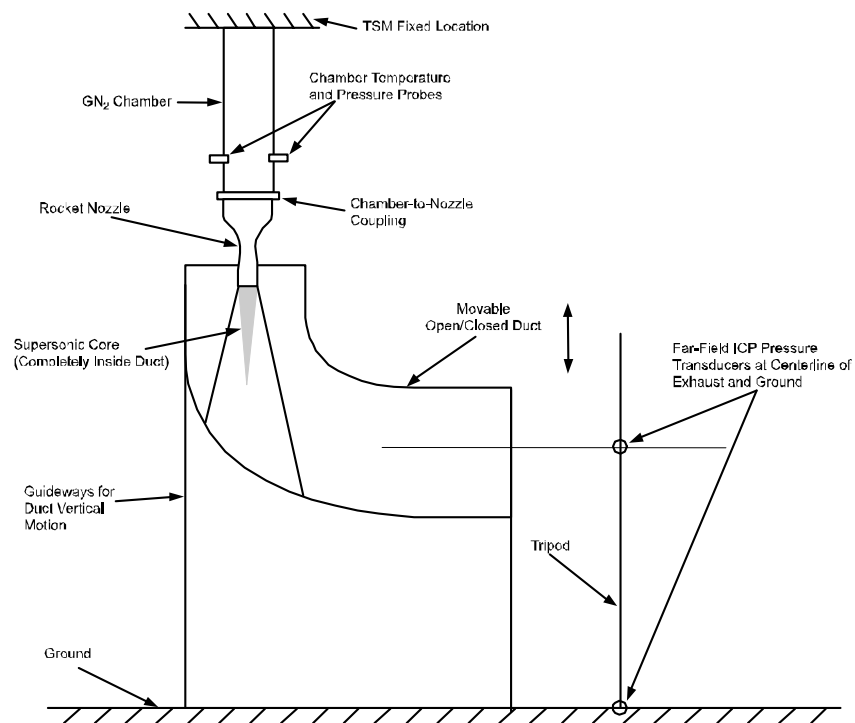Figure 6. Duct inlet at -1 inch above the NEP.
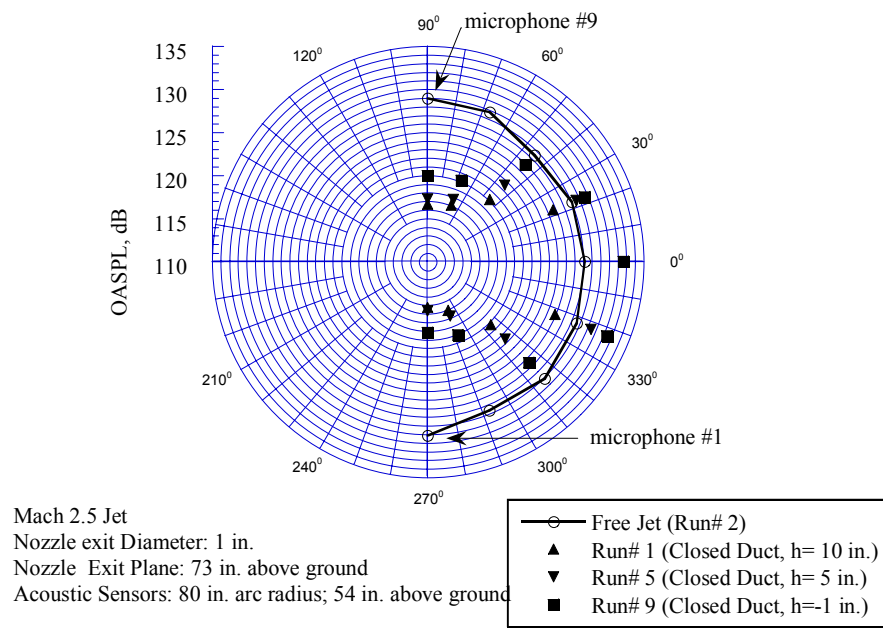

Mach 2.5 Jet
Nozzle exit Diameter: 1 in.
Nozzle Exit Plane: 73 in. above ground
Acoustic Sensors: 80 in. arc radius; 54 in. above ground

Figure 7. Comparison of OASPL for free jet and with a closed duct.

8

Mach 2.5 Jet
Nozzle exit Diameter: 1 in.
Nozzle Exit Plane: 73 in. above ground
Acoustic Sensors: 80 in. arc radius; 54 in. above ground
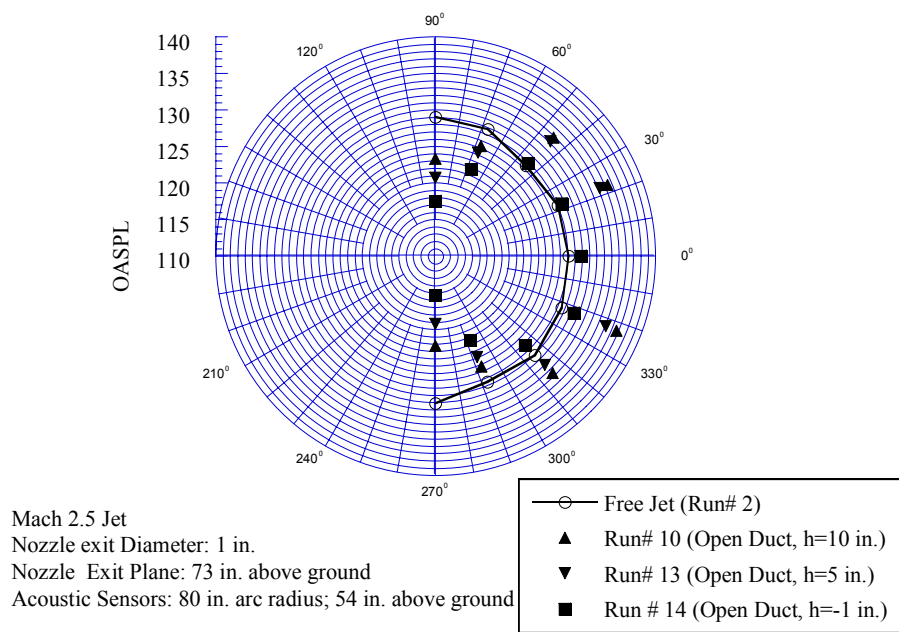
Figure 8. Comparison of OASPL for free jet and with a partially open duct.

Run#2
Mach 2.5 Free Jet
Nozzle Exit Diameter: 1 in.
Nozzle Exit Plane: 73 in. above gound
Acoustic Sensors: 80 in. arc radius; 54 in. above ground
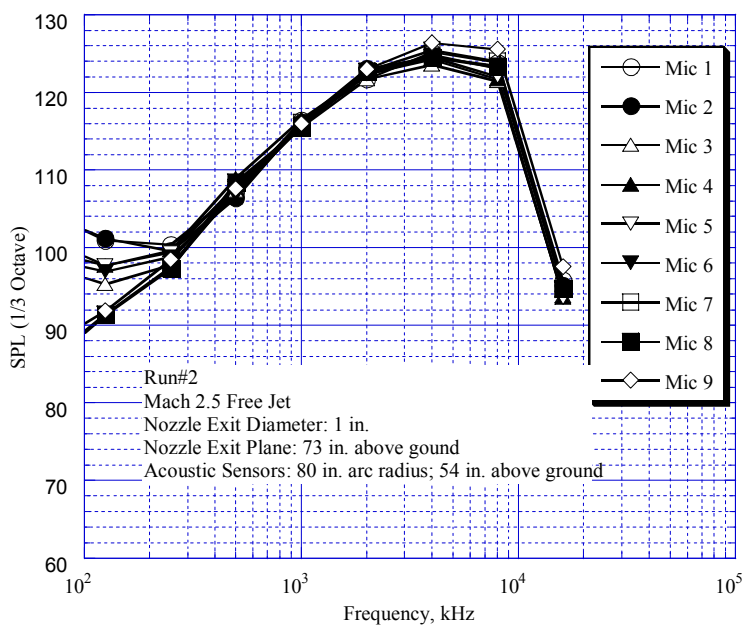
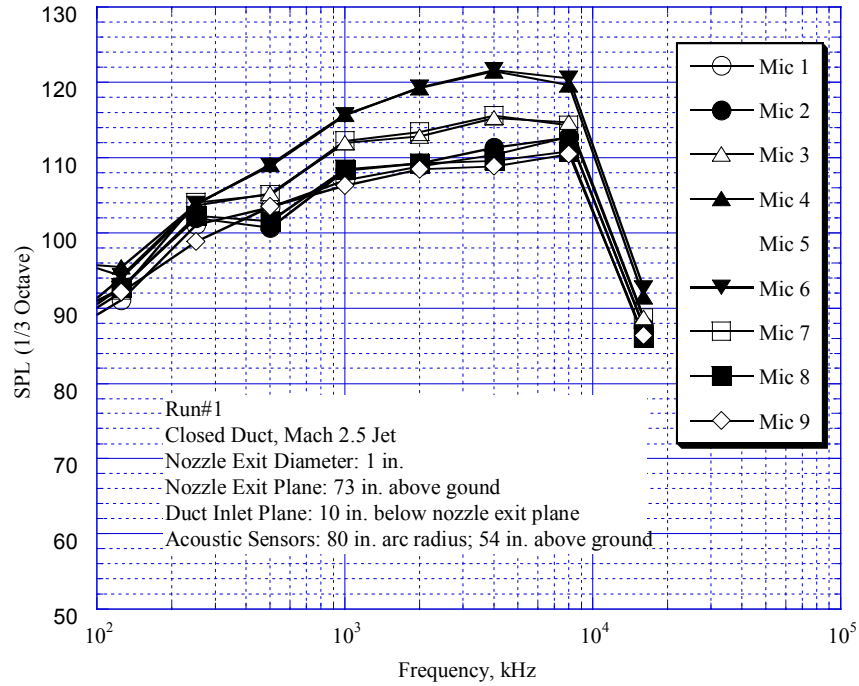Figure 9. Spectral sound power for the free jet.

9

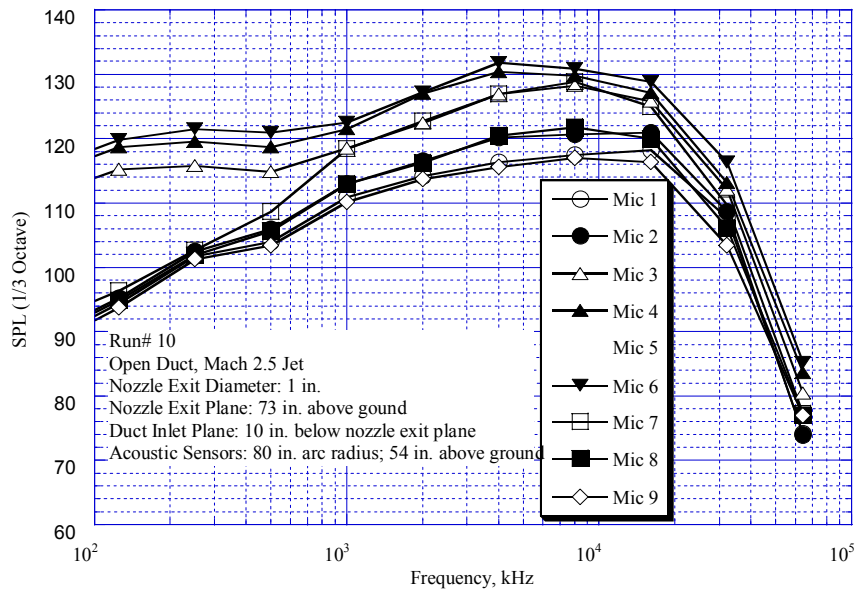Figure 10. Spectral sound power for the jet flowing in a closed duct.

Figure 11. Spectral sound power for the jet flowing in a partially open duct.

10